P.L. ~~MATTERN~~, 8342; ~~ATTN:~~
~~J. VITKO, Jr.~~

SAND78-8192
Unlimited Release
Printed March 1981

UC-62d

MCDONNELL DOUGLAS
CORPORATION

SECOND GENERATION HELIOSTAT DETAIL DESIGN REPORT

AUGUST 1980

MDC G8631
CONTRACT 83-0024A

Prepared by:
R. K. Knowles
Chief Program Engineer
Second Generation Heliostats

Approved by: D A. Steinmeyer
D. A. Steinmeyer
Program Manager
Second Generation

MCDONNELL DOUGLAS ASTRONAUTICS COMPANY-HUNTINGTON BEACH
5301 Bolsa Avenue Huntington Beach, California 92647 (714) 896-3311

Printed in the United States of America
Available from
National Technical Information Service
U. S. Department of Commerce
5285 Port Royal Road
Springfield, VA 22161
Price: Printed Copy $9.25 ; Microfiche $3.00

PREFACE

This document contains the Second Generation heliostat design prepared by McDonnell Douglas Astronautics Company (MDAC) under Contract 83-0024A for Sandia Laboratories, Livermore, California.

TABLE OF CONTENTS

TABLE OF CONTENTS
(Continued)

LIST OF FIGURES

LIST OF FIGURES
(Continued)

LIST OF TABLES

LIST OF TABLES
(Continued)

Section 1
INTRODUCTION AND SUMMARY

1.1 INTRODUCTION

1.1.1 Program Objective

This report provides the results of the design phase of the McDonnell Douglas Astronuatics Company (MDAC) Second Generation heliostat program. The overall goal of the program is the development of a heliostat which can be produced at low cost in high volume. The program includes: (1) heliostat design, (2) high volume manufacturing and deployment process definition, (3) volume cost projections, and (4) fabrication and test of two heliostats demonstrating the features of the high volume design.

The baseline production heliostat design as well as the modifications to this design for fabrication of the two test units are defined in this report. Also included is the initial definition of the production and deployment processes. The final report to be prepared in the fourth quarter of 1980 will provide completed manufacturing installation plans as well as cost projections for 50,000 heliostats/year.

1.1.2 Design Approach

The MDAC Second Generation heliostat configuration, Figure 1-1, is based on the results of the prototype heliostats study, completed in July 1978 and reported in MDC G7399, "Prototype Heliostat Final Technical Report." However, between the completion of the prototype study and the start of the Second Generation program in September 1979, several significant sources of new data have provided the impetus for additional cost reduction modifications for the Second Generation heliostat. These data sources are shown in Table 1-1.

The design conforms to the performance requirements of Sandia Specification No. A10772, Issue D.

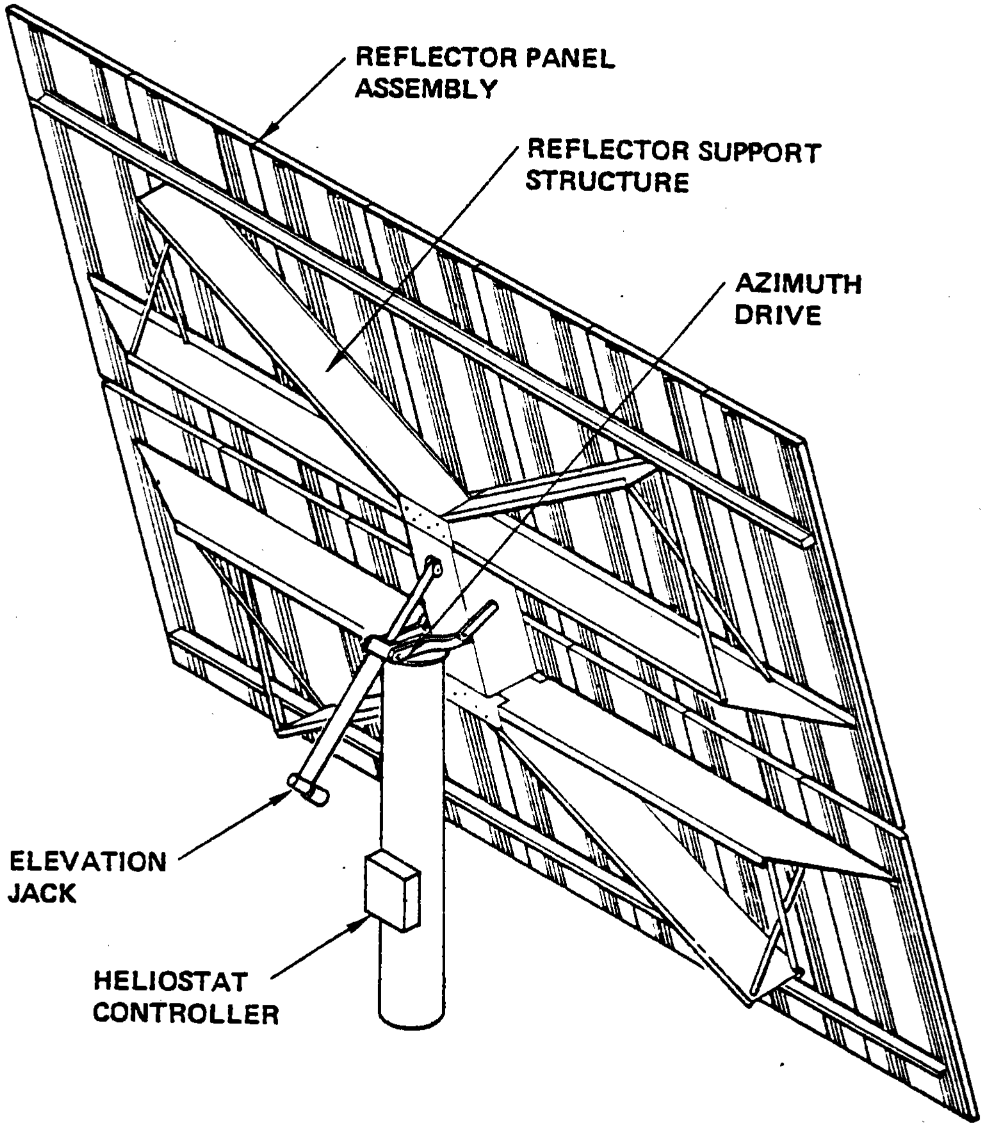

- VERTICAL STOW
- HORIZONTAL SURVIVAL
- REFLECTIVE AREA - 612 FT^2 (57 M^2)
- 1.27-1 ASPECT RATIO

Figure 1-1. Second Generation Heliostat

Table 1-1

SECOND GENERATION HELIOSTAT DESIGN DATA BASE

- Solar Central Receiver Prototype Heliostat CDRL Item B.d, Final Technical Report, Volume II, MDAC MDC G7399, August 1978.
- Noninverting Heliostat Study, MDAC MDC G7876, July 1979, Contract No. 18-7872
- Heliostat Production Evaluation and Cost Analysis, SERI/TR-8052-1, December 1979
- Heliostat Manufacturing Cost Analysis, SERI/TR-8043-1, October 1979.
- Colorado State Wind Tunnel Test - CER79-80JEC-JAP23
- Full Scale Wind Tunnel Test, SAND79-8034
- Pilot Plant Heliostat Development, Phase I, Contract 21006, September 1979
- Second Generation Program, Sandia Contract 83-0024A
- Sandia Studies, Program Kickoff, July 1979
    - Heliostat Cost/Performance Trades
    - Heliostat Stow Position Cost Benefit Analysis
    - CRTF Dust Buildup Experience
    - Eye Hazards Associated with Heliostats

1.1.3 Design Status

This report is provided at the completion of the detail design phase of the Second Generation heliostat program. Component level tests associated with obtaining design data have been completed. This design has been reviewed by Sandia in a formal review. Hardware fabrication for two test heliostats is now underway for testing at MDAC in the third quarter of 1980 and testing at Central Receiver Testing Facility (CRTF) starting 1 December 1980.

1.2 DESIGN SUMMARY

The major features of the MDAC design are shown in Figure 1-2. Changes from previously developed heliostats have all been made for reduction of life cycle cost without sacrifice of performance.

The most beneficial configuration change is selection of vertical stow, face up survival instead of inverted stow. The benefits obtained by this change are summarized in Table 1-2. In addition to drive parts reduction, this change allows rearrangement of the structure, with a resulting capability to increase the reflector area. The rearrangement provides a more favorable aspect ratio, while maintaining the same clearout radius required for smaller inverting designs and thereby significantly reduces land requirements as well as collector subsystem costs.

The field effect gain identified in the prototype study for this type of area increase is greater than a 1.2 factor for the area added.* The reduced blocking and shading results from the height decrease, and increased area associated with filling the slot.

1.2.1 Component Design Summary

Component level improvements in the Second Generation heliostat involve the mirror module, support structure, and drives.

A laminated mirror module is used providing a 0.059 inch fusion glass mirror with white backing paint laminated to a 0.190 inch float glass by the conventional PVB (poly vinyl butyral), autoclave process. For the test heliostats, 0.095 inch

---

*Solar Central Receiver Prototype Heliostat CDRL Item B.d, Final Technical Report, Volume II, MDAC MDC G7399, August 1978.

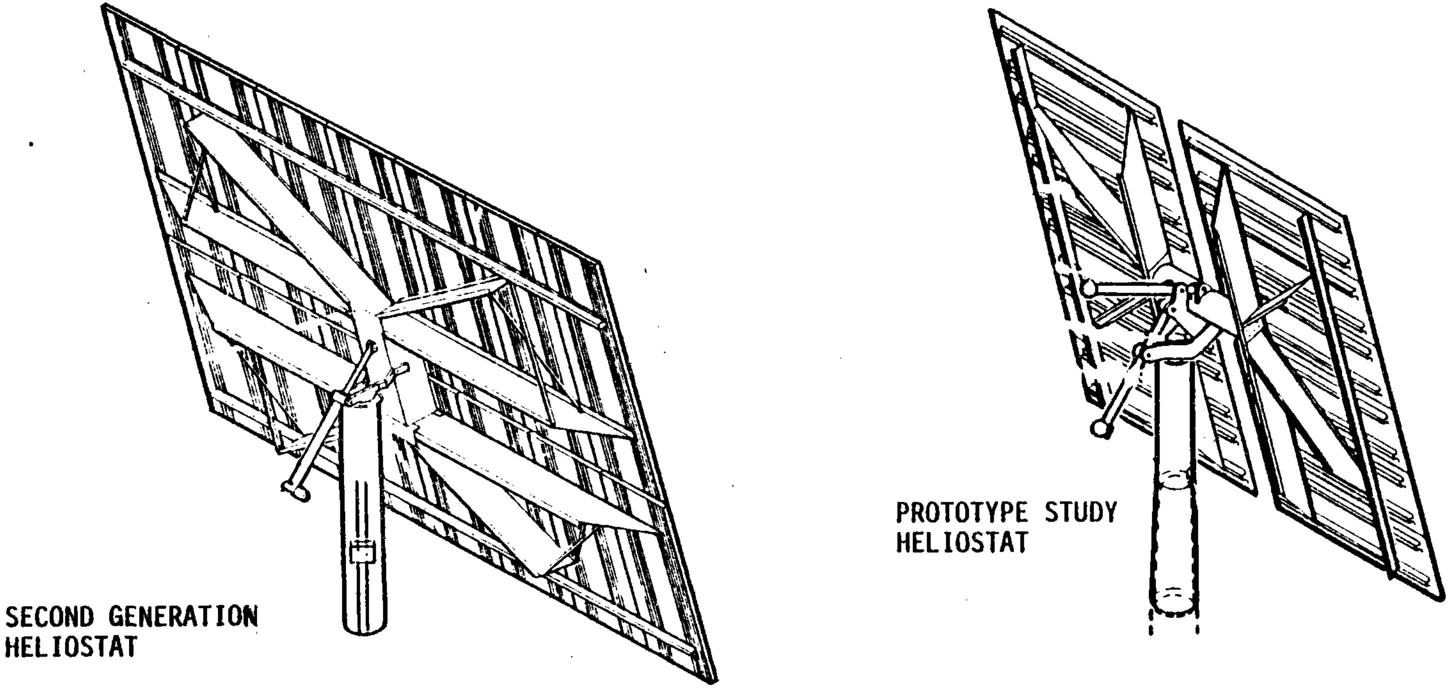

HELIOSTAT

- o ELIMINATED INVERTED STOW HARDWARE
- o INCREASED REFLECTOR AREA
- o ROTATED REFLECTOR PANEL FOR IMPROVED ASPECT RATIO
- o RECONFIGURED DRIVE GEOMETRY FOR REDUCED LOADS-WEIGHTS
- o REPACKAGED CONTROLLER

COLLECTOR SYSTEM

- o REDUCED NUMBER OF HELIOSTATS/FIELD
- o DECREASED FIELD AREA REQUIREMENTS
- o DECREASED MAXIMUM FIELD SLANT RANGE

Figure 1-2. Design Improvements

Table 1-2
COST REDUCTION FEATURES*
MDAC SECOND GENERATION CONFIGURATION

DRIVE COMPONENT PARTS REDUCTION	∿30%
DRIVE WEIGHT REDUCTION	∿350 lbs
INCREASED AREA WITH SAME SUBSYSTEMS	∿17%
UNMODIFIED ELEMENTS	
CONTROLLER AND ELECTRICAL COMPONENTS	
AZIMUTH DRIVE	
FOUNDATION	
FIELD INSTALLATION LABOR AND SERVICES	
AREA INCREASE WITHIN SAME CLEAROUT RADIUS	
COLLECTOR SYSTEM COST REDUCTION	∿5%
REDUCED BLOCKING AND SHADOWING	
INCREASED FIELD COVERAGE RATIO	
REDUCED FIELD PERIMETERS	
REDUCED ATTENUATION	
REDUCED TOWER HEIGHT	

*COMPARISONS BASED ON MDAC PROTOTYPE STUDY RESULTS float glass is used for the mirror because full size fusion glass panels were not available in a timely manner. The mirror panel is supported by low carbon steel hat sections bonded to the panel. The edge is sealed with silicone and protected by metal edge member. The laminated mirror module provides significant cost reduction over the currently qualified MDAC foam core panel. In the future, lower production costs will be available for this configuration from an adhesive bonding process, investigated in this program, to replace the PVB autoclave process. However, more extensive development is required before use in full scale heliostats is warranted.

Structural parts are predominantly roll formed low carbon steel with spot welding and fusion welding assembly. In a significant departure from previous designs, the reflector assembly consisting of the support structure and mirror modules is bolted together and aligned in the factory. This results in major field installation cost reduction.

The azimuth and elevation drives are both two stage mechanisms rather than the previously used three stages, with components selected from those used on virtually all MDAC heliostats since 1973. The harmonic drive used in azimuth has proven to provide low backlash under load conditions of the large area of this heliostat, with a minimum number of parts. A helicon gear provides the input stage of the Second Generation drive. A welded housing, coupled with revised load paths, has reduced weight significantly since the prototype study. A wire race turret bearing was selected also for cost reductions. The elevation drive is a roll formed ball screw jack driven by a helicon gear. Both drives are factory lubricated and sealed.

Significant field installation cost reductions are achieved by providing three factory assembled and prealigned assemblies to the field installation site. As shown in Figure 1-3, the drive assembly consists of the main beam, azimuth and elevation drives, pedestal, and heliostat controller. Factory adjustments of the drive assemblies and position sensors are performed to facilitate later on heliostat track alignment. The two reflector assemblies consist of support structure and seven mirror modules each. The reflector assemblies are prealigned with respect to curvature and cant for the field site. A tapered joint foundation

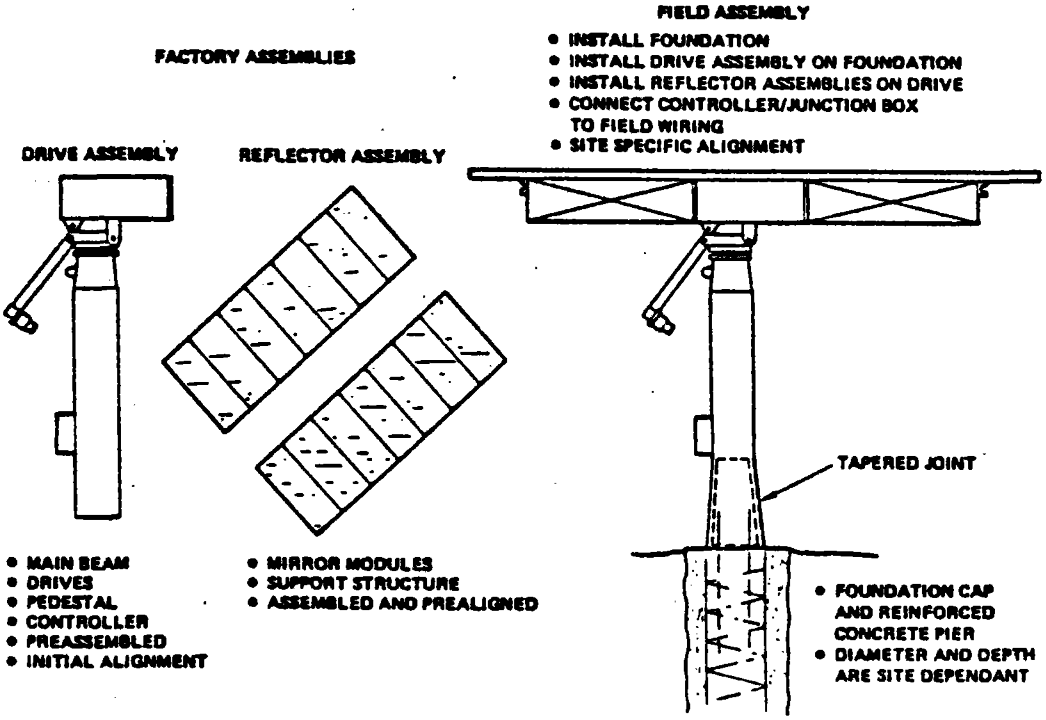

Figure 1-3. Field Installation

is installed with the field wiring terminated at a facility junction box adjacent to its base. Heliostat installation consists of emplacing the drive assembly tapered pedestal on the foundation, installing the reflector assemblies, connecting the controller to the field wiring, and inputting site specific alignment data into the controller. In response to user preference, the heliostat may also be supplied with a more conventional bolting flange pedestal.

1.2.2 Hardware Testing Summary

Testing to provide design data has been accomplished to date on the mirror bonding process and the drive hardware. Additional testing for design verification will be accomplished and reported in the program final report. Available test data are summarized in Table 1-3.

1.2.3 Production Planning Summary

Production process flows are currently under development reflecting the heliostat design. A central factory concept is being postulated with tradeoffs on the detail level of make or buy for components such as the mirror laminate and steel piece parts. Under MDAC supervision General Motors Transportation Systems Center (GM TSC) and the F. Joseph Lamb Company will perform these analyses for production planning and costing definition. The results of this effort will be provided in the final report.

1.2.4 Cost Projections Summary

Following completion of the production planning, the production cost and life cycle costs will be developed. The results of this effort will be provided in the final report.

Table 1-3

COMPLETED COMPONENT TESTS

TEST	CONFIGURATION	SUMMARY RESULTS
Development of Mirror Laminate Bonding Process Using Adhesives	Fusion glass mirror, no backing paint, and backlite glass.	Bond capability achieved. Long term degradation of mirror without backing paint requires additional development. Conventional PVB process chosen for Second Generation hardware.
Hail Tests	Adhesive bonded and PVB laminates 0.059 and 0.095 inch front lite	No failures with 1 inch dia. ice balls
Hat Stiffener to Laminate Bonding Accelerated Environmental Load Test	Three adhesives 2 urethane 1 epoxy 1 ft x 8 in weighted samples	Steel to adhesive bond. Successfully acheived all candidates. Glass to adhesive: Stabond Urethane selected, others failed test
Azimuth Drive	Barstow Prototype drive assembly	Demonstrated harmonic drive capability for Second Generation heliostat loads.
Wire Race Bearing	Second Generation bearing and drive housing	Meets all specification requirements Load-Deflection-Life. No assembly difficulties.
Mirror Stiffener Configuration	Hat section and C section stiffeners	Hat section selected for bond peel area, stiffness.

The heliostat is mounted on a single pedestal (approximately 20 inches in diameter) that has a taper and is emplaced over a matching taper cone on the foundation for quick installation. The heliostat is noninverting and moves about 96 degrees in the elevation direction. Vertical stowage is the normal stowage mode and the heliostat design accommodates -2 degrees from vertical stowage to ensure reflected beam is on the ground in the near vicinity even for low sun angles.

The elevation drive is actuated by a linear jack system. Azimuth movement is achieved by a harmonic drive system. Both drive systems are environmentally sealed,

Heliostat control is achieved by a three-tier open loop control system. The three-tier configuration provides a Heliostat Array Controller (HAC) which provides overall field control and interface to the rest of the plant, a Heliostat Field Controller (HFC) which provides control of up to 32 heliostats, and the individual Heliostat Controller (HC). The control system is based on the heliostat control system developed by MDAC for the Barstow Pilot Plant heliostat with a simplified reference update technique which provides additional reduction in control system costs. The HC is housed in a raintight NEMA box mounted on the pedestal at eye level providing easy access for maintenance purposes. All heliostat wiring is protected with much of it internal to the pedestal or drive system.

Detailed design descriptions of each of the heliostat subsystems are provided in Section 3 of this report.

Section 2

DESIGN OVERVIEW

An overview of the Second Generation heliostat design is provided in this section. The presented material also includes a summary of the compliance of the design to the key heliostat requirements as contained in the Sandia Specification A10772, Issue D.

2.1 REQUIREMENTS

The basic requirements for the Second Generation heliostat design results from the Sandia Collector Subsystem Specification. The MDAC Second Generation heliostat has been designed to fulfill the requirements and intent of the specification. Analysis and/or test verification of many of the parameters are included with the design and development activity in progress at MDAC Huntington Beach.

Results to date indicate that the design is within full compliance of the specification. Tables 2-1 through 2-3 list the key performance, operational, and environmental requirements from the Sandia specification. These tables also summarize the current predicted performance of the MDAC design and note the methodology verifying the specific capability. Current performance meets or exceeds the specified requirements.

2.2 GENERAL DESCRIPTION

2.2.1 Configuration Selection

As noted in Section 1, the MDAC Second Generation heliostat configuration and design approach is based on the results of the prototype heliostat study activity completed in July 1978 and several subsequent studies conducted by Sandia, MDAC and Solar Energy Research Institute (SERI). This total data base has been utilized in determining the selected heliostat configuration for the MDAC Second Generation heliostat. Some of the key system trade parameters and the data base sources are shown in Table 2-4.

Table 2-1

KEY PERFORMANCE REQUIREMENTS

Paragraph No./Requirement	Predicted Capability	Verification Method
3.2.1 95% Redirected Energy on Target (5% Spillage)	2-3% Spillage Annual Average	Analysis
a. Beam Pointing 1.5 mrad Beam Error.	1.5 mrad	Allocation/Analysis
b. Beam Quality 1.4 mrad Fringe Width	Capability dependent on specific field location and temperature conditions (see separate discussion in paragraph 3.1.4).	Analysis Test
c. Reflective Surface Deflection - 3.6 mrad maximum (less foundation) Each Axis at 27 mph	2.5 mrad 3σ Elevation 2.9 mrad 3σ Azimuth	Analysis

Table 2-2

KEY OPERATIONAL REQUIREMENTS

Paragraph No./Requirement	Predicted Capability	Verification Method
3.2.2 (a) Function for All Steady-State Modes, etc.	N/A - Plant Oriented	N/A
(b) Position to Any Orientation Within 15 Minutes	Within 12 Minutes	Test
(c) No Drive Drift Due to Loading	No Backdrive	Test
(d) Resolve Singularity Within 15 Minutes	Within 12 Minutes	Test
(e) Provide Cost Effective Stowage	-2° Vertical Face Up 90 MPH	Demonstration Demonstration
Provide Orientation to Master Control	Provided to HAC	Test
(f) Control by Computer, Provide Basic Control Functions	Provided, Except Interfaces to BCS,* MCS and DAS not provided in CRTF test hardware	Test - 2 Heliostats

*BCS Beam Characterization System
MCS Master Control System
DAS Data Acquisition System

Table 2-3

KEY ENVIRONMENTAL REQUIREMENTS

Paragraph No./Requirement		Predicted Capability	Verification Method
3.2.6.1	Wind Loading - Withstand Gust, Vortex Shedding, Vibrations, Etc.	Comply - $F_N^* \geq 1$ CPS	Analysis
3.2.6.2	Operational Limits Wind - 12 m/s (27 MPH) Temperature - 0°C - 50°C Gravity - All Elevation Angles Function with -9°C + 50°C Plus Thermal Lag	Comply with Specification	Analysis Test
3.2.6.3	Stowage Initiator Track to 16 m/s (35 MPH) and Initiate Stow, and Withstand Loads 50 MPH Non-Operational	Comply	Analysis
3.2.6.4 Appendix 1 3.3.3	Hail 0.75" at 65 ft/sec 1.0" at 75 ft/sec (stow position)	>1" at 75 Ft/Sec any orientation	Test
3.2.6.5	Lightning - Survive Other Than Direct Hit	Controller has Lightning Arrestors	Analysis

*Natural Frequency

Table 2-4

SYSTEM TRADEOFF DATA BASE

	Source
Factory versus field labor	Solar Central Receiver Prototype Heliostat CDRL Item B.d, Final Technical Report, Volume II, MDAC MDC G7399, August 1978
Inversion	Noninverting Heliostat Study, MDAC MDC G7876, July 1979, Contract No. 18-7872
Aspect ratio	Sandia Letter dated November 6, 1979, Graph showing calculation of heliostat breakeven cost vs. aspect ratio
Rotation Axis	Second Generation Program, Sandia Contract 83-0024A
Heliostat Size	Second Generation Program, Sandia Contract 83-0024A
Error budget distribution	Second Generation Program, Sandia Contract 83-0024A
Open loop control logic	Second Generation Program, Sandia Contract 83-0024A
Array control distrubiton	Solar Central Receiver Prototype Heliostat CDRL Item B.d, Final Technical Report, Volume II, MDAC MDC G7399, August 1978
Maintenance approach	Solar Central Receiver Prototype Heliostat CDRL Item B.d, Final Technical Report, Volume II, MDAC MDC G7399, August 1978; and Second Generation Program, Sandia Contract 83-0024A

As an example of the trade studies, the selected configuration is compared to other configurations evaluated in Table 2-5 and Figure 2-1. The vertical stow configuration with a 1.27 to 1 aspect ratio results in the lowest weight per ft^2 of heliostat area. The increased area is available without elevation load increase. At the same time, increased load capability of the azimuth drive (verified by test) is utilized. The effect of eliminating inversion on the heliostat and area availability with the same clearout radius is also shown.

Figure 2-2 relates heliostat cost in $\$/m^2$ for varying mirror area where the design is limited by strength critical or stiffness critical criteria. The selected 616 ft^2 area (approximately 57 m^2) is in the bottom area of both curves indicating the appropriate choice for the overall area.

The above discussions indicates the methodology and type of data base that was used in the determination of the MDAC Second Generation heliostat configuration.

2.2.2 Heliostat Description

The MDAC heliostat configuration has a total of 14 mirror modules, each approximately 4 x 11 ft, providing a total reflective area of 612 ft^2. Seven of the mirror modules are assembled to a support structure as an assembly which is then attached to the main beam. This approach allows maximum use of the automated factory labor in lieu of field labor to assemble mirror modules on the structure. Mirror reflectivity is 0.89 for the prototype heliostats and 0.92 for production. Production will utilize a 0.059 inch fusion glass/mirror for the top lite of the laminated sandwich as opposed to the 0.093 inch clear float being used for the prototype units. The mirror modules have a common curvature in the 11-foot direction, but are individually canted on the support structure. The laminated glass mirror module has a simple painted stub edge member to ensure long life and protect against silver corrosion at the edges. This edge member reduces the reflective area to 612 ft^2 from the total heliostat mirror area of 616 ft^2.

Table 2-5
SECOND GENERATION CONFIGURATION SELECTION LOADS AND WEIGHT TRADES

	AREA ASPECT RATIO	DRIVE LOADS		DRIVE WEIGHT		SUPPORT STRUCTURE WEIGHT	MAIN BEAM WEIGHT	PEDESTAL WEIGHT	TOTAL WEIGHT	LB/ft^2
		EL	AZ	EL	AZ					
VERTICAL STOW RECTANGULAR MAIN BEAM	616 ▭	320	144	242	315	1262	324	436	5575	9.05
VERTICAL STOW TUBULAR MAIN BEAM	616 ▯	440	129	340	315	1262	430	823	6166	10.01
VERTICAL STOW TUBULAR MAIN BEAM	528 ▯	316	105	242	315	1150	370	432	5077	9.62
INVERTED STOW UPDATED PROTOTYPE	528 ▯▯	320	105	535	315	1150	410	432	5126	9.71

Note: All configurations use laminated glass mirror modules.

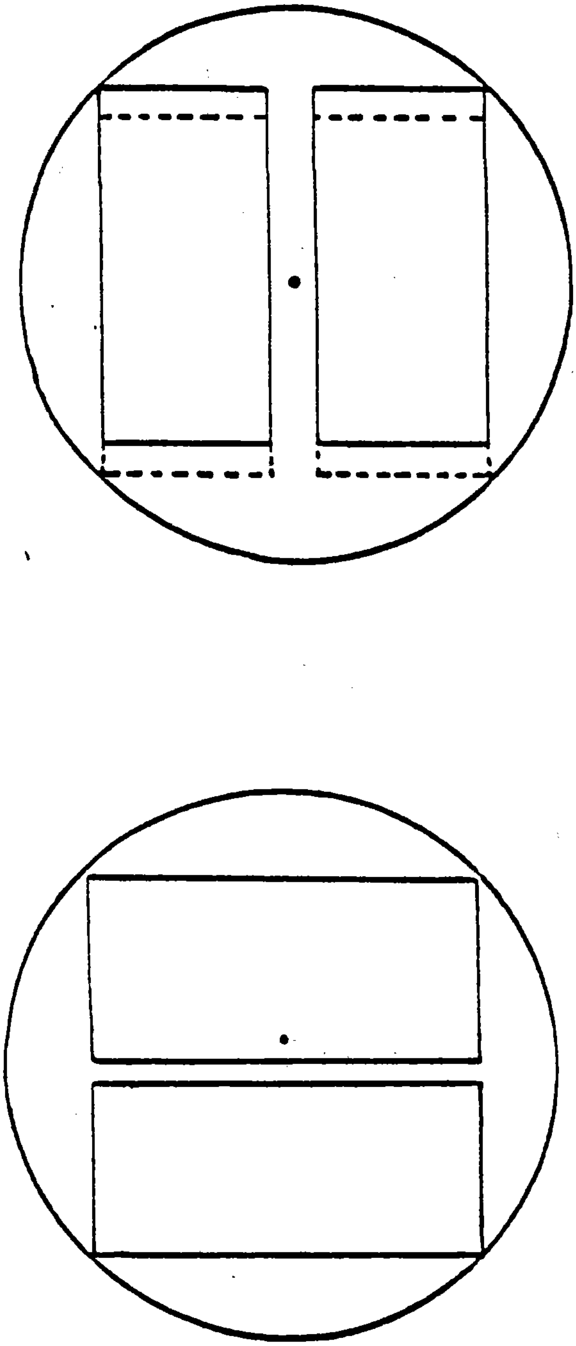

528 FT^2 - INVERTING, CENTROID OVER AZIMUTH AXIS, CLEAROUT CIRCLE RADIUS 222 INCHES

Dashed line indicates inverted position.

616 FT^2 - VERTICAL STOW CENTROID DISPLACED 11 1/2 INCH FROM AZIMUTH AXIS, CLEAROUT CIRCLE RADIUS 225 INCHES

Figure 2-1. Impact of Configuration on Clearout Circle.

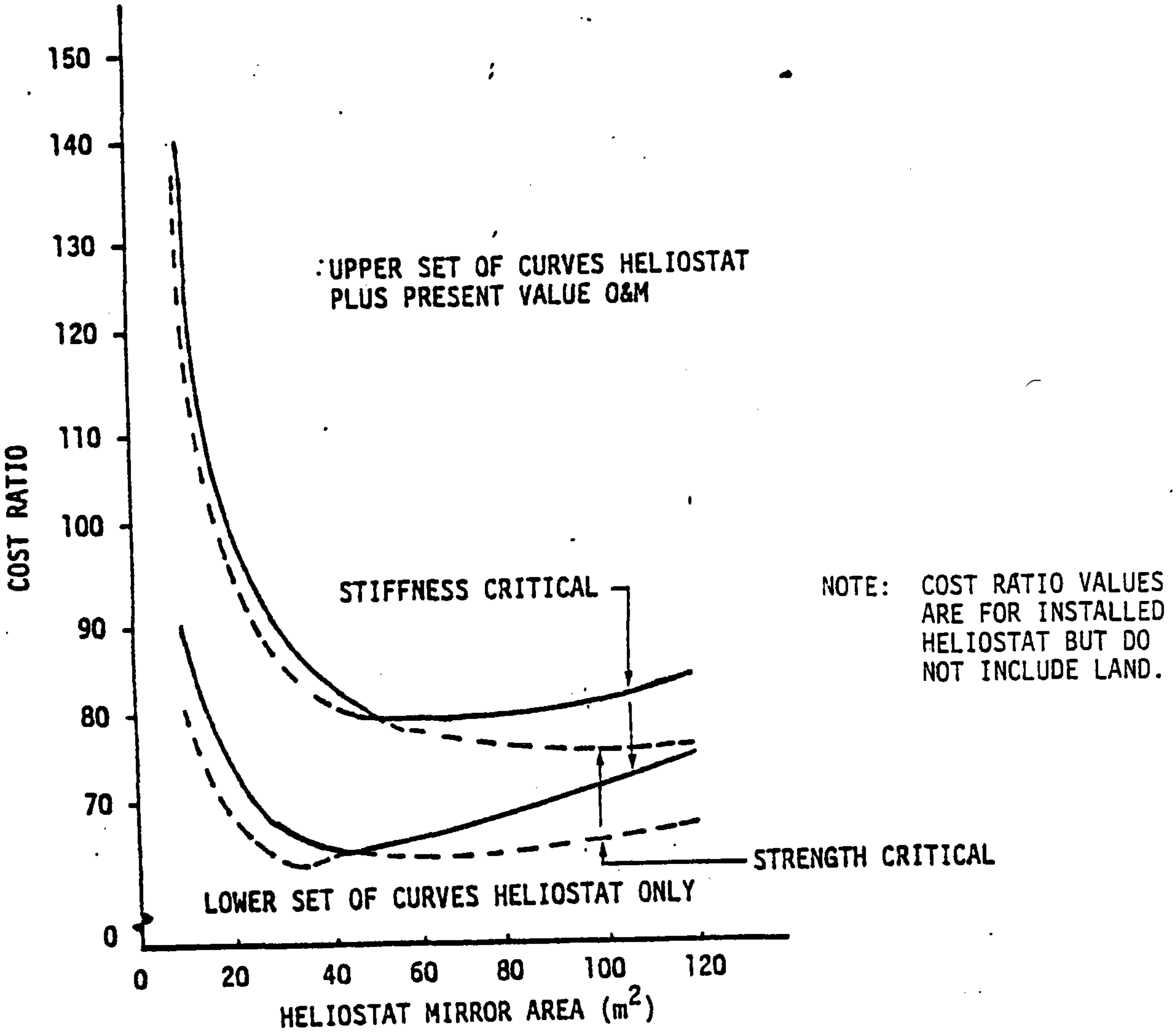

Figure 2-2. Effect of Heliostat Size/Cost (Prototype Study)

The heliostat is mounted on a single pedestal (approximately 20" in diameter) that has a taper and is forced down over a matching taper cone on the foundation for quick installation. The heliostat is noninverting and moves about 96 degrees in the elevation direction. Vertical stowage is the normal stowage mode and the heliostat design accommodates -2 degrees from vertical stowage to ensure reflected beam is on the ground in the near vicinity even for low sun angles.

The elevation drive is actuated by a linear jack system. Azimuth movement is achieved by a harmonic drive system. It provides ± 270 degrees of movement. Both drive systems are environmentally sealed.

Heliostat control is achieved by a three-tier open loop control system. The three-tier configuration provides a Heliostat Array Controller (HAC) which provides overall field control and interface to the rest of the plant, a Heliostat Field Controller (HFC) which provides control of up to 32 heliostats, and the individual Heliostat Controller (HC). The control system is based on the heliostat control system developed by MDAC for the Barstow Pilot Plant heliostat with adaptations for compatibility with the Second Generation heliostat configuration and a simplified reference update scheme which provides additional reduction in control system costs. The HC is housed in a raintight box mounted on the pedestal at eye level providing easy access for maintenance purposes. All heliostat wiring is protected with much of it internal to the pedestal or drive system.

Detailed design descriptions of each of the heliostat subsystems is provided in Section 3 of this report.

Section 3
DESIGN DESCRIPTION

The heliostat hardware is described in this section. The material presents requirements, the hardware and software design used to fulfill these requirements and the analysis and test used to evaluate related performance.

3.1 SYSTEM DESIGN AND CONFIGURATION

The design of the MDAC Second Generation components, described in Section 3.2, is based on and fully supports the system design and configuration described in this section. The design meets the specified performance requirements with heliostat components which can be produced at a high rate with a low unit cost. The cost of field installation and checkout received close attention in the design, with the result that, other than the foundation, only three heliostat components are sent to the field for installation.

Component design requirements were derived from the system analyses performed to define performance compliance and an economic configuration. These analyses are described in the following subsections.

3.1.1 Structure Requirements and Analysis

3.1.1.1 Basic Requirements and Capabilities

The requirements coupled with the capabilities of the resulting heliostat configuration are as follows.

Configuration

Figure 3-1 shows the overall configuration of the MDAC Second Generation heliostat. The heliostat has overall reflective surface dimensions of 340.75 inches in width and 270.5 inches in height and reflective area of 612 ft^2. The height of the pedestal is 141 inches above ground and the frontal area for load calculation purposes is 640 ft^2, including all gaps between mirror surfaces. Table 3-1 shows a comparison of the weight of the Second Generation heliostat

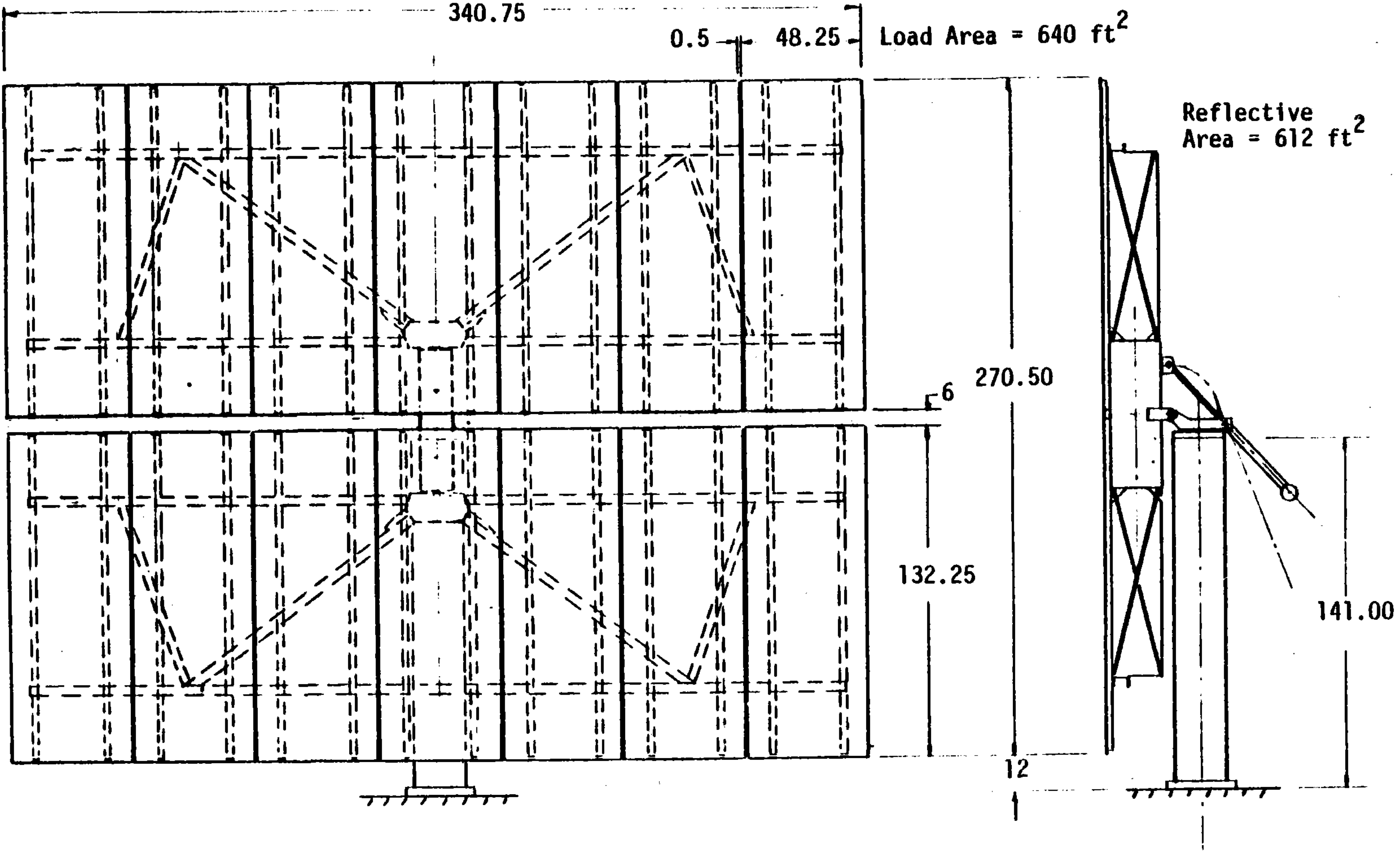

Figure 3-1. Heliostat Configuration

Table 3-1
HELIOSTAT WEIGHT COMPARISONS

	Second Generation Production (612 ft^2)		Modified Prototype Heliostat (528 ft^2)		Barstow** Pilot Plant Heliostat (522 ft^2)		Barstow** Pilot Plant Heliostat (479 ft^2)	
	lb	lb/ft^2	lb	lb/ft^2	lb	lb/ft^2	lb	lb/ft^2
Mirror Modules (include hat sections)	2996*	4.90	2568*	4.86	1533	2.95	1442	3.01
Support Structure (include main beam)	1586	2.59	1412	2.67	1152	2.21	1132	2.36
Drive Units	557	0.91	907	1.72	907	1.74	907	1.89
Pedestal	436	0.71	373	0.71	415	0.80	415	0.86
TOTAL	5575*	9.11	5260*	9.96	4007	7.68	3896	8.13
*With 0.059 inch fusion glass the values are:								
Mirror Modules	2721	4.45	2332	4.42				
TOTAL	5300	8.66	5024	9.52				

Note: All areas are reflective

**MDAC Barstow Pilot Plant design

with other MDAC heliostats. The major weight differences are in the mirror module and the drive unit. The Barstow Pilot Plant mirror module weighed 1.5 lb/ft^2 less than Second Generation while the inverting drive unit assembly weighed 0.84 lb/ft^2 more than the noninverting drive assembly for Second Generation. Also, if the modified prototype did not invert, its total weight could be reduced to approximately 4674 lb or 8.85 lb/ft^2 which is more than the 8.66 lb/ft^2 of Second Generation production. This shows a design improvement since heliostat weight (for two equally designed heliostats) increases at a rate higher than the ratio of the areas.

Requirements and Capabilities

The major design requirements/capabilities for the structural subsystem of the heliostat are given in Table 3-2. This shows the specification requirements, the MDAC drive requirement, the MDAC capability and the verification method. As the table shows, all of the specification requirements are met and compliance will be demonstrated by test or detailed analysis.

3.1.1.2 Design Analysis

Critical Load Conditions

The Collector Subsystems Requirements No. A10772 specifies the environmental design conditions. Performance criteria must be met in any position when subjected to the effects of gravity, temperature, and maximum of 27 mph wind. The heliostat must track with wind speeds to 35 mph at which time stowage action will be initiated. The maximum wind rise rate is 0.02 mph/sec. The heliostat must survive, in a nonoperational state, a 50 mph wind in any position and a 90 mph wind when stowed horizontally. In some instances the heliostat may be starting or driving against a 50 mph wind. For elevation reflector angles greater than 45 degrees the azimuth drive capability may be exceeded in worst case orientation. For those rare worst case conditions heliostat azimuth travel may be delayed until elevation angles less than 45 degrees have been achieved. This may be accomplished by control logic. The loading on the heliostat for these environmental conditions can be obtained from aerodynamic coefficients and the dynamic pressure associated with the condition's wind speed. The following summarizes these conditions:

Table 3-2

STRUCTURAL REQUIREMENTS/CAPABILITY

SPECIFICATION REQUIREMENT	DERIVED REQUIREMENT	MDAC CAPABILITY	VERIFICATION METHOD
3.2.1 PERFORMANCE			
B. Beam Quality - 90% of reflected energy within theoretical +1.4 mrad fringe	Mirror module radius of curvature at 77°F equal to 24,600 in. ±3000 in.	R = 24,600 ± 3000 in.	Measurement
	Mirror module surface waviness <0.5 mrad rms	Waviness 0.4 mrad rms	Measurement
	Mirror module end slope in temperature range 32°F to 122°F		
	Long direction - 0.4 $\leq$ - $\leq$ 5.7 mrad Short direction 0.4 $\leq$ - $\leq$ 2.3 mrad	Long direction - 0.2 $\leq$ - $\leq$ 5.2 mrad Short direction 0.3 $\leq$ - $\leq$ 0.3 mrad	NASTRAN and measurements
	Mirror module alignment within 0.5 mrad rms (including gravity substructure)	Mirror modules aligned within 0.5 mrad rms	Measurement
	Mirror module rms slope error due to gravity $\leq$ 0.5 mrad rms	RMS slope error due to gravity = 0.37 mrad	NASTRAN

Table 3-2

STRUCTURAL REQUIREMENTS/CAPABILITY
(Continued)

SPECIFICATION REQUIREMENT	DERIVED REQUIREMENT	MDAC CAPABILITY	VERIFICATION METHOD
3.2.1 PERFORMANCE			
C. Structural support total rms less than 3.6 mrad under 27 mph wind conditions in each axis.	Mirror module and support structure Elevation (α = 40°) $\leq$ 0.65 mrad Azimuth (α = 90°) $\leq$ 0.7 mrad	Mirror module and support structure Elevation = 0.61 mrad Azimuth = 0.65 mrad	NASTRAN
	Pedestal rotation Elevation (α = 40°) $\leq$ 0.7 mrad Azimuth (α = 90°) $\leq$ 0.40 mrad	Pedestal rotation Elevation = 0.57 mrad Azimuth = 0.40 mrad	Analysis
D. Foundation elastic rotation $\leq$ 1.5 mrad in each axis under 27 mph operating loads	Foundation elastic rotation $\leq$ 1.5 mrad	Foundation rotation = 0.52 mrad	NASTRAN (preliminary results for CRTF)
Foundation plastic rotation $\leq$ 0.45 mrad in each axis	Plastic deformation $\leq$ 0.45 mrad	Plastic rotation = 0.51 mrad	NASTRAN
32.6 WIND LOADING Heliostat must survive 50 mph wind in any orientation or 90 mph wind in storage position	M.S. $\geq$ 0 for all loads Corresponding survival conditions	All M.S. > 0	Analysis

Aerodynamic Load Conditions

	Wind Speed	Dynamic Pressure	Orientation
Performance	27 mph	1.87 psf	Any position
Stowage Initiation	35 mph	3.14 psf	Any position
Wind Rise Rate	.02 mph/sec	3.14-4.96 psf	Any position
Gust Front	50 mph	6.40 psf	Any position
Survival	90 mph	20.74 psf	Stowed horizontally

Aerodynamic Coefficients

The following sources of aerodynamic coefficients have been reviewed in depth to define the applicable coefficients for Second Generation design:

Heliostat Wind Tunnel Data

Colorado State University	Power Law		Aug. 1979
Colorado State University	Uniform		Sept. 1979
Ames Research Center	Uniform	Large Blockage/Corrections	Dec. 1978
Colorado State University	Power Law	Data Too High	July 1978
DAC Long Beach	Uniform	Blockage Uncorrected	May 1976

Flat Plate Data

"Wind Forces on Structures"	ASCE Paper No. 3269
Building Code Requirements for Minimum Design Loads in Buildings	ANSI A58.1-1972
International Critical Tables	
Fluid Dynamic Drag, S. F. Hoerner	
Standard Handbook for Mechanical Engineers, Marks	

As a result of this review, MDAC has taken the conservative approach of using the maximum coefficient from either the 1979 Colorado State University (CSU) Power Law profile data or the ASCE data as modified to account for the heliostat height. This approach revealed that the CSU data was the maximum except for the azimuth moment coefficient CMZ. Plots of the coefficients versus angle of attack were developed and are included as Figures 3-2 through 3-6. A summary of critical coefficients is included as Table 3-3.

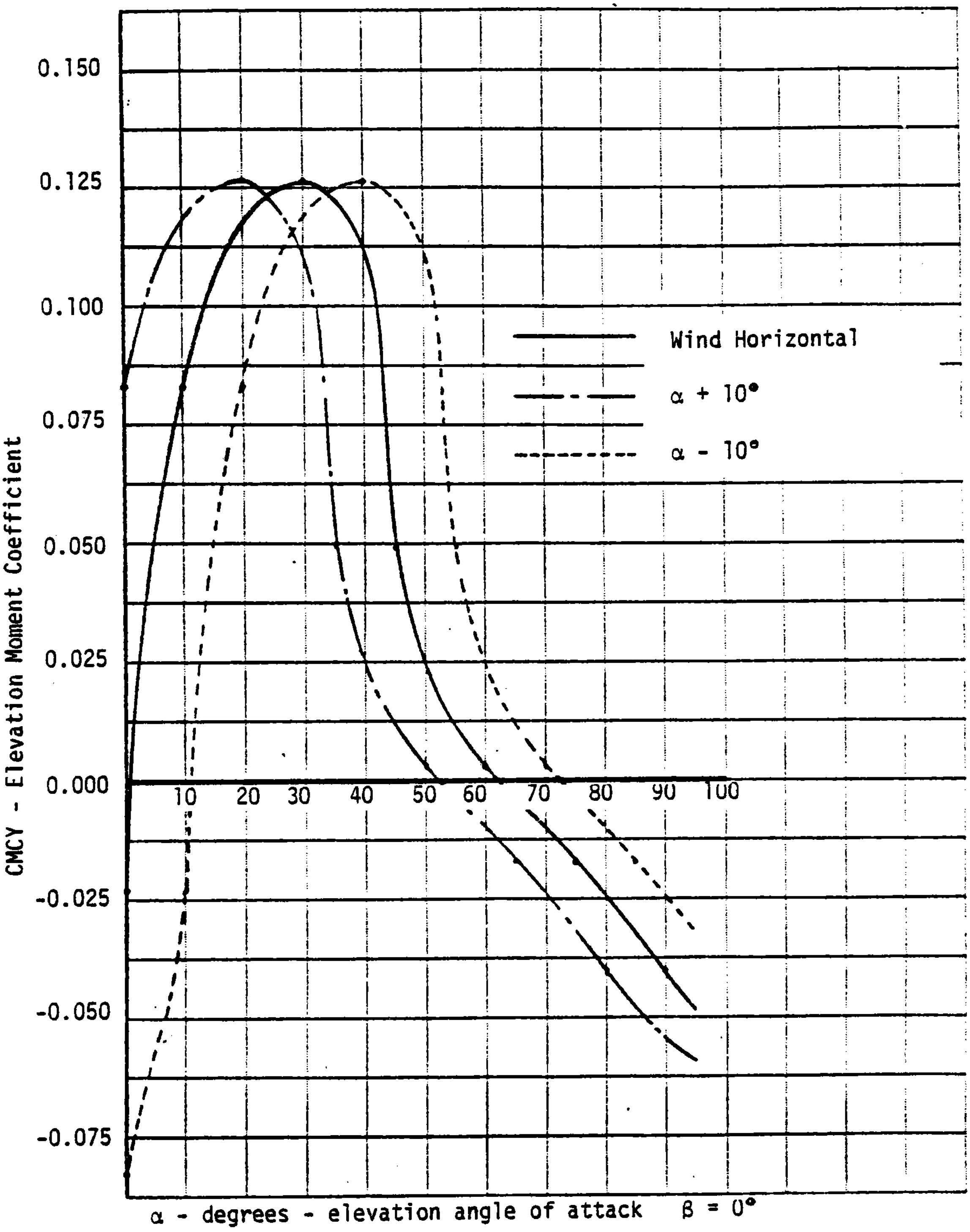

Figure 3-2. Elevation Moment Coefficient vs α for β = 0

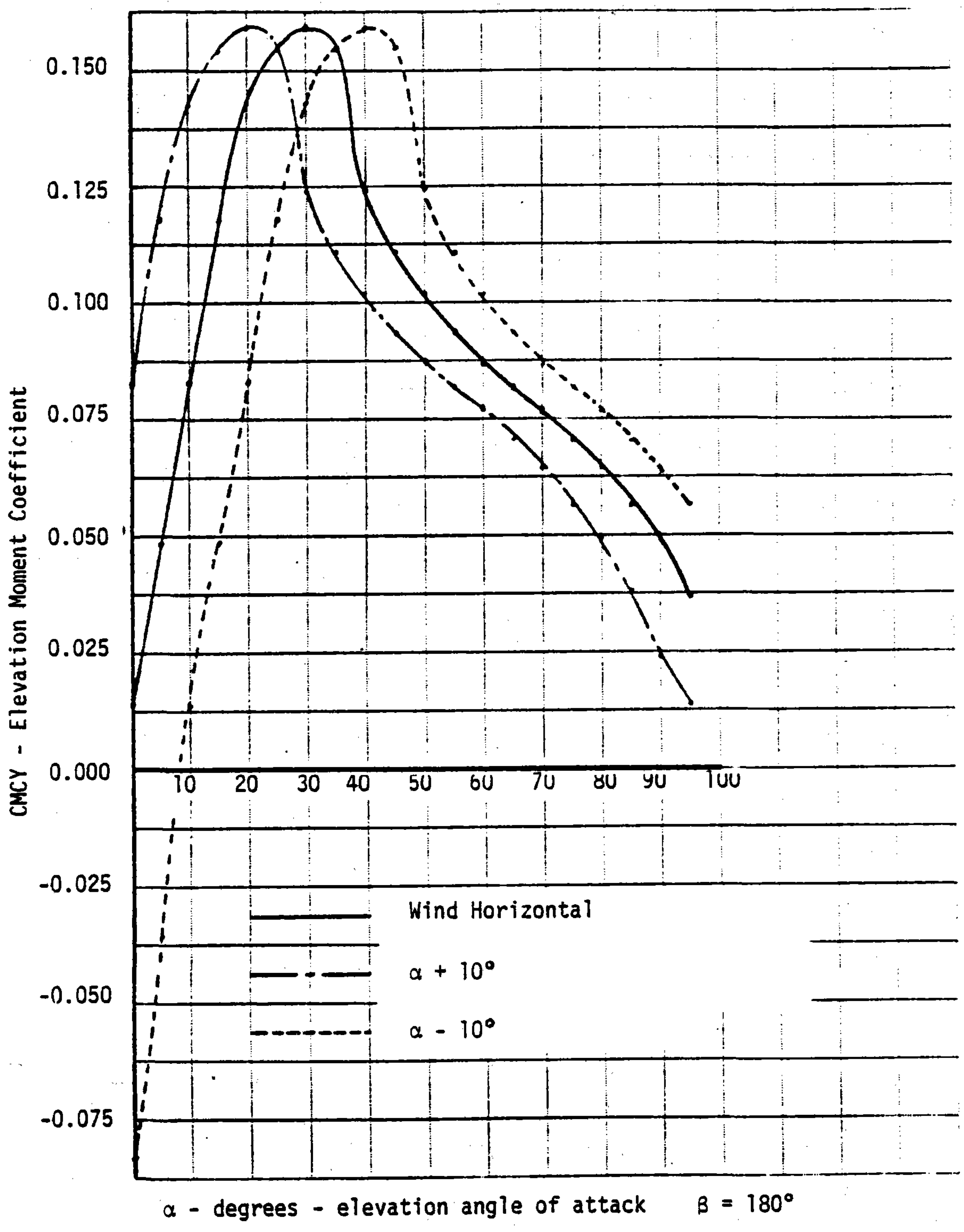

Figure 3-3. Elevation Moment Coefficient vs α for β = 180°

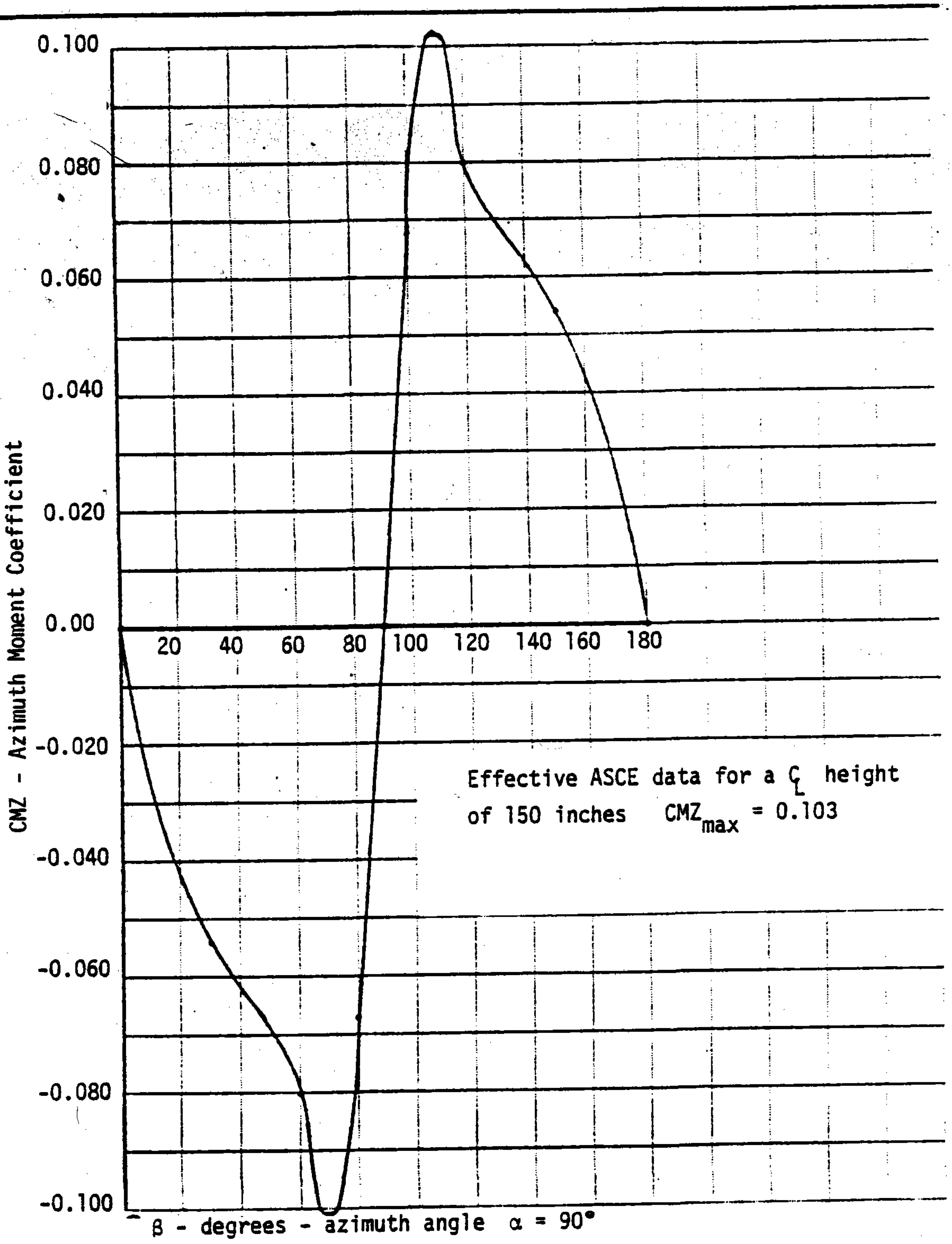

Figure 3-4. Azimuth Moment Coefficient vs β for α = 90°

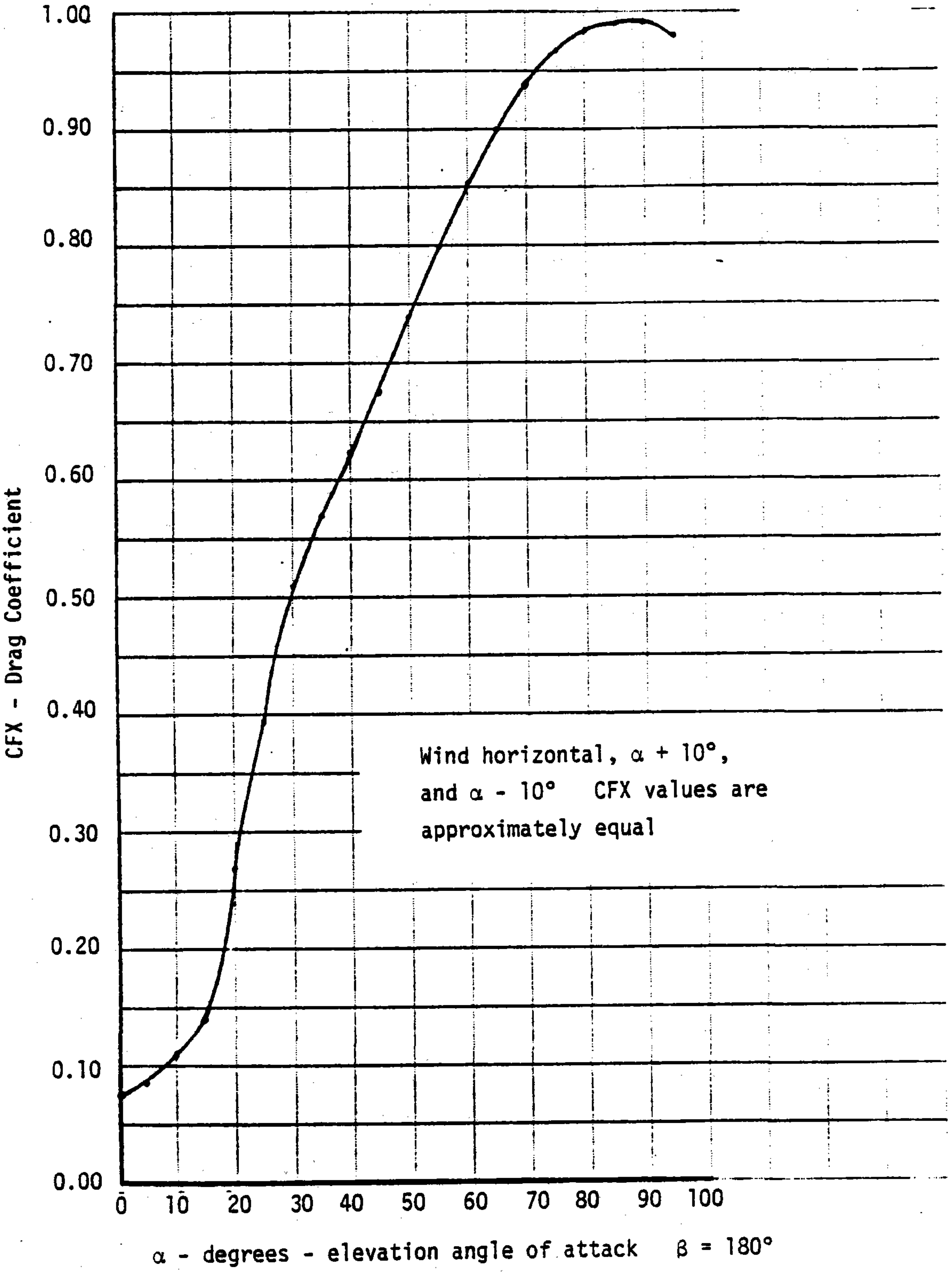

Figure 3-5. Drag Coefficient vs α for β = 180°

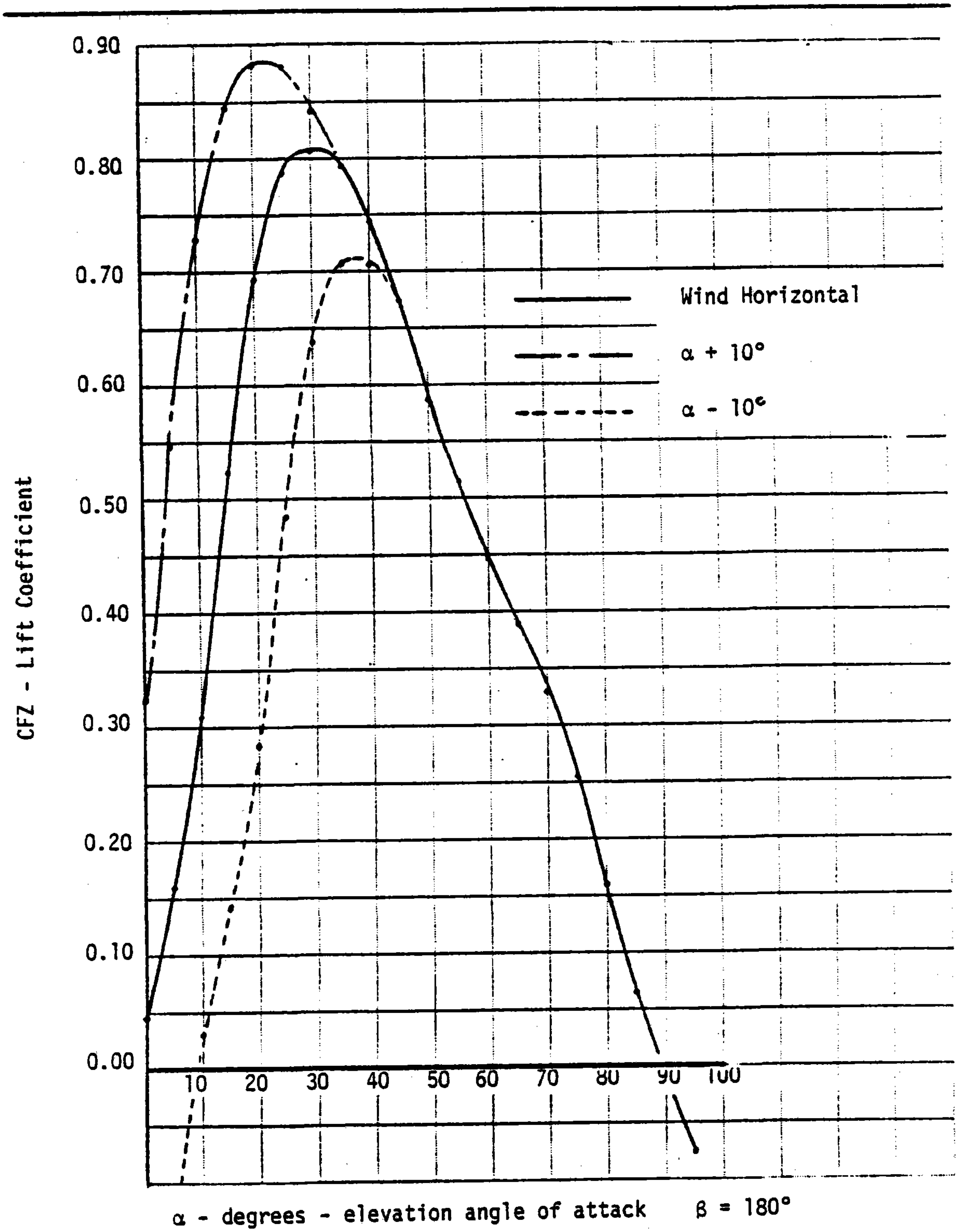

Figure 3-6. Lift Coefficient vs α for β = 180°

Table 3-3

SUMMARY OF CRITICAL AIRLOAD COEFFICIENTS

	MIRROR POSITION	WIND ANGLE OF ATTACK	AZIMUTH ANGLE	AERODYNAMIC COEFFICIENTS					
	ϕ^o	α^o	β^o	CFX	CFY	CFZ	CMCX	CMCY	CMZ
	0	+10	0	-.057	0	-.324	-.023	.083	0
	0	-10	0	-.057	0	.324	-.023	-.083	0
	0	+10	90	0	.057	-.324	.083	.023	0
Maximum Survival Loads	0	-10	90	0	.057	.324	-.083	.023	0
	0	+10	180	.057	0	.324	.023	.083	0
	0	-10	180	.057	0	-.324	.023	-.083	0
	0	+10	270	0	-.057	-.324	-.083	-.023	0
	0	-10	270	0	-.057	.324	.083	.023	0
	20	30	180	.362	.004	.883	-.033	.160	-.011
Maximum Hinge Moment	30	30	180	.510	.004	.807	-.033	.160	-.011
	40	30	180	.642	.004	.706	-.033	.160	-.011
Maximum Pedestal & Found.Load	90	80	180	.998	.011	-.013	-.012	.065	.012
Maximum Azimuth Moment	90	90	70,110,250, 290	.62	.22	0	0	0	.103

The coefficients and dynamic pressures were used in conjunction with the heliostat geometry to determine the design loads on the drive system and heliostat structure. The critical design loads are as follows:

Drive System

		Elevation Jack Load (lbs)	Azimuth Drive Moment (in-lbs)
Maximum Performance	27 mph	9,800	41,900
Maximum Starting	35 mph	10,800	80,900
Maximum Operating	35 + mph	10,800	80,900
Maximum Static*	50 mph	13,900	144,000
Maximum Survival, Stowed	90 mph	±27,300	99,500
Maximum Overturning	90 mph	N/A	401,000

*Same load value for 50 mph gust front

Structure

Maximum Elevation Moment on Support Structure	298,000 in-lb
Maximum Overturning Moment on Support Structure	375,000 in-lb
Maximum Moment at Pedestal/Foundation Interface	635,000 in-lb
Maximum Moment at Ground	840,000 in-lb

In addition, the aerodynamic data was used to develop the loading for a NASTRAN model of the heliostat. Pressure distributions from an early wind tunnel test and the current overall coefficients were used to determine a C_p value for each NASTRAN CQUAD4 element used to model the mirror. Figure 3-7 shows the NASTRAN CQUAD4 elements and their numbering system. The C_p values along length and width are shown in Figures 3-8 and 3-9. The C_p value for a given element is obtained by multiplying the two values corresponding to its length and width position. The C_p value is for a unit dynamic pressure so that when multiplied by a dynamic pressure for a particular wind speed, the pressure on an element is obtained.

NASTRAN Models

The Second Generation heliostat has been modeled to perform a NASTRAN analysis. The results of the NASTRAN analysis provide stresses and margins of safety for various elements, forces in the elements which are used in buckling analysis, and deflections which are used to evaluate conformance with the performance requirements. Two models have been used. One model is

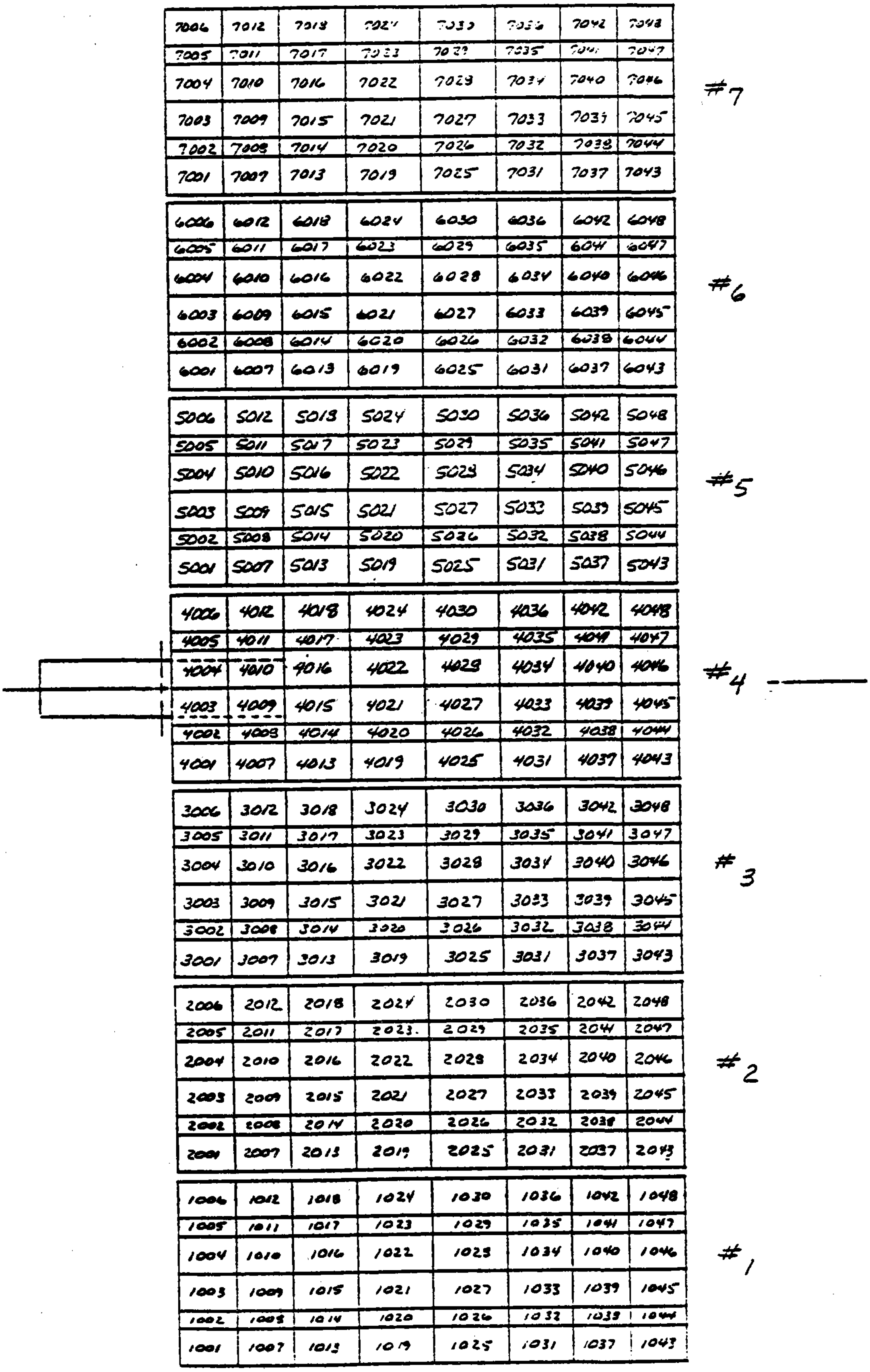

7006	7012	7018	7024	7030	7036	7042	7048	
7005	7011	7017	7023	7029	7035	7041	7047	
7004	7010	7016	7022	7028	7034	7040	7046	#7
7003	7009	7015	7021	7027	7033	7039	7045	
7002	7008	7014	7020	7026	7032	7038	7044	
7001	7007	7013	7019	7025	7031	7037	7043	
6006	6012	6018	6024	6030	6036	6042	6048	
6005	6011	6017	6023	6029	6035	6041	6047	
6004	6010	6016	6022	6028	6034	6040	6046	#6
6003	6009	6015	6021	6027	6033	6039	6045	
6002	6008	6014	6020	6026	6032	6038	6044	
6001	6007	6013	6019	6025	6031	6037	6043	
5006	5012	5018	5024	5030	5036	5042	5048	
5005	5011	5017	5023	5029	5035	5041	5047	
5004	5010	5016	5022	5028	5034	5040	5046	#5
5003	5009	5015	5021	5027	5033	5039	5045	
5002	5008	5014	5020	5026	5032	5038	5044	
5001	5007	5013	5019	5025	5031	5037	5043	
4006	4012	4018	4024	4030	4036	4042	4048	
4005	4011	4017	4023	4029	4035	4041	4047	
4004	4010	4016	4022	4028	4034	4040	4046	#4
4003	4009	4015	4021	4027	4033	4039	4045	
4002	4008	4014	4020	4026	4032	4038	4044	
4001	4007	4013	4019	4025	4031	4037	4043	
3006	3012	3018	3024	3030	3036	3042	3048	
3005	3011	3017	3023	3029	3035	3041	3047	
3004	3010	3016	3022	3028	3034	3040	3046	#3
3003	3009	3015	3021	3027	3033	3039	3045	
3002	3008	3014	3020	3026	3032	3038	3044	
3001	3007	3013	3019	3025	3031	3037	3043	
2006	2012	2018	2024	2030	2036	2042	2048	
2005	2011	2017	2023.	2029	2035	2041	2047	
2004	2010	2016	2022	2028	2034	2040	2046	#2
2003	2009	2015	2021	2027	2033	2039	2045	
2002	2008	2014	2020	2026	2032	2038	2044	
2001	2007	2013	2019	2025	2031	2037	2043	
1006	1012	1018	1024	1030	1036	1042	1048	
1005	1011	1017	1023	1029	1035	1041	1047	
1004	1010	1016	1022	1028	1034	1040	1046	#1
1003	1009	1015	1021	1027	1033	1039	1045	
1002	1008	1014	1020	1026	1032	1038	1044	
1001	1007	1013	1019	1025	1031	1037	1043	

Figure 3-7. NASTRAN CQUAD Element Numbers

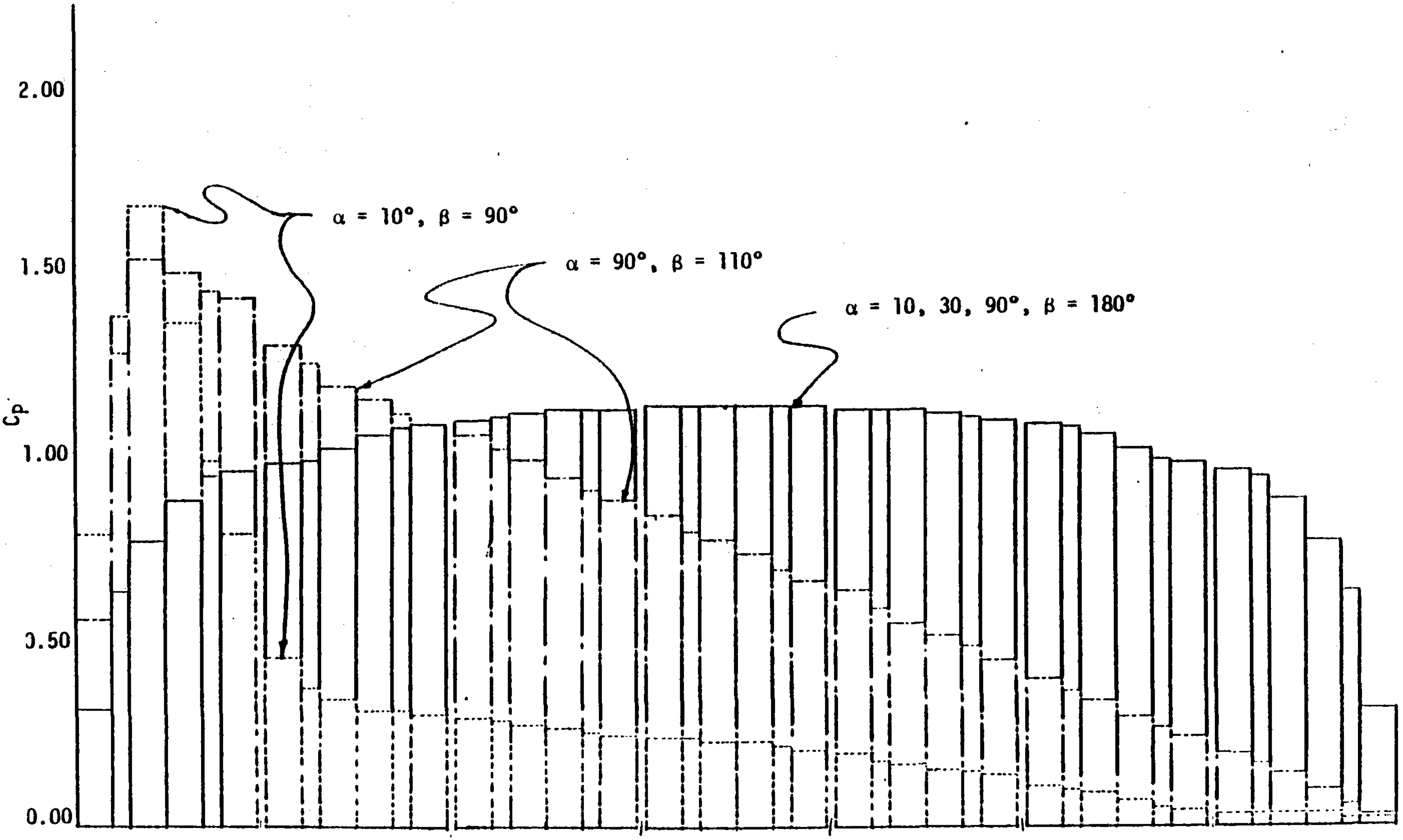

Figure 3-8. Pressure Coefficient Along Length

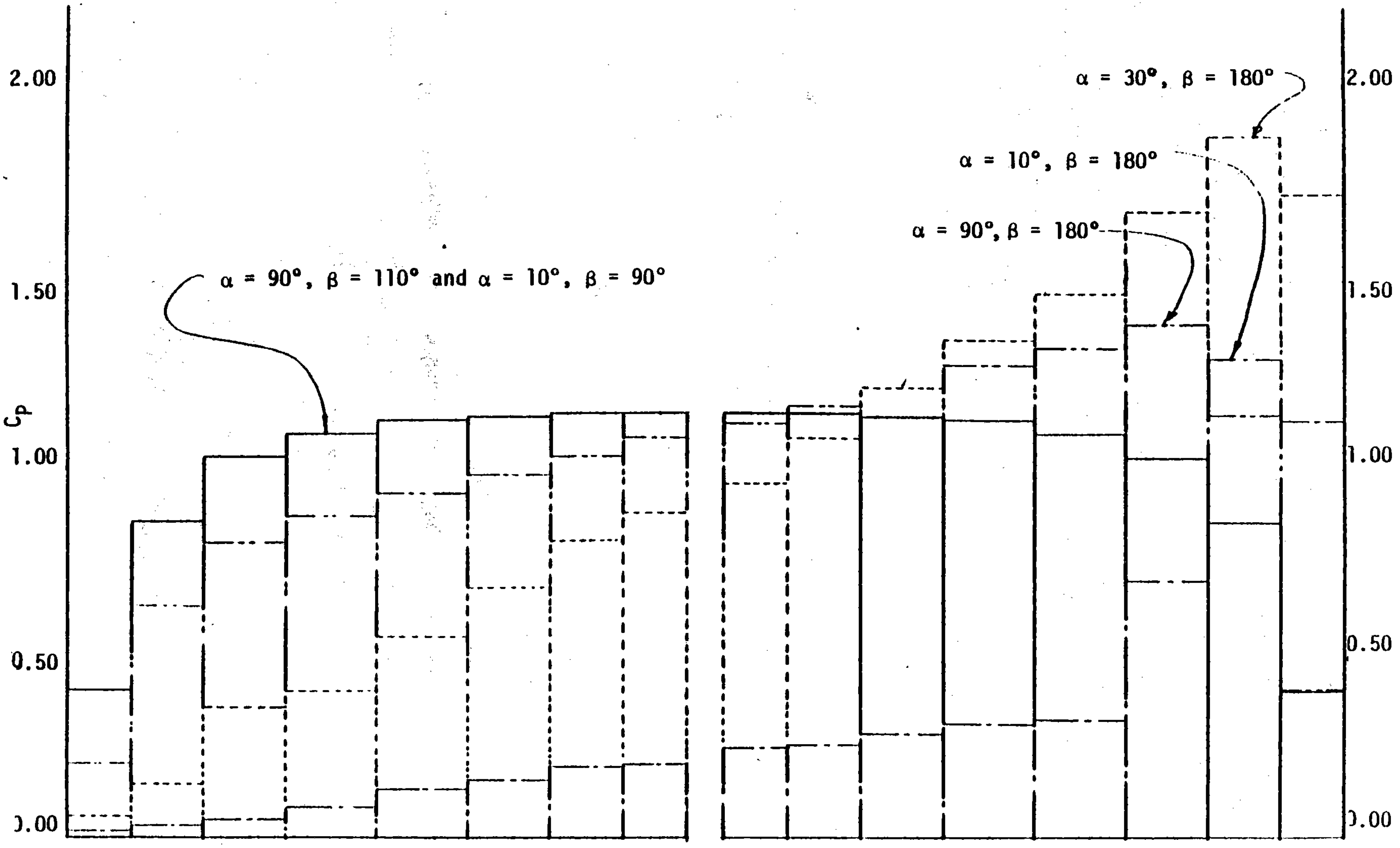

Figure 3-9. Pressure Coefficient Along Width

single mirror module. It is used primarily to evaluate gravity and temperature effects on the beam quality aspect of performance. The other represents half of the heliostat including seven mirror modules, a reflector support structure, and the main beam. Each mirror module uses 48 CQUAD4 elements to represent the laminated mirror, 8 CBAR elements to represent each of the two stringers, and CELAS 1 elements to represent the bond between the hat and the stringers with elastic properties in the x, y, z, θ_x, θ_y directions. The support structure uses CBEAM elements to model the inboard and outboard cross-beams and the diagonal beam. CBAR elements are used to model the cross bracing. The main beam is modeled with CQUAD4 and CTR1A2 plate elements. See Figures 3-10 and 3-11.

Analysis Results

NASTRAN displacement data of the mirror module grid points were analyzed to determine RMS and average rotations. These were combined with predicted rotations of the drive unit and pedestal to obtain a total RMS rotation value. The predicted rotations are compared to the budget assigned to each component in Table 3-4.

Margins of safety are summarized in Table 3-5. MDAC determines its margins of safety as follows:

$$\text{Margin of Safety} = MS = \frac{F_A}{F} - 1.0$$

Where: F_A = $K(1+1/3)\ F_Y$ = The allowable working stress

F_Y = The yield stress of the material

$(1+1/3)$ = The increase in allowable permitted for wind loads by the AISC Specification, Section 1.5.6.

K = The reduction factor as specified by the AISC Specification, Section 1.5.

F = Applied stress for the critical design condition.

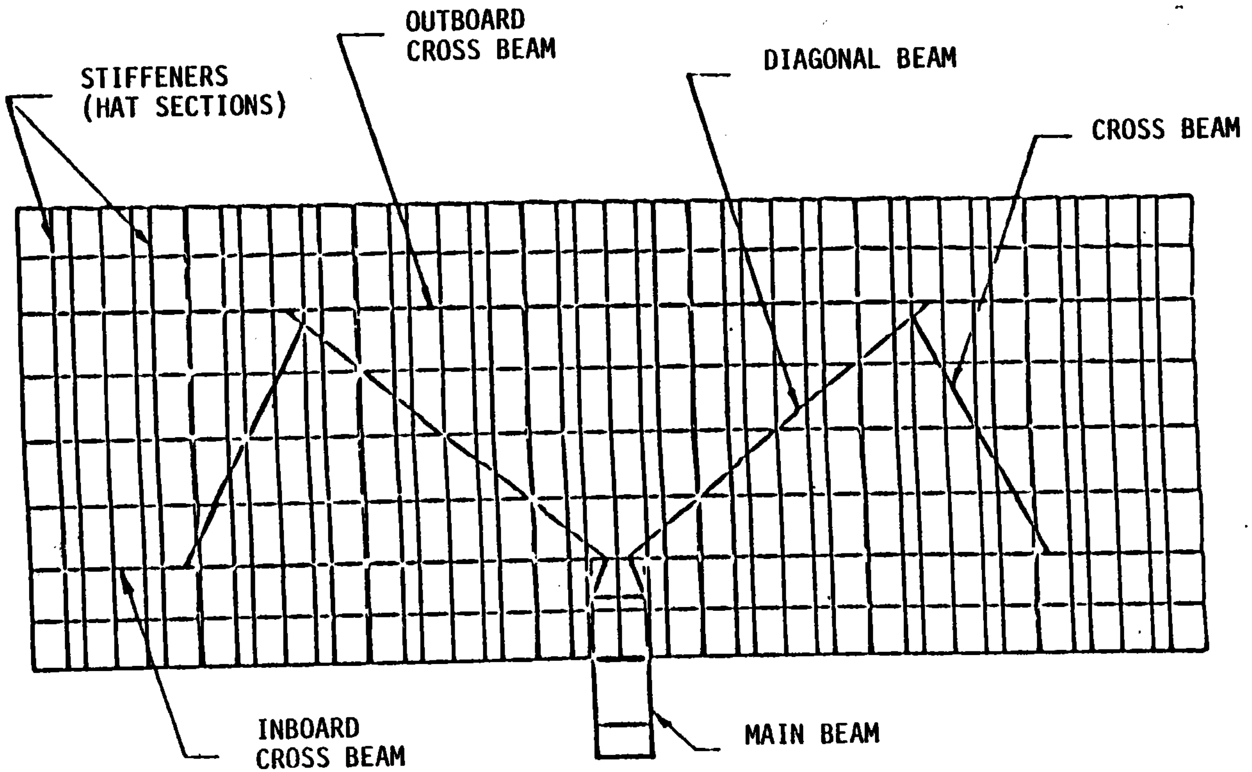

Figure 3-10. NASTRAN Model, Plan View - Second Generation Heliostat Reflector Panel and Support Structure

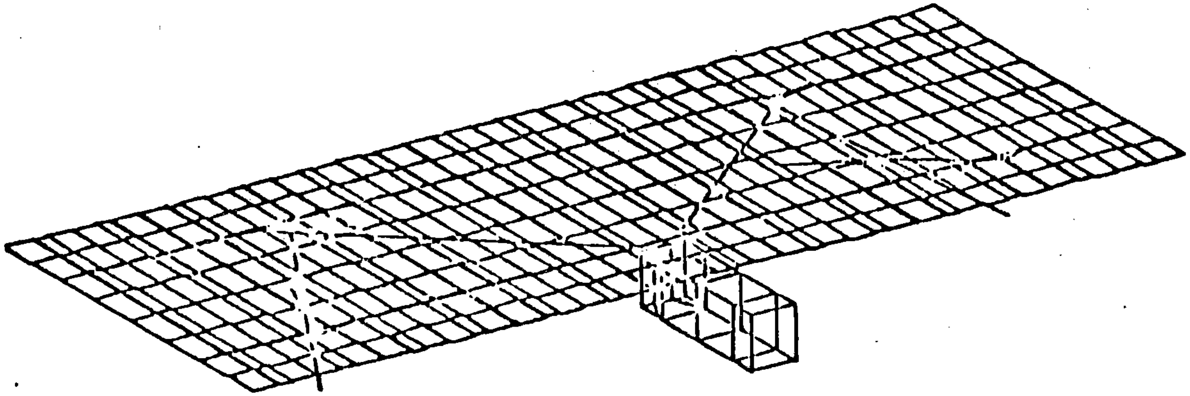

Figure 3-11. NASTRAN Model - Second Generation Heliostat Reflector Panel and Support Structure

Table 3-4

SPECIFICATION PERFORMANCE STRUCTURAL ROTATIONS ~ MRAD

	ELEVATION AXIS						AZIMUTH AXIS	
	$\varphi = 0$		$\varphi = 40$		$\varphi = 90$		$\varphi = 90$	
	PREDICTED	BUDGET	PREDICTED	BUDGET	PREDICTED	BUDGET	PREDICTED	BUDGET
STRUCTURE	.22	.40	.61	.65	.11	.40	.64	.70
RMS	.35	-	.64	-	.35	-	.66	-
AV	.20	-	.61	-	.08	-	.64	-
DRIVE UNIT	1.79	2.50	1.25	1.85	1.60	2.00	1.80	2.40
PEDESTAL	.20	.30	.57	.70	.57	.80	.41	.40
MARGIN	0	.40	0	.40	0	.40	0	.20
TOTAL	2.21	3.60	2.44	3.60	2.28	3.60	2.85	3.60

$$\theta_T = \sqrt{\left(\theta_{DR} + \theta_{PED}\right)^2 + 2\left(\theta_{DR} + \theta_{PED}\right)\left(\theta_{STR_{AV}}\right) + \left(\theta_{STR_{RMS}}\right)^2}$$

Table 3-5

SUMMARY OF MARGINS OF SAFETY

1D22459-1	Heliostat Assembly				+ .03
1D11469-1	Foundation			TBD	
	Foundation Cap		TBD		
	Steel Rebar		TBD		
	Concrete		TBD		
1D22456-1	Reflector Assembly			+ .12	
1D11471-1	Mirror Attach Kit		+ .18		
1D11462-1	Mirror Module		+ .12		
1D22428-1	Laminated Mirror	+ .16*			
1D22462-9	Stiffener	+ 4.51			
1D22462-15	Miscellaneous Details	+ .12			
1D22463-1	Reflector Support Structure Assembly		+ .03		
1D22465-1	Inboard Crossbeam	+ .03			
1D22466-1 & -2	Diagonal Beam	+ .32			
1D22467-1	Outboard Crossbeam	+ .10			
1D22470-1	Braces	+ 3.58			
1D22463-3 & -5	Miscellaneous Details	+ .14			
1D22475-1	Drive Unit/Pedestal/ Main Beam				+ .05
1D22405-1, -501, -503	Hinge			OK	
1D22424-2, -501	Switch			N/A	
1D22416-1	Cover			OK	
1D22417-1	Mount			OK	
1D22418-1	Bracket			OK	
1D22429-1	Bracket			OK	
1D22432-1	Pin, Trunnion			+ 9.62	
1D22433-1	Mount			OK	
1D22438-1	Cap			OK	
1D22439-1	Support Assembly, Elevation Drive			+ .11	

*Margin on 1000 psi stress allowable

Table 3-5 (Continued)

SUMMARY OF MARGINS OF SAFETY

1D22475-1 (Cont'd)					
1D22445-1	Pedestal Electrical Assembly			N/A	
1D22455-1	Pin, Hinge			+ 1.62	
1D22461-1	Pedestal			+ .48	
1D22464-1	Main Beam			+ .14	
1D22478-1	Pin, Rod End			+ .26	
1D22513-1	Controller			N/A	
1D22594-1	Cover			OK	
1D22496-1	Actuator			N/A	OK
1D22497-1	Jack		N/A		
1D22487-1	Motor	N/A			
1D22415 503	Bearing	N/A			
1D22575-1	Incremental Encoder Inst.		N/A		
	Miscellaneous Details				
1D22494-1	Drive Assembly, Azimuth				+.05
1D22411-501	Bracket			OK	
1D22414-1	Switch			N/A	
1D22420-1	Clip			OK	
1D22421-1	Block			OK	
1D22422-1	Block			OK	
1D22424-1	Support			+ 19.00	
1D22429-1	Cover			OK	
1D22442-1	Lub Pan			+ .57	
1D22443-1	Shim			High	
1D22449-1	Spacer			OK	
1D22474-1	Support			+ .26	
1D22481-1	Bushing			OK	
1D22482-1	Retainer			+ .38	
1D22485-1	Shim			OK	
1D22486-1	Gear			N/A	
1D22489-1	Retainer			+ 4.78	
1D22490-1	Bearing Kit			N/A	
1D22495-1	Shaft, Drive			+ .05	

Table 3-5 (Continued)

SUMMARY OF MARGINS OF SAFETY

1D22499-1	Harmonic Drive Kit	N/A
1D224514-1	Wire Harness	N/A
1D22575-1	Motor	N/A
1D22593-1	Tube Assembly	OK
1D22596-1	Electrical Installation	N/A

N/A = Not Analyzed - Electrical or Purchased Part

OK = Not Analyzed - Unloaded or Negligible and Indeterminate Loads

All structural and mechanical drawings are listed for completeness as well as electrical top drawings which are a part of the major assemblies. Where an N/A is noted, the part was not analyzed because it is an electrical or a purchased part. Where an OK is noted, the part was not analyzed because the part was either not loaded or was lightly loaded in an indeterminant manner.

3.1.2 Drive Configuration and Performance Assessment

The drive requirements are presented together with a performance assessment for the given configuration.

3.1.2.1 Configuration

As shown by Figure 1-1, the electromechanical drives are configured with a linear actuator in elevation and a rotational gear drive in azimuth. A ball-screw jack coupled with helicon input gearing and driven by 1/3 HP, 208 VAC motor comprise the elevation drive. Rotational output motion is accomplished kinematically with a simple lever arm. Variable lever arm effective length results in an overall gear reduction ranging from 20950:1 with the reflector in a face-up horizontal attitude to 48760:1 in the vertical attitude.

The azimuth drive combines the same type of helicon gearing (different size and reduction ratio) with a harmonic reducer resulting in a total gear ratio of 43090:1. The torque loads are smaller in azimuth so a 1/4 HP motor is used for the input drive. The turret type bearing which supports the rotational portion of the heliostat is also an integral part of the azimuth drive.

3.1.2.2 Requirements and Capabilities

The drives requirements and capabilities are summarized in Table 3-6. Maximum motor speeds are 1750 rpm which provides the required 180 degrees of azimuth travel in less than 12.5 minutes, and the 90 degree elevation travel is in approximately 6 minutes. The azimuth drive is capable of ± 270 degrees total rotation, thus, making the heliostat independent of site location within a field. Control system logic provides azimuth rotational limits rather than physical hardware. Hard limits are not necessary in azimuth since multiple full rotations in either direction can be tolerated. In elevation the jack has

Table 3-6

DRIVE REQUIREMENTS CAPABILITY

Parameter	Origin	Azimuth		Elevation	
		Requirement	Capability	Requirement	Capability
Travel					
Rate	Specification Paragraph 3.2.2.b	180° in 15 min.	180° in 12.5 min.	90° in 15 min.	∿ 90° in 6 min.
Rotation	Derived	± 180°	± 270°	90°	98°
Survival load at 90 mph wind					
Stowed face up	Derived	99,500 in-lbs	> 178,000 in-lbs	27,300 lbs	28,000 lbs
Overturning moment	Derived	401,000 in-lbs	No visible Brinelling at 401,000 in-lbs	-----	-----
Static load at any orientation and 50 mph wind	Derived	144,000 in-lbs	> 178,000 in-lbs	13,900 lbs	18,600 lbs
Maximum operating load during stowage with >35 mph wind	Derived	80,900 in-lbs**	> 80,900 in-lbs	10,816 lbs 13,800 lbs*	> 13,900 lbs
Radial deflection at 27 mph wind (no gravity)	Derived	2.4 mrad at 41900 in-lbs	1.90 mrad (estimated)	1.85 mrad at 52,900 in-lbs and α = 40°	1.25 mrad (estimated)

*50 mph gust front produces worst case loads equivalent to 50 mph static. Load dependent on azimuth and elevation angle of attack.

**Azimuth operating load at 50 mph may be limited by initiating azimuth travel when heliostat elevation attitude is less than 45 degrees.

hard stops and so physical limit switches are used to prevent bottoming which could cause component damage. A total stroke of 98 degrees is provided with 5 degrees overtravel from the vertical position and 3 degrees from the horizontal position.

As the table indicates, the drive hardware in all cases has the capability to meet and in some cases to exceed requirements.

3.1.2.3 Performance Assessment

This section is concerned with the assessment of the actual hardware design with respect to required performance.

Azimuth Operational Torque

The critical operational torque is at start-up conditions. Using the maximum operational wind load of 80,900 in-lbs, a minimum estimated efficiency of 9 to 10 percent (turret bearing, harmonic drive, helicon gearing) and an overall reduction of 43,090 in-lbs, the required calculated motor torque is 20 in-lbs. Initial 1/4 HP motor data indicate an available start-up torque of 37.5 in-lbs. under ambient conditions. This results in a substantial margin especially since minimum efficiencies were used in the required torque estimate. Subsequent loaded drive testing will determine actual margins under ambient as well as low voltage and cold conditions.

Elevation Operational Torque

In elevation the maximum operational jack load of 13,900 lbs results from a combination of wind and gravity. This load combined with a minimum efficiency estimate of 10 to 11 percent (ball screw, jack bearings, helicon gearing) and a reduction ratio of 2664 (jack only) results in a required motor torque of 20 in-lbs. The 1/3 HP motor has a start-up torque of 42 in-lbs at ambient temperature and thus provides sufficient margins for cold ambients and low voltage conditions.

Azimuth Radial Deflections

The allowable deflection under a 27 mph wind (41,900 in-lbs load) budgeted for the azimuth drive is 2.4 mrad. Test data from an existing drive was used to estimate Second Generation deflections. This data indicated a deflection of 1.9 mrad for the above load. Later testing on the Second Generation drive hardware will be used to determine actual deflections.

Elevation Radial Deflections

In elevation the deflection for a 27 mph wind load of 52,900 in-lbs was calculated to be 1.25 mrad at an elevation angle of 40 degrees. The drive budget is 1.85 mrad. The calculated deflection which includes backlash plus compliance was based upon a sum of maximum hardware dimensions and so the estimate should be pessimistic. Components included in the calculation are the jack, trunnion joint, rod end joint, hinge joint and wire race turret bearing. Hardware testing will be used to determine actual deflections at 0 degrees and 90 degrees as well as at 40 degrees. As noted in the next paragraph, the kinematics were designed to provide a near maximum torque arm length (18 inches) at 40 degrees in order to minimize associated deflections.

Jack Stroke

The kinematic relationships between jack stroke and torque arm length versus elevation angle are shown in Figure 3-12. As indicated, the jack stroke for the basic 90 degrees of travel is 25.9 inches. The 8 degree overtravel allocation requires an additional 1.6 inches, thus resulting in a total stroke of 27.5 inches. The overtravel is based on the following factors:

- Pedestal tilt (1 degree at each end of travel) = 2.0°
- Beam safety at vertical position = 1.5°
- Limit sensor adjustment range (0.4° at each end of travel) = 0.8°
- Motor coast (0.5° at each end of travel) = 1.0°
- Total tolerance allowance = 2.7°
- Total Overtravel = 8.0°

Self Lubricated Bearings

The self lubricated bearings used throughout the elevation drive have been selected so that the imposed loads are well within the recommended capability

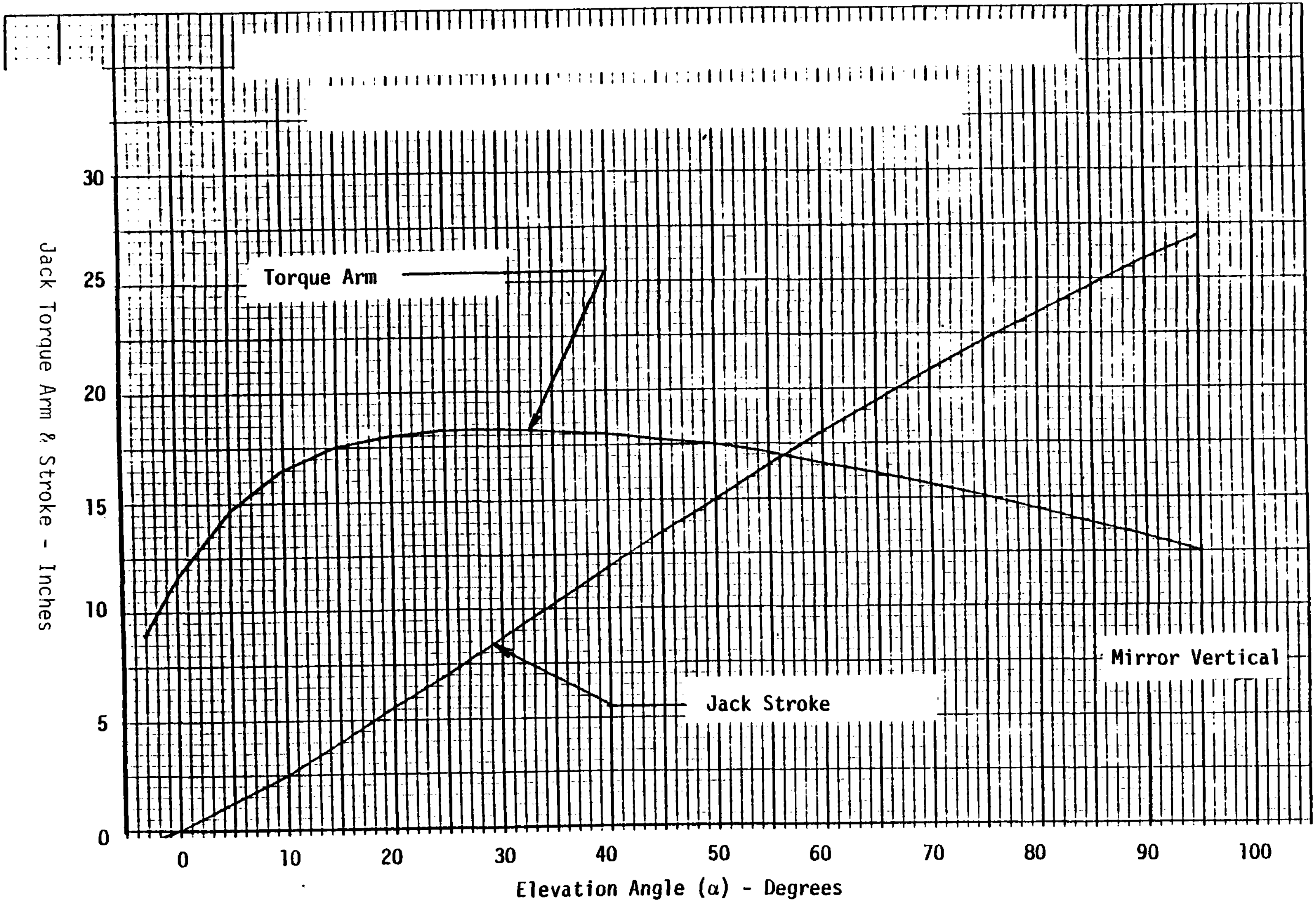

Figure 3-12. Second Generation Heliostat Elevation Drive Kinematics

of the bearing. The interfacing pins have smooth corrosion resistant finishes and are sealed at both ends to prevent entry of contaminants, thus maximizing life expectancy. The bearings can be machined or sized after installation, thus providing the capability for low tolerance assemblies. Also interference fits up to 0.002 inch can be utilized to eliminate unloaded clearances if assembly problems are not encountered. The trunnion pins and bearings are dimensioned in this manner since the threaded pins provide excellent alignment and assembly conditions.

The following comparisons between the applied loads and bearing capabilities show that ample margins have been designed into the hardware thus providing an additional factor for extending life expectancy.

	Maximum Static (psi)	Maximum Dynamic (psi)	Best Operation (psi)
Sleeve Bearing Capability	50,000	20,000	< 5,000
Imposed Loads	12,000-20,000	5,000-7,000	2,500-3,500

The spherical self lubricating bearing at one of the elevation hinge joints has ample margins also as indicated by the following data:

	Static Radial (lbs)	Axial (lbs)	Staking (lbs)
Bearing Capability	104,000	19,300	3,600 (Proof)
Imposed Loads	28,700	1,700	1,700

3.1.3 Controls Configuration and Requirements

The amount of energy incident upon the receiver is directly related to the pointing accuracy of the reflected beam from the heliostat to the receiver. This section will describe how the collector control system will achieve the required beam pointing accuracy and how it will implement all other control system functional requirements.

Heliostat reflective beam pointing is achieved using open-loop command algorithms. A set of ephemeris equations is used to calculate the azimuth and elevation position of the sun for a given time of day. Knowing the relative position of the receiver and heliostat, the required heliostat gimbal angles can be calculated to reflect the beam to the aimpoint. The gimbal angles are modified to account for atmospheric refraction, gravitational structure bending, non-orthogonality error, tilt errors, etc. The transfer function of the azimuth and elevation drive system are used to transform the modified gimbal angles into motor turns. The motors are turned on until an incremental encoder mounted on the motor shaft indicates that the desired number of motor turns have been achieved. Sensors mounted on the outer gimbals and helicon gear are used to determine the reference position.

3.1.3.1 Control Subsystem Functional Description

The key electronic components that are used in controlling the heliostats in the collector field are:

- o Heliostat Array Controller (HAC) - Serves as an interface between operator and control system, obtains data for displays to the operator, executes operate commands, maintains status of heliostat field.
- o Heliostat Field Controller (HFC) - Calculates the desired heliostat position, transmits commands to heliostat controller, maintains status of heliostats under its control.
- o Heliostat Controller (HC) - Calculates a motor signal which will be used to turn motor on/off in order to maintain the HFC command position. Reads external sensors such as the incremental encoders and reference sensors.

- Motor Control Board - Applies the proper voltage to the motor upon receiving a signal from the HC such that the heliostat will turn in the correct direction.

- Motor - Moves the heliostat to a new physical location.

- Incremental Encoder - Furnishes a pulse to the HC each time the motor makes one complete revolution.

- Reference Sensors - Furnishes a pulse to the HC each time the helicon gear or the heliostat makes one complete revolution or travels to end points in elevation.

The functions of these components and the information flow between them is summarized in Figure 3-13.

The location and wire connections for the control hardware located on the heliostat are shown in Figure 3-14. At the front of the heliostat is a circuit breaker junction box which contains a circuit breaker, plug connectors, and terminators for the incoming power and communication wires. Power to a heliostat can be controlled by activating the switch on the circuit breaker. There is a motor mounted on the jack and one on the azimuth drive. Each of these drive motors has an incremental encoder mounted on it.

3.1.3.2 Requirements and Capabilities

The requirements for the control system are defined in the Second Generation Heliostat Specification.

Top level requirements and capabilities for a 50 MWe plant and CRTF are shown in Table 3-7. Since only two heliostats are going to be tested at CRTF, the capability for CRTF in some cases will be somewhat different than that for a 50 MWe plant.

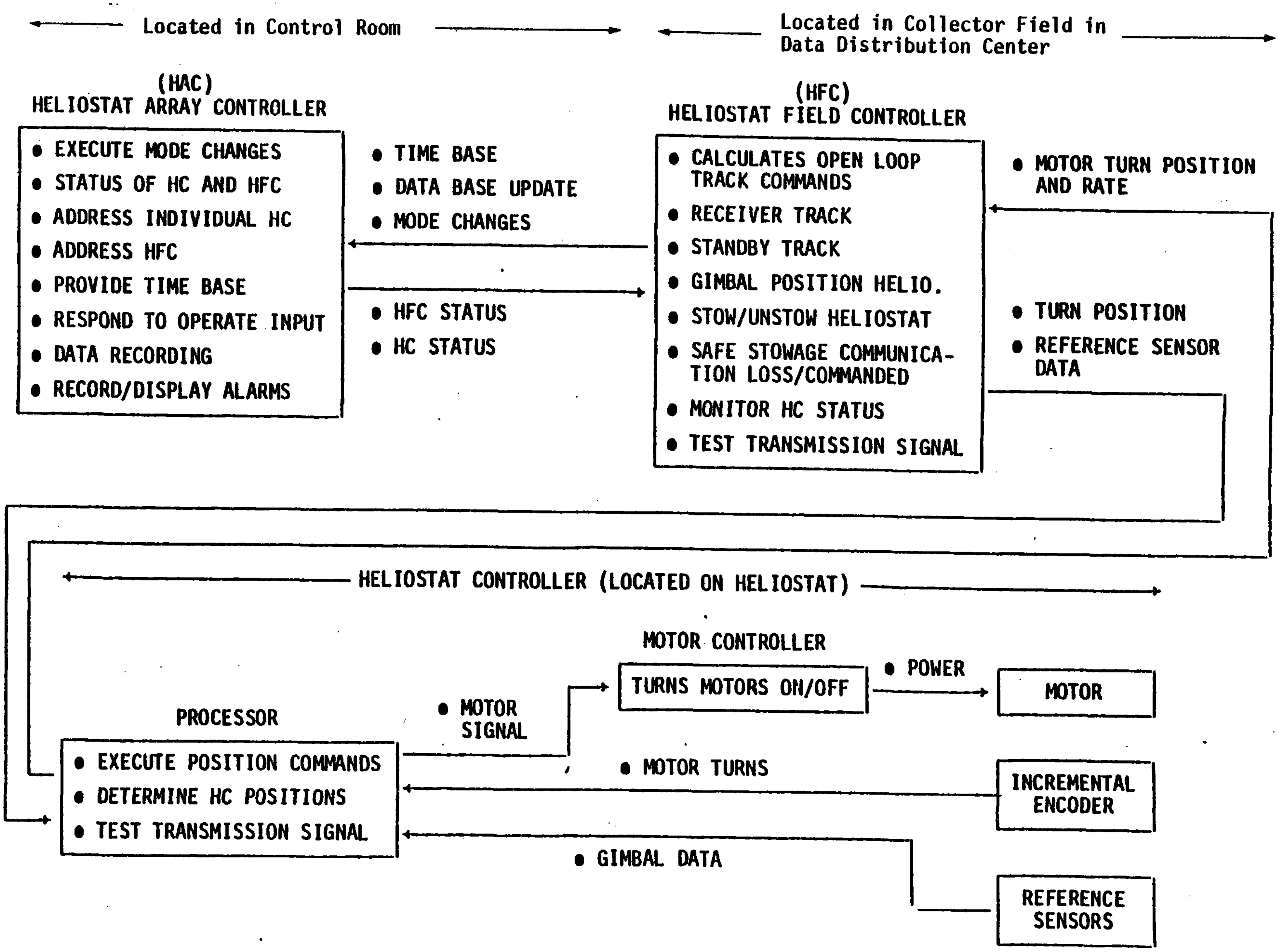

Figure 3-13. Controls Subsystem

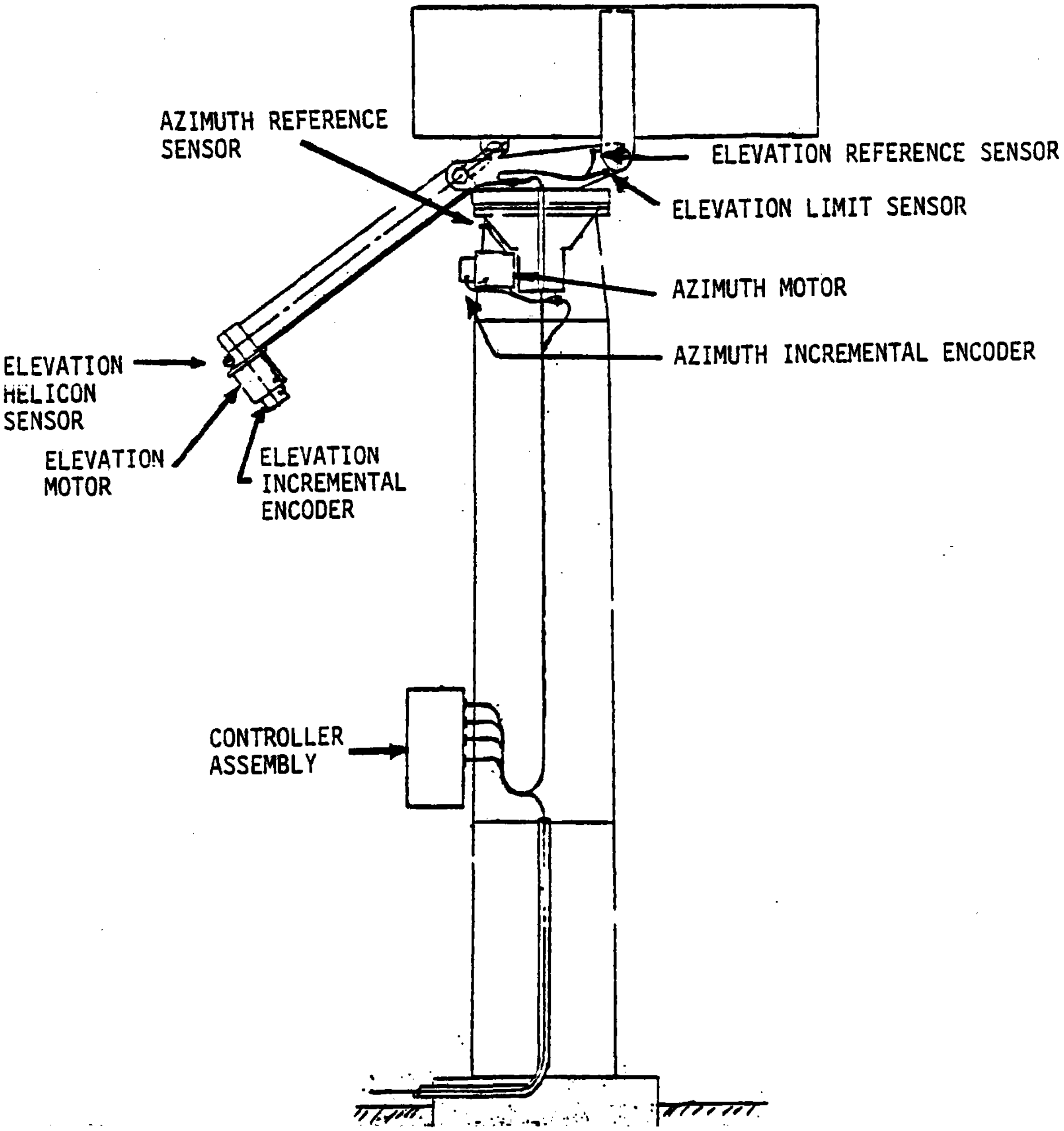

Figure 3-14. Key Control Components

Table 3-7
TOP LEVEL CONTROL SYSTEM REQUIREMENTS

	CAPABILITIES	
	50 MWe Plant	CRTF
o HAC interface with MCS, BCS, DAS	Same	None
o Beam pointing error less than 1.5 mrad	1.5 mrad	1.5 mrad
o Resolve singularity control in 15 minutes	12 min	12 min
o Position heliostat to an orientation within 15 minutes	14 min	12 min
o Control a field of heliostats as a group or individual basis	Same	Individual only
o Defocus from receiver within 120 seconds	<30 sec	<15 sec
o Local override of HC	Same	Same
o Electrical transients of 1.7 overshoot for 5 cycles and dropout for 3 cycles	Same	Same
o Temperature requirements	Same	Same
- Performance 0°C to 50°C		
- Function -9°C to 50°C		
- Survival -30°C to 50°C		
o HFC initiate safe stowage upon loss of communication with HAC	Same	Same
o Lightning protection from a strike to an adjacent heliostat	Same	Same
o Minimize susceptability to electromagnetic interference	Same	Same

The track accuracy requirement for 1.5 mrad beam error generates a number of subsystem requirements not only on the control system, but the structural and mechanical parts of the heliostat as well. Through testing of the heliostat and tolerance analysis, different errors have been identified. These errors plus the subsystem requirements are given in Table 3-8.

3.1.4 Optical Performance

A study was made of the optical performance of the Second Generation heliostat in terms of the energy spillage characteristics in a representative 50 MWe array, and the single-heliostat beam quality at various locations in the array. This analysis included the effects of panel curvature changes due to temperature variations. Using the Sandia DELSOL code, the general field layout of a 50 MWe collector array was determined. From this a row-by-row layout with individual heliostat locations was produced. Figure 3-15 shows a diagram of the 37-row array as used for input data for the MDAC CONCEN code. Comparison runs with both codes showed essentially equivalent results. The system parameter values assumed for the study are given in Table 3-9. The results of this study are as follows.

The relative differences in annual energy spillage for heliostat panels which change in curvature due to normal temperature variations and heliostat panels which are flat or at fixed optimum curvature are small.

Beam quality from individual heliostats at all locations in the field is adequate to be included within the receiver cross-section, although the beam quality for close-in heliostats does not meet the 1.4 mrad fringe width specification for some conditions.

The theoretical beam-shape may be determined by simulation with either the HELIOS or the CONCEN code.

As related to the design of a central receiver system of the 50 MWe size category, it is evident that the 95 percent energy - received specification can be met even though the beam quality for close-in heliostats does not

Table 3-8

SUBSYSTEM REQUIREMENTS AND BEAM ERROR SOURCES

			BEAM ERROR (RMS)	
Error Source	Subsystem Requirements	Description	Azimuth (mrad)	Elevation (mrad)
Sun position calculation	Electrical	Calculation of sun position, earth obliquity, refraction model	0.35	0.35
HC position control	Electrical	Sensor granularity, integration error, etc.	0.4	0.4
HC control lag	Electrical	The control system lags the commanded position	0.4	0.4
HFC calculations	Electrical	Time drift of processor, 16 bit calculation. Approximation of pivot point offset.	0.5	0.5
Drive backlash	Mechanical	Difference in turn position between CW and CCW movement	0.14	0.14
Pedestal bending from sun	Structural	The sun shining on one side of the pedestal will cause pedestal to bend	0.10	0.3
Track reference alignment	Electrical	Difference between true north/south and vertical and heliostat reference system. Alignment plate not accurate enough, used BCS system.	0.3	0.3
Tilt and nonorthogonality alignment	Electrical	Difference between true tilt and nonorthogonality and estimated. Caused from alignment plate, instrument error, wind, etc.	0.5	0.5
Elevation transfer function	Mechanical Structural	Difference in gravitational bending from model, from one heliostat to the next heliostat, and pivot point tolerance	0.0	0.3
Azimuth drive elevation variation	Mechanical	Rotation of azimuth drive in CW direction produces a different elevation angle than CCW	0.0	0.3
Elevation repeatability	Mechanical	Variation in elevation system from one test to next test caused by temperature, load, etc.	0.0	0.3
		Stochastic Summation =	1.29	1.43

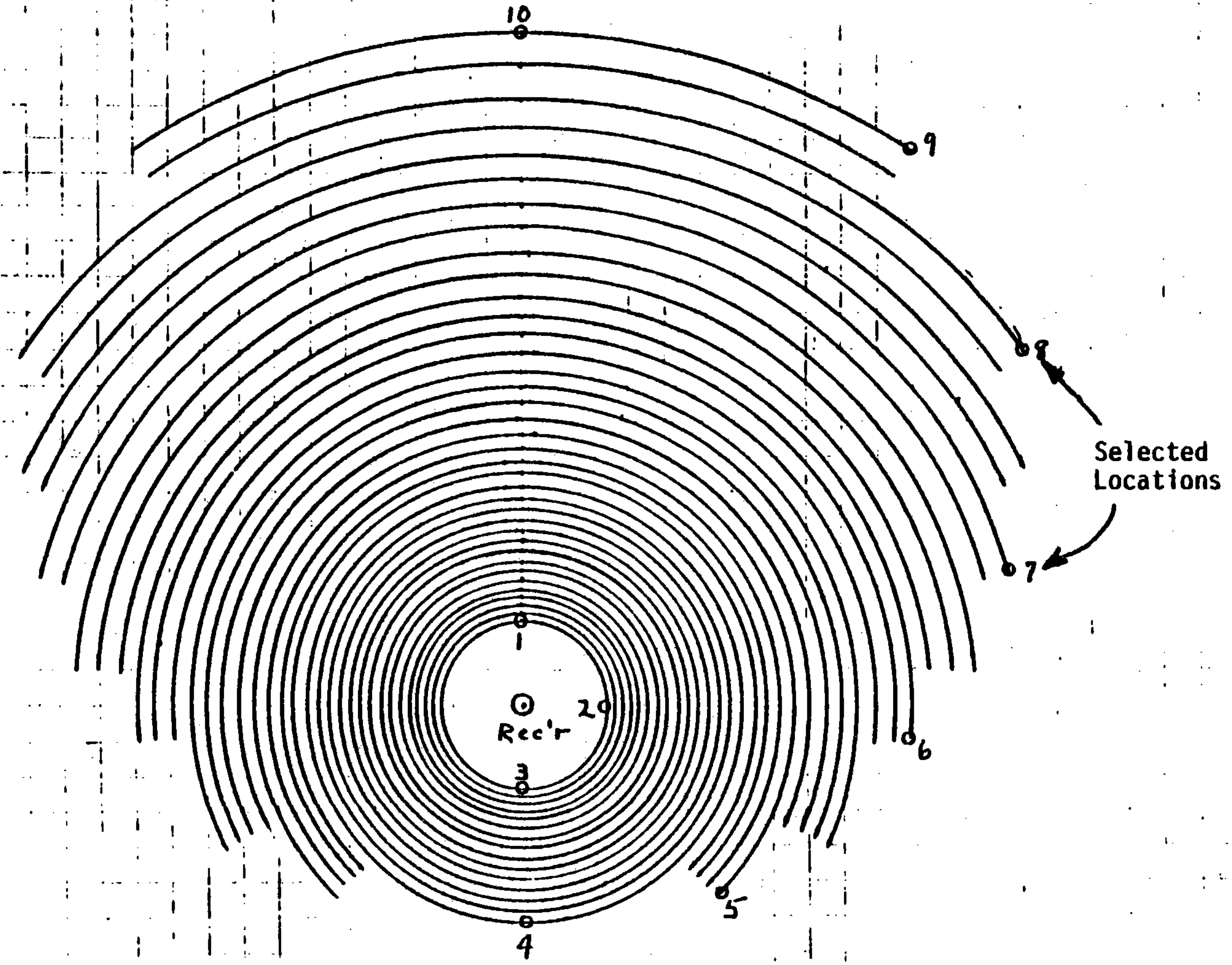

Figure 3-15. 50 MWe Heliostat Field Layout Staggered-Radial Locations

Table 3-9

SYSTEM PARAMETER DATA

- Number of Heliostats = 5609
- Number of Rows = 37
- Field Extent = 123.2 M to 972.2 M
- Tower Height = 136.4 M above Heliostat Center Plane
- Heliostat Width = 8.66 M
- Heliostat Height = 6.87 M
- Mirror Reflectance = 0.89
- Mirror Waviness = 1.0 MR, 1 Sigma
- Gimbal Axis Pointing Error = 0.75 MR, 1 Sigma, Each Axis
- Panel Cant Error = 0.5 MR, 1 Sigma, Each Component
- Receiver Diameter = 12 M
- Receiver Height = 14 M

meet the theoretical beam shape - plus - 1.4 mrad fringe specification. The 95% requirement is preeminent and the beam quality specification is subsidiary. Utilizing this philosophy, 97% of annual energy is provided to the receiver. The following paragraph describes the technique used by MDAC to perform the analysis.

3.1.4.1 Total Energy

Using the CONCEN code with representative hour-by-hour insolation and ambient temperature data for the Barstow location, received-energy figures were computed. The diurnal energy for one day in each month was determined by integration under the hourly received power curves for the day. The annual energy was then calculated by integrating the diurnal energies over the year. Since the ambient temperatures varied throughout the day and year unsymmetrically about noon and summer solstice, it was necessary to include the full day and full year in the integration. By ratioing the received energy to the incident energy, percent spillage figures were computed for each day and for the year. The results of this calculation are shown in Table 3-10. The diurnal spillage shows a minimum near the summer solstice of 1.57 percent and a maximum near the winter solstice of 2.89 percent. The annual spillage, which is determined from the ratio of the received annual energy to the incident annual energy, is 2.04 percent. Wind effects were not accounted for in this computation.

Diurnal energy spillage computations were run for four representative days for panels with different curvature/temperature characteristics. The figures selected from Table 3-10 were compared with similar runs made for conditions of flat panels and for panels with a fixed curvature for proper focus at the location. Table 3-11 gives the energy and spillage for the three conditions. Although, as expected, the spillage figures are best for the fixed curvature condition (non varying with temperature) and worst for the flat panel condition, the differences are small and all are under 3 percent.

3.1.4.2 Beam Quality

The effects of extreme temperature conditions on the beam quality for single heliostats of various locations in the collector field were investigated by comparing the beam shape with the corresponding specification shape. The latter was determined from the theoretical beam shape for heliostats with

Table 3-10
ENERGY DATA

DAY	RECEIVED DIURNAL ENERGY (MW Hr)	SPILLAGE (%)
March 21	1843.1	1.99
April 20	1990.1	2.03
May 20	1980.3	1.58
June 19	2179.0	1.57
July 19	1966.6	1.58
August 18	2038.5	1.72
September 17	1571.9	1.90
October 17	1773.1	2.06
November 16	1447.1	2.57
December 16	1480.9	2.89
January 15	1495.7	2.73
February 14	1460.7	2.31

Annual Received Energy = 6.43×10^5 MW hr

Annual Energy Spillage = 2.04%

Table 3-11

DIURNAL ENERGY VARIATION WITH PANEL CURVATURE
BARSTOW PILOT PLANT PHASE I FOAM CORE MIRROR MODULE

			BARSTOW INSOLATION			
	BARSTOW INSOL & TEMP.		FLAT PANELS		FIXED CURVATURE	
DAY	DIUR. EN.	SPILLAGE	DIUR. EN.	SPILLAGE	DIUR. EN.	SPILLAGE
MAR. 21	1843.1 MW Hr	1.99%	1839.0 MW Hr	2.36%	1846.3 MW Hr	1.85%
JUNE 19	2179.0	1.57	2175.1	1.94	2184.0	1.56
SEPT. 17	1571.0	1.90	1565.7	2.41	1571.9	1.85
DEC. 16	1480.9	2.89	1480.7	2.86	1483.1	2.54

error-free flat panels at each location, with the addition of a 1.4 mrad fringe around the 90 percent power contour which defines the beam shape. The locations are identified by number in Figure 3-15. CONCEN was used to determine the 90 percent power contour for both theoretical beam shape and actual heliostat beam shape. A comparison was run with the Sandia HELIOS code for the definition of the theoretical beam shape. Figure 3-16 shows cross-sections of the beam as computed by the two codes for representative conditions, showing good agreement.

Beam shapes were determined for each of the ten locations for the extreme conditions of early AM on summer solstice, ambient temperature 116°F, and early AM on winter solstice, ambient temperature 32°F. In general, the 90 percent power contour of the beam shape was comparable to or inside the specification contour except for the close-in heliostats. Figures 3-17 and 3-18 show diagrams for Locations 1 and 10 as determined by interpolation in the flux distribution over an imaginary screen normal to the beam, located at the receiver. The specification contour is shown as a solid line; the computed 90 percent contour appears as a series of dots. It is seen that, although the beam from the heliostat at Location 1 is outside the specification, it is still well within the diameter of the receiver (indicated by the rows of asterisks at the sides). For the outer heliostat at Location 10, the 90 percent contour is inside the specification and comparable in size to the receiver diameter. The comparisons for the other locations for summer and winter fall in between the extremes at Locations 1 and 10.

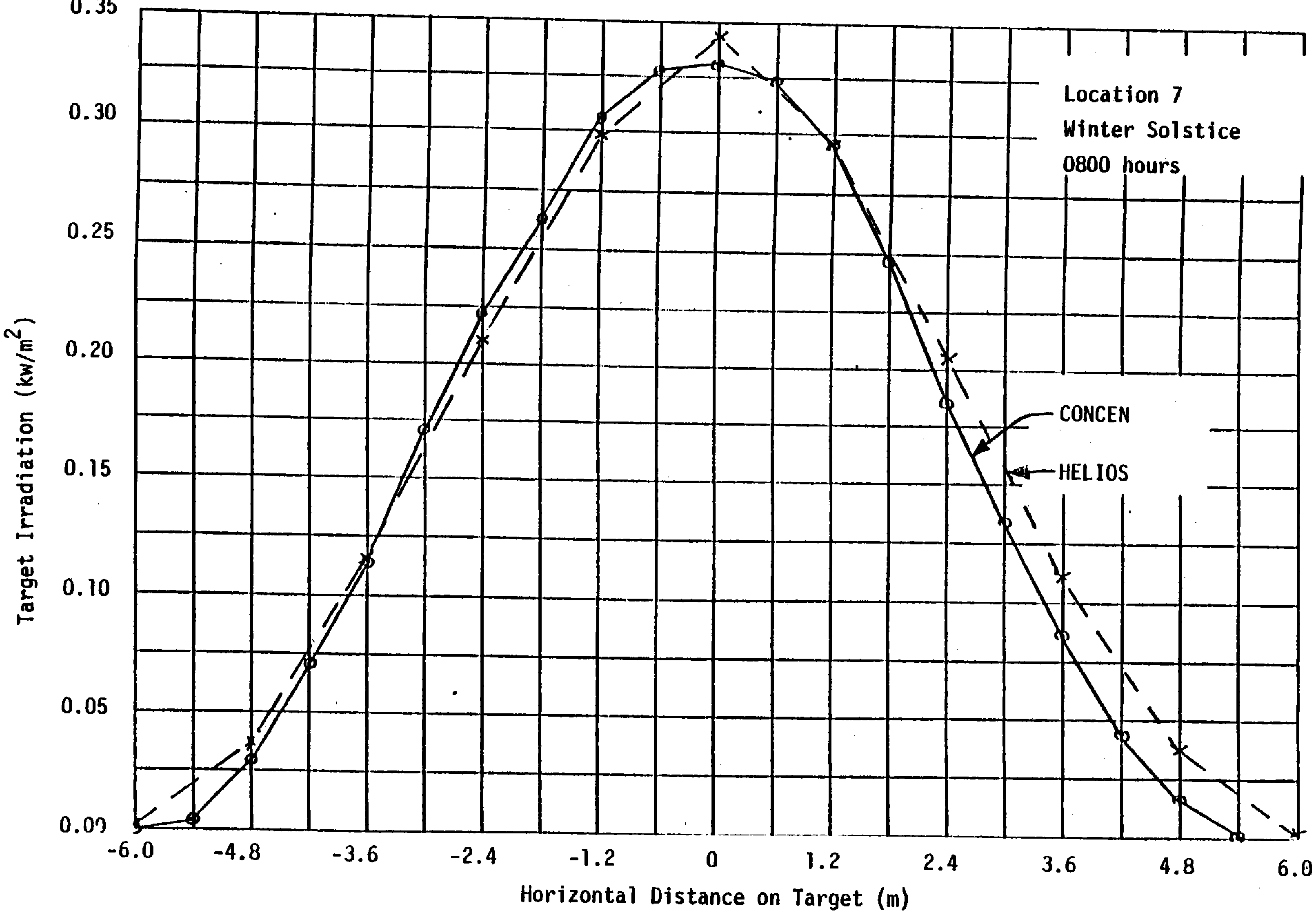

Figure 3-16. Comparison Between Theoretical Beam Shape by HELIOS and CONCEN

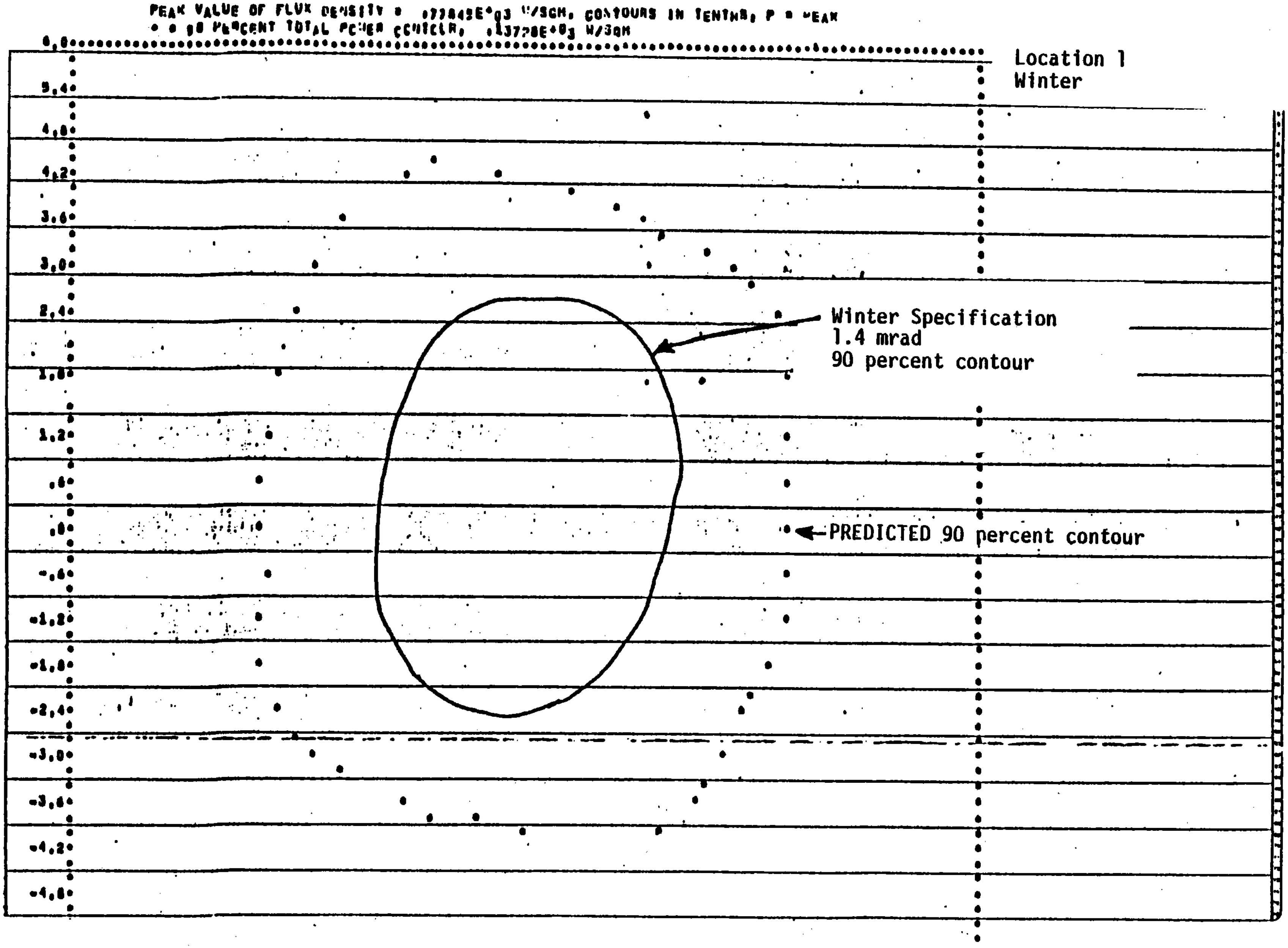

Figure 3-17. Beam Quality Compared to Specification

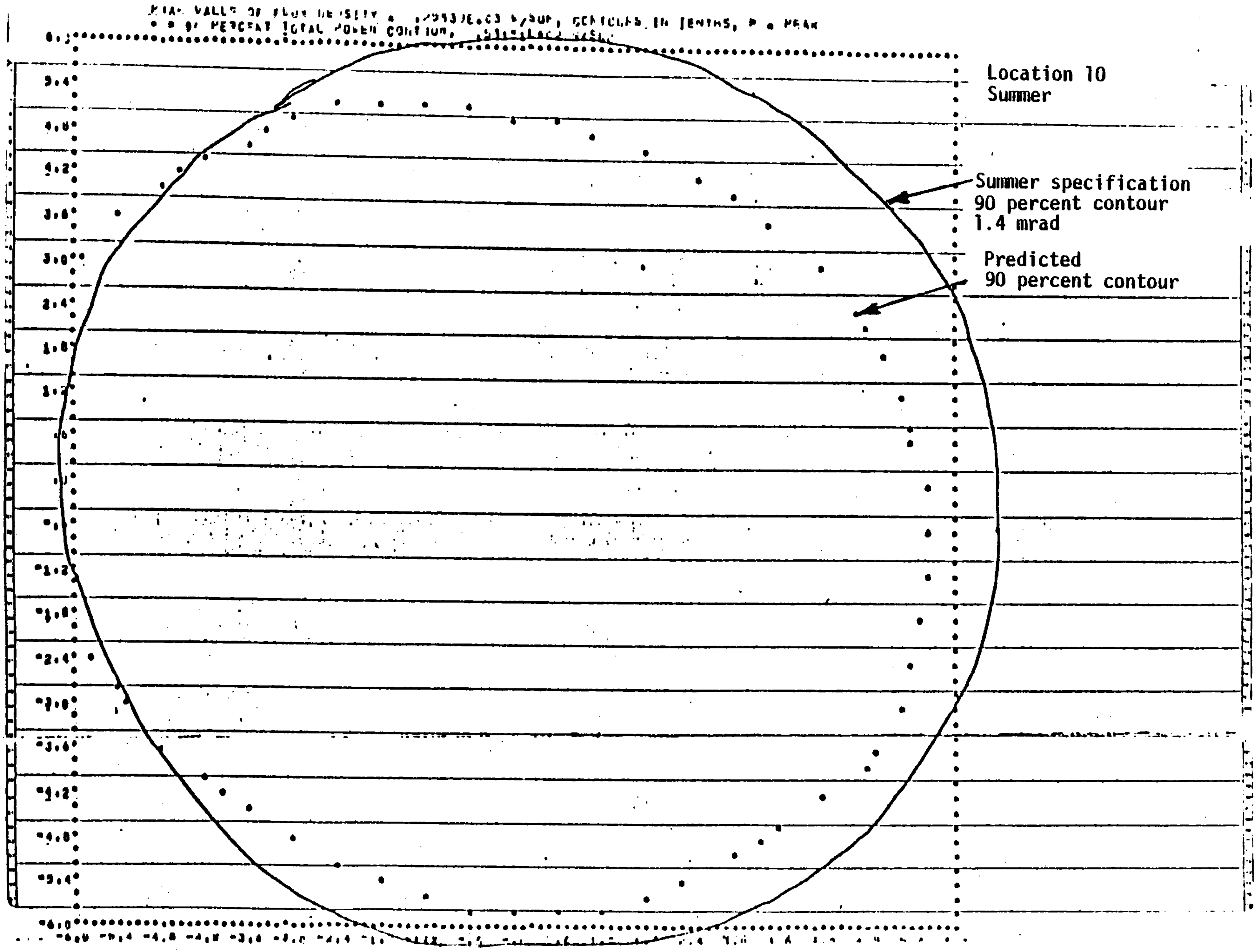

Figure 3-18. Beam Quality Compared to Specification

3.2 DETAILED DESIGN AND TESTING

This section presents the heliostat detail design and the testing utilized to verify performance.

3.2.1 Structural Design

This subsection describes the details of each of the structural components. The component is described along with selection rationale and development testing done to confirm the design selected. Additional test plans and results to date are given in Appendix A.

Figure 3-19 shows the mirror module configuration. It consists of a laminated mirror bonded to two galvanized steel shims. Two galvanized steel hat section stringers are then bonded to the shims. The laminated mirror for the Second Generation prototype units is comprised of a 0.093 clear float glass mirror laminated to 0.188 float glass substrate. The production design will utilize a 0.059 fusion glass mirror and the same 0.188 substrate. The mirror is sealed around the edges with a metal edge member and silicone. The overall dimensions of the panel are 40 1/4 x 132 1/4 inches. Each panel has a reflective surface of 43.7 ft^2.

The mirror module size was chosen on the basis of available glass size, shipping constraints and a desire to minimize parts count. The mirror module is curved in the long direction to enhance performance and sealed for long life. The two-stringer support system provides adequate stiffness and the panel has demonstrated hail survival of one inch diameter hail stones at over 100 fps for both front and back surface impacts, which is in excess of the requirements.

The mirror module design was selected based upon trade study evaluations, desert aging tests and preliminary development tests. Tables 3-12, 3-13 and 3-14 show the results of a trade study based upon the Second Generation rating criteria given in the RFP. Table 3-12 shows the rating given in the various categories for the different configurations considered. Table 3-13 shows the estimated relative costs based on 1979 dollars for the configurations considered. It should be noted that the cost of pinch rolling includes an extra \$.04/ft^2 when a backing paint is used to cover the cost of handling/storage to allow

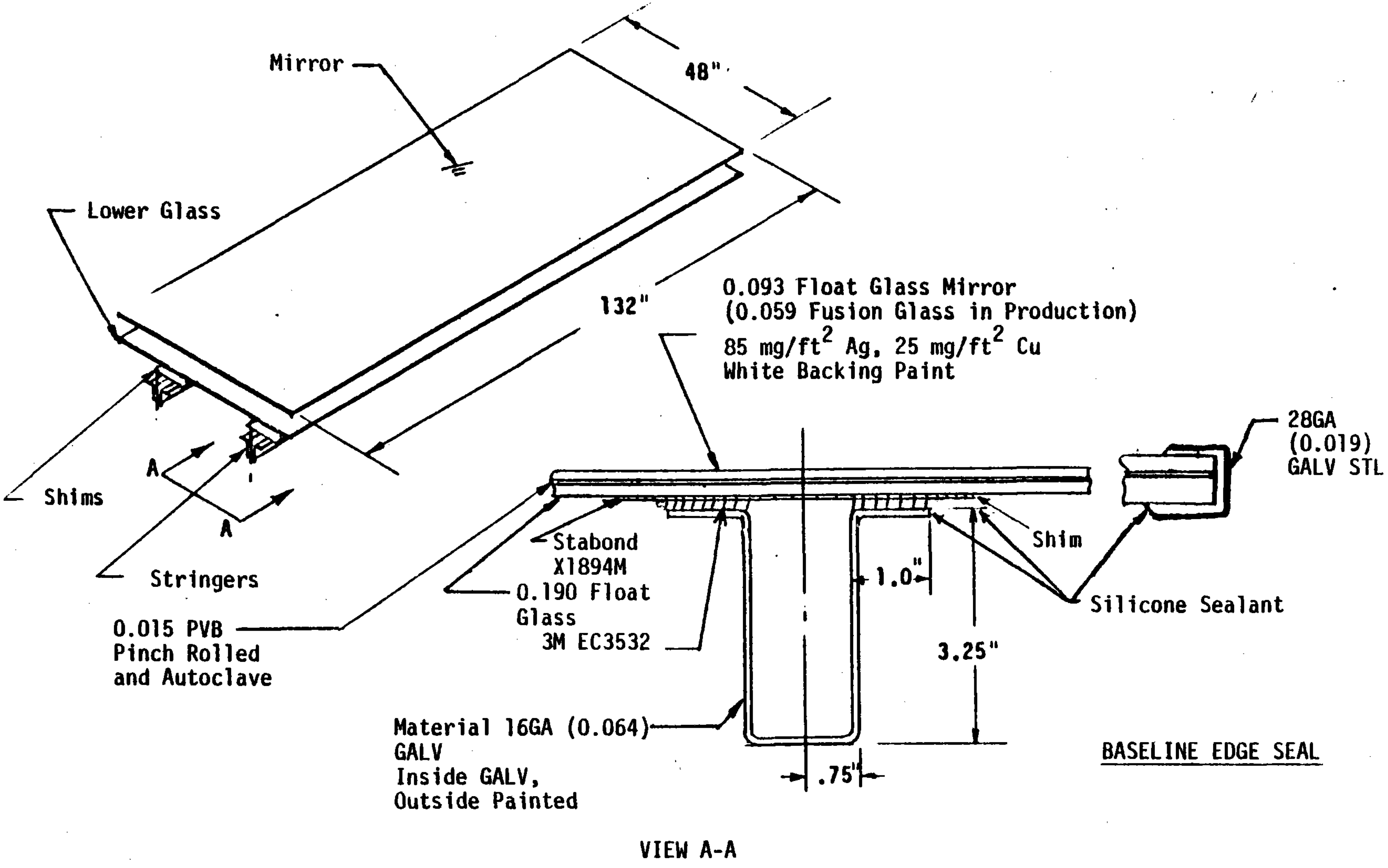

Figure 3-19. Second Generation Heliostat Mirror Module

Table 3-12

SECOND GENERATION RATING CRITERIA

1. Cost 40 points - lowest cost configuration assigned 40 points - others are determined by ratio of costs

$$\frac{\text{lowest cost}}{\text{cost}} \times 40.$$

2. Technical Risk - 30 points (delivery + 2 years)

Clear PVB gray mirror backing paint, autoclave	30
Clear PVB white mirror backing paint, autoclave	29
Clear PVB gray mirror backing paint, no autoclave	28
Clear PVB white mirror backing paint, no autoclave	27
White PVB gray mirror backing paint, no autoclave	27
White PVB white mirror backing paint, no autoclave	26
Clear PVB on copper, no autoclave	24
White PVB on copper, no autoclave	23
Polyurethane	20

3. Survivability - 20 points (greater than 10 year lite)

Clear PVB gray mirror backing paint, autoclave	20
Clear PVB white mirror backing paint, autoclave	19
Clear PVB gray mirror backing paint, no autoclave	18
Clear PVB white mirror backing paint, no autoclave	17
White PVB gray mirror backing paint, no autoclave	17
White PVB white mirror backing paint, no autoclave	16
Clear PVB on copper, no autoclave	15
White PVB on copper, no autoclave	14
Polyurethane	10

4. Performance - 10 points

-1 point - no autoclave
-1 point - no PVB

+0.25 point - white paint + white PVB

Table 3-13

COST RATIO COMPARISONS
MIRROR MODULE CONFIGURATIONS AND EDGE SEALS

MIRROR MODULE CONFIGURATIONS ($\$/ft^2$)

Item	1	2	3	4	5	6	7	8	9	Foamcore	
3/32 inch glass	0.40	0.40	0.40	0.40	0.40	0.40	0.40	0.40	0.40	0.60	1/8 inch LIF Glass
Silvering	0.33	0.33	0.33	0.33	0.33	0.33	0.33	0.33	0.33	0.33	Silvering
Mirror Backing Paint	----	----	----				0.02	0.02	0.02	0.02	Mirror Backing Paint
Adhesive PVB or PU	0.07	0.36	0.24	0.46	0.36	0.24	0.24	0.24	0.24	0.15	Adhesive
Pinch Rolling	0.16	0.16	0.16	0.20	0.20	0.20	0.20	0.20	0.20	0.61	Foam
Autoclaving	----	----	----	----	----	----	----	0.07	0.07	0.60	Bonding
3/16 inch Backlite	0.60	0.60	0.60	0.60	0.60	0.60	0.60	0.60	0.60	0.40	Backsheet (Painted)
Stringers	0.19	0.19	0.19	0.19	0.19	0.19	0.19	0.19	0.19	0.08	Cups
Adhesive	0.03	0.03	0.03	0.03	0.03	0.03	0.03	0.03	0.03	0.02	Adhesive
Bonding	0.15	0.15	0.15	0.15	0.15	0.15	0.15	0.15	0.15	0.08	Cup Bonding
Backside Painting							0.30		0.30		
Total	1.93	2.22	2.10	2.36	2.28	2.16	2.46	2.23	2.53	2.89	

EDGE SEALS

Item	Metal, Butyl Silicone	Silicone	Foamcore
Edge Members	2.52		3.68
Corner Caps			4.60
Butyl	1.25		3.00
Silicone	0.76	0.38	1.88
Labor	25.00	6.25	37.50
Total	29.53	6.63	50.66
Cost/Ratio	0.67	0.15	1.23

Table 3-14

SECOND GENERATION MIRROR MODULE CONFIGURATION

Decreasing Risk

Configuration	Description	Cost	Test Results/Remarks	Edge Seal		Total Cost	Cost	Risk	Survivability	Performance	Total
				Type	Cost						
1	Ag + Cu + Pu	1.93	1. Complete silver corrosion after 1 month with no edge seal.	S	0.15	2.08	40	20	8	8	76
			2. No corrosion with mirror backing paint - 1 yr HB experience	MBS	0.67	2.60	32	20	10	8	70
2	Ag + Cu + white PVB	2.22		S	0.15	2.37	35	23	12	9	79
				MBS	0.67	2.89	29	23	14	9	75
3	Ag + Cu + clear PVB	2.10	1. Slight corrosion of Cu on 4 year old piece kept indoors	S	0.15	2.25	37	24	13	9	83
				MBS	0.67	2.77	30	24	15	9	78
4	Ag + Cu + white MBP + specification PVB	2.36		S	0.15	2.51	33	26	15	9	83
				MBS	0.67	3.03	27	26	17	9	79
5	Ag + Cu + GMBP + white PVB	2.28		S	0.15	2.43	34	27	15	9	86
				MBS	0.67	2.95	28	27	17	9	81
6	Ag + Cu + WMPB + clear PVB	2.16		S	0.15	2.31	36	27	15	9	87
				MBS	0.67	2.83	29	27	17	9	82
7	Ag + Cu + GMBP + clear PVB + WBP	2.46		S	0.15	2.61	32	28	16	9	85
				MBS	0.67	3.13	27	28	18	9	82
8	Ag + Cu + WMBP + clear PVB + auto	2.23	A3 and desert exposure 3 years 1/2" to 1" edge corrosion without seal	S	0.15	2.38	35	29	17	10	91
				MBS	0.67	2.90	29	29	19	10	87
9	Ag + Cu + GMBP + clear PVB + auto to WBP	2.53	1. CRTF configuration no edge seal. No degradation after 3 years	S	0.15	2.68	31	30	18	10	89
				MBS	0.67	3.20	26	30	20	10	86
10	Foamcore	2.89			1.23	4.12	20	30	20	10	80

the paint to cure. Table 3-14 shows that Configuration 8 with the simple edge seal has the highest rating and this configuration was chosen for the Second Generation design. The edge seal has been modified to include a metal edge member over the silicone mainly for the purposes of providing edge protection from chipping.

A second trade study involved the selection of the stringer material. Table 3-15 shows the results of this study. The carbon steel stringer was selected because the very slight performance gain using the stainless steel stringer could not justify the added cost.

To verify the design selection, several mirror module development tests were performed. The first step consisted of evaluating results of the desert aging of different configurations. Table 3-16 summarizes the results of the laminated mirrors subjected to desert exposure for periods of nine months to three years. These show that:

- o Mirrors bonded with polyurethane show the largest amount of corrosion due to large air voids.
- o Panels bonded with PVB without autoclaving show light corrosion in air voids.
- o Mirror backing paint is required
- o Edge seals are required for long service life.

A second development test involved the stiffener shape study. Table 3-17 summarizes this effort. The hat section was selected because of greater load capability (larger peel area) and a higher stiffness.

The third development test was the stress durability tests for the stringer/glass adhesive. Table 3-18 shows the details of these tests. Both the EC3532 and the HYSOL ADX414 have failed in these tests. The Stabond x 1894M has survived this test to date and has survived four years of desert exposure with minimum degradation effects. This is the choice to bond the stringers to the glass, but its 18-hour cure time prohibits its use on line. A design change has been implemented using a shim approach where 28 gage galvanized steel

Table 3-15

STRINGER MATERIAL COMPARISON

	Carbon Steel Stringer ($.30/lb)	404 Stainless Stringer ($1.00/lb)
CONFIGURATION	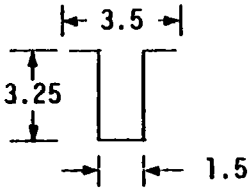	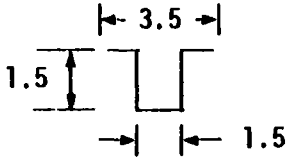
WEIGHT PER STRINGER	23.16	14.63
COST PER STRINGER	$ 6.95	$ 14.63
COST PER HELIOSTAT	$195.00	$410.00
COEFFICIENT OF EXPANSION (α_s)	6.3×10^{-6}	4.8×10^{-6}
$\alpha_s - \alpha_g$ ($\alpha_g = 4.0 \times 10^{-6}$)	2.3×10^{-6}	0.8×10^{-6}
MIRROR MODULE PERFORMANCE (132 inch PANEL)		
Initial R at 77 degrees	24,600	24,600
Initial End Scope at 77 degrees	2.7	2.7
End Slope at T = 32PF (Allow = -0.4 mrad)	+0.20	+0.95
End Slope at T = 122°F (Allow = +5.7 mrad)	+5.2	+4.5
MAXIMUM TENSILE STRESS (ELASTIC + THERMAL)	230	125
	↑ CARBON STEEL STRINGER SELECTED	

Table 3-16

LAMINATED MIRROR DESERT EXPOSURE RESULTS

Sample No.	Configuration	Bond	Edge Seal	Exposure	Results
X 1	Ag, Cu + Glass	Polyurethane	MBS	9 Mo.	Corrosion in void areas
X 1A	Ag, Cu + Glass	Polyurethane	None	9 Mo.	Edge corrosion
X 4	Ag, Cu + Glass	Polyurethane	MBS	9 Mo.	Corrosion in voids
X 4A	Ag, Cu + Glass	Polyurethane	None	9 Mo.	Edge Corrosion and corrosion in voids
X 6	Ag, Cu + Glass	PVB + Auto	MBS	9 Mo.	Edge corrosion of Cu
X 6A	Ag, Cu + Glass	PVB + Auto	None	9 Mo.	Edge corrosion + interior corrosion of Cu
X 7	Ag, Cu + Glass	PVB	MBS	9 Mo.	Cu corrosion
X 7A	Ag, Cu + Glass	PVB	None	9 Mo.	Cu corrosion
X 11	Ag + Glass	PVB	MBS	9 Mo.	Air voids growing
X 11A	Ag + Glass	PVB	None	9 Mo.	Edge corrosion
X 12	Ag + Glass	PVB + Auto	MBS	9 Mo.	Slight edge corrosion
X 12A	Ag + Glass	PVB + Auto	None	9 Mo.	Edge corrosion
X 14	Ag, Cu + Glass	Polyurethane	MBS	9 Mos.	Corrosion in voids
66-4	Ag, Cu, GMBP + Glass	PVB + Auto	None	36 Mos.	1" Edge discoloration of paint
65-4	Ag, Cu, GMBP + Glass	PVB + Auto	None	36 Mos.	1/2" Edge discoloration of paint
65-13	Ag, Cu, GMBP + Glass	PVB + Auto	None	36 Mos.	1/2-3/4" Edge discoloration of paint

Table 3-17

STIFFENER SHAPE STUDY

- HAT SECTION VS C SECTION

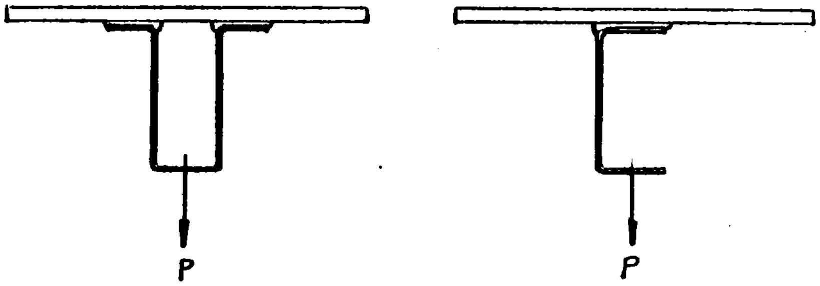

- TENSILE LOAD AT RT, 140° F, 160° F

TEMPERATURE	HAT SECTION	C SECTION
160°	FAILED AT 460 LB LOADED TO 150 LB - HELD 30 MIN.	FAILED AT 318 LB LOADED TO 150 LB - HOLD FAILED AFTER 35 MIN.
140°	NOT TESTED	LOAD TO 150 LB - HELD FOR 30 MIN. RAISE TO 200 LB - FAILED AFTER 20 MIN.
RT	NOT TESTED	NO FAILURE AT 1000 LB

- HAT SECTION SELECTED BECAUSE OF GREATER LOAD CAPABILITY (LARGER PEEL AREA) AT TEMPERATURE AND LARGER STIFFNESS

Table 3-18

ADHESIVE STRESS DURABILITY TEST

- TEST SAMPLES - 12" LONG HAT SECTION BONDED TO LAMINATED MIRROR
  3 ADHESIVES EC 3532, ADX 414, X1894M
- TEST SETUP

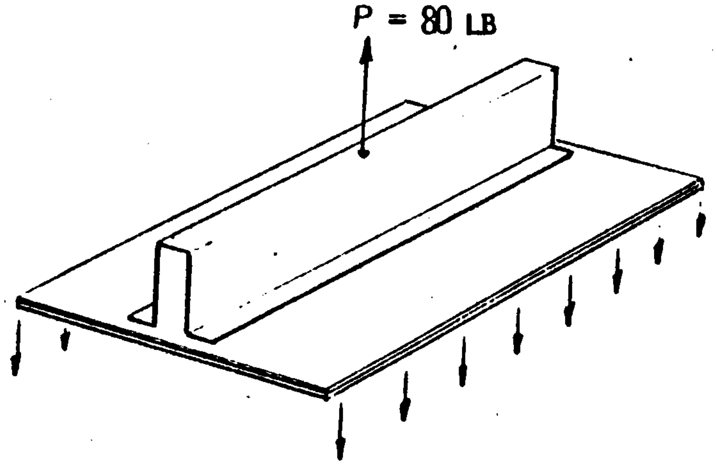

- TEST CYCLE
  4 HRS. AT 140^0 F 100% RELATIVE HUMIDITY
  20 HRS. AT 100^0 F AT AMBIENT HUMIDITY
  1 HR OF WATER SPRAY
  U V EXPOSURE
- RESULTS
  EC 3532 SAMPLES FAILED WITHIN 24 HRS.
  ADX 414 SAMPLES FAILED IN 34 DAYS.

o STABOND X1894M SAMPLES INTACT AFTER 60 DAYS

o DESIGN CHANGE IMPLEMENTED USING STABOND X2894M FOR SHIM/GLASS BOND AND EC 3532 FOR STRINGER/SHIM BOND.

o SAMPLES OF THIS DESIGN HAVE BEEN FABRICATED AND ARE IN TEST shims are bonded to the mirror off line with this adhesive. The hat sections are then bonded to the shim using the EC3532 adhesive which was verified during the cup debond evaluation testing.

Creep tests on the three adhesives are also being performed. They consist of double lap shear specimens under constant loading at three temperatures, 70°F, 140°F, and 160°F. Preliminary results show acceptable creep.

To determine the bond tool curvature and the amount of springback, curvature determination tests were performed. The objective of these tests was to determine the bond tool curvature to obtain a mirror module curvature of R = 24,000 inches. The approach was to fabricate full size mirror modules on the existing tooling, measure the curvature, correlate the data/analysis and modify the tooling as required.

Four panels were fabricated with an existing 11,000 inch R tool. These results show consistent curvature and minimum springback. Figures 3-20 and 3-21 show the contours of panels SN01 and SN04. The panels were subsequently thermal cycled between -20°F and 120°F for five cycles and remeasured. No significant contour changes were observed.

In addition to the development tests, the MDAC laminated mirror specification calls for a series of tests to be performed by the supplier on both the laminated and unlaminated mirror prior to commencing production. These tests include mirror defects, silver thickness, copper thickness, paint thickness, salt spray, boiling water, humidity and compressive shear.

The support structure is shown in Figures 3-22 and 3-23. It consists of an inboard cross beam, two diagonal beams, an outboard cross beam and two sets of diagonal braces. The support structure is made from mill galvanized steel and is entirely spot welded together for low cost, high quantity production. The deep roll formed sections provide high stiffness, low weight and ease of fabrication in production. The design of the support structure minimizes field assembly time.

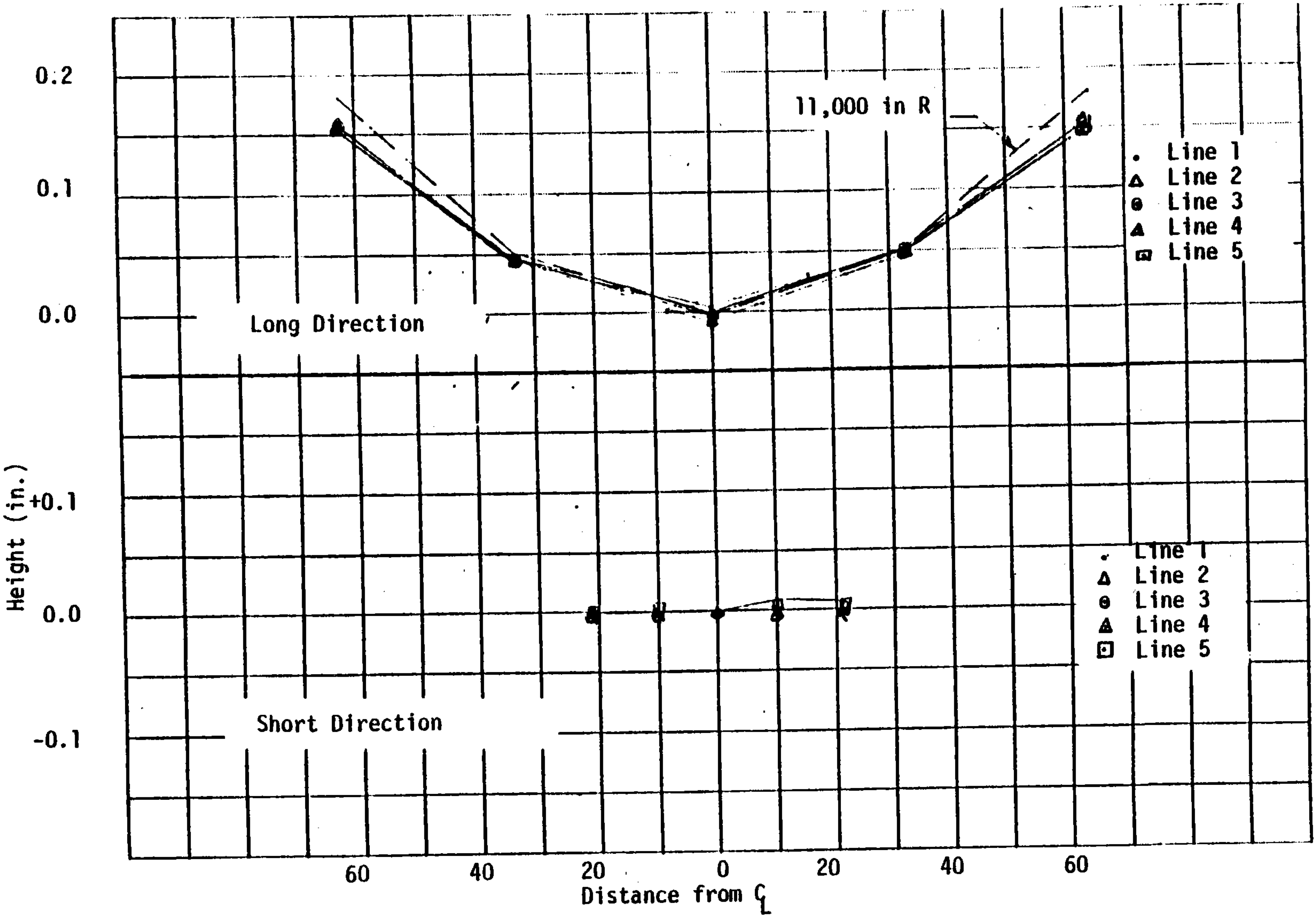

Figure 3-20. Laminated Mirror Module Contour SN01

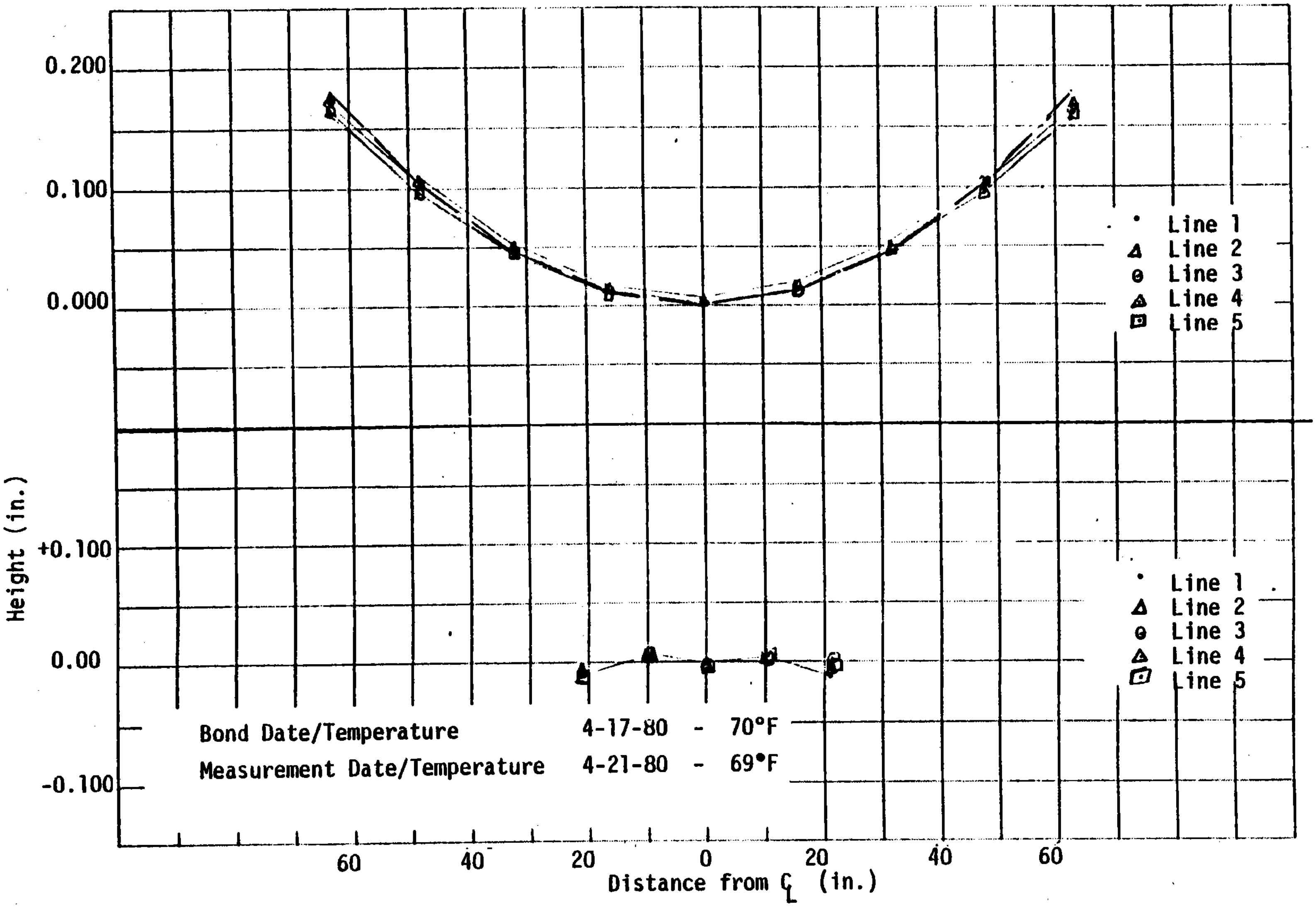

Figure 3-21. Laminated Mirror Module Contour SN04

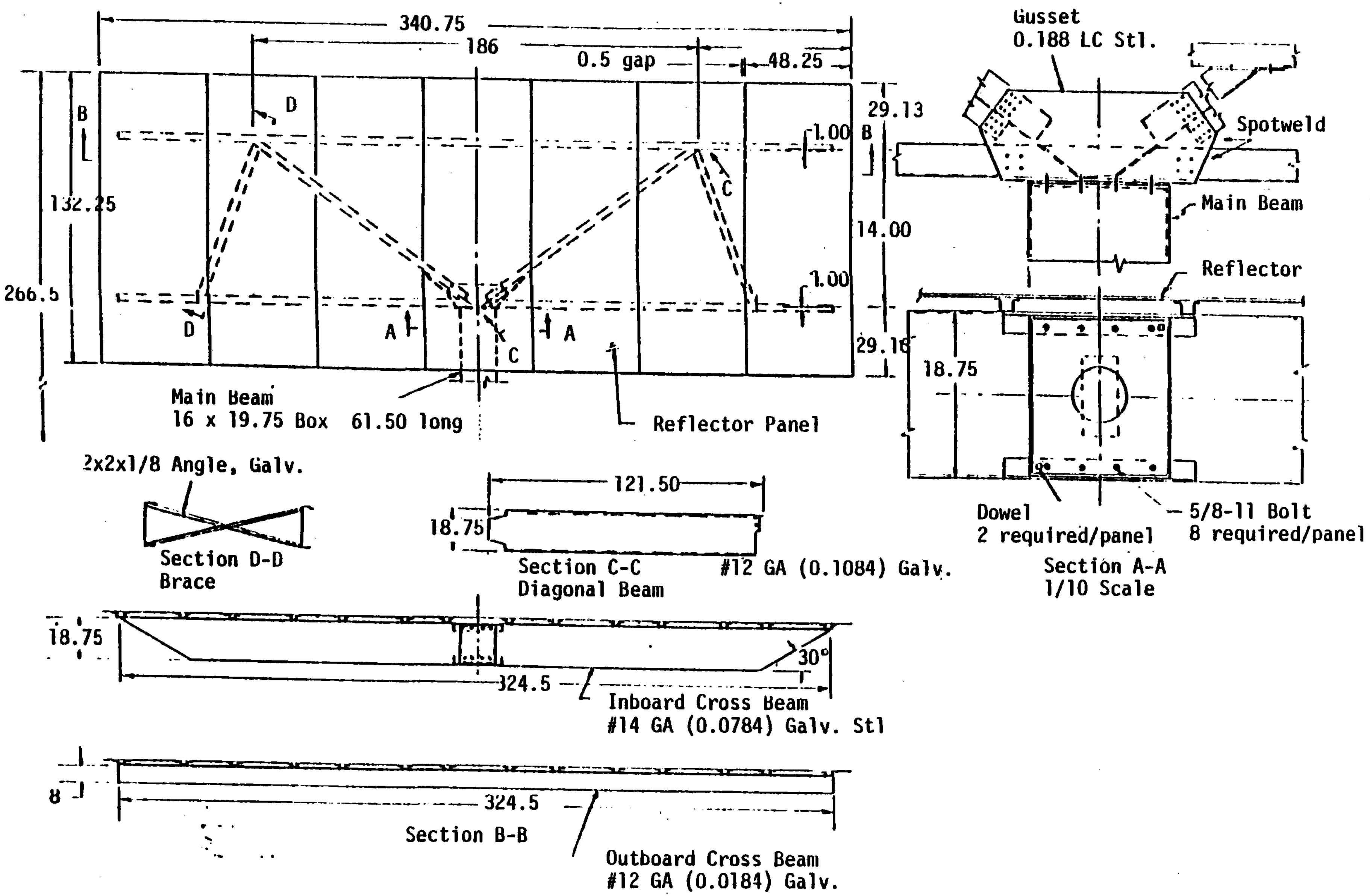

Figure 3-22, Support Structure Assembly

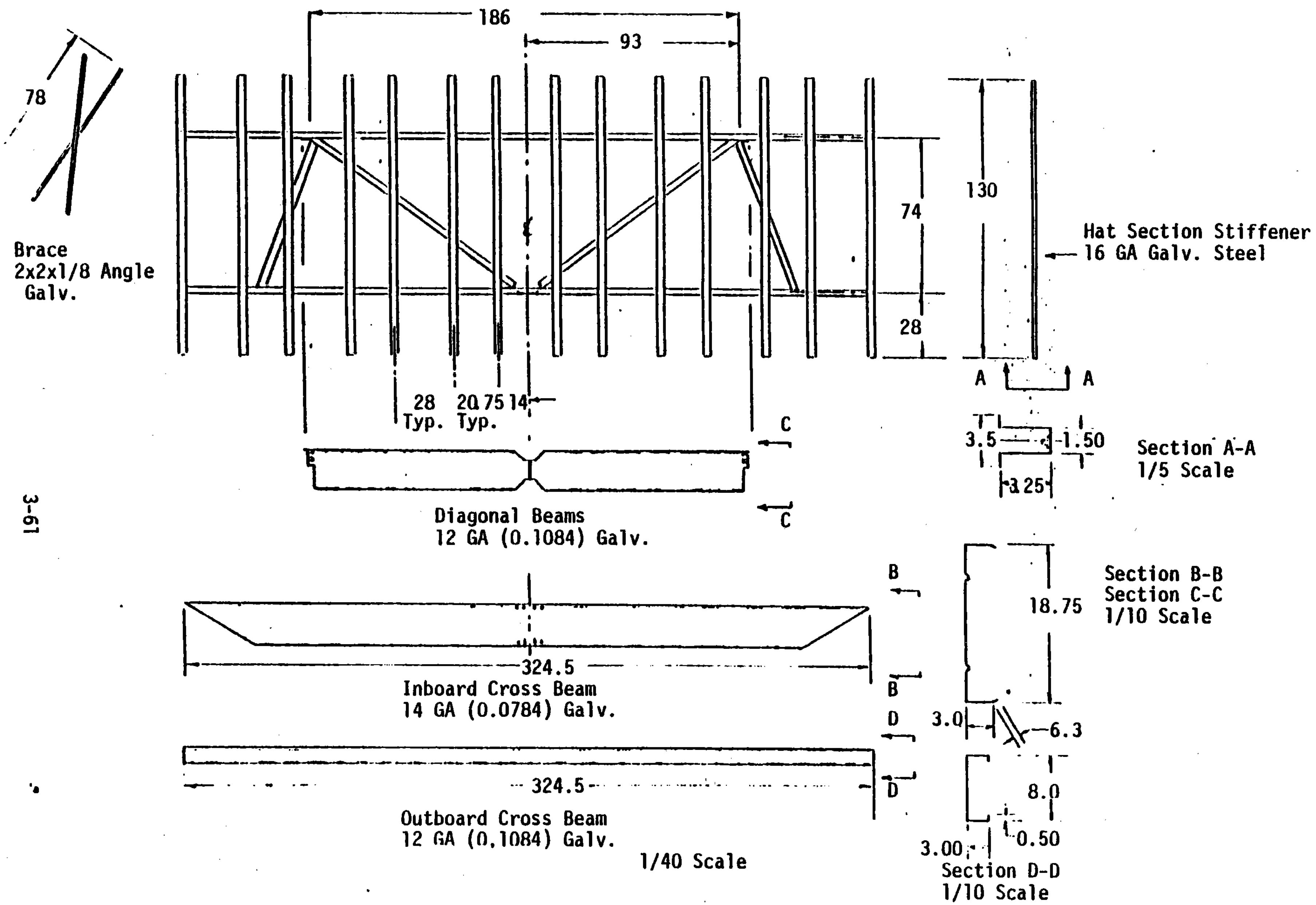

Figure 3-23. Support Structure

The attachment of the mirror modules to the support structure is shown in Figure 3-24. The attachment will be either three point or four point depending on a field evaluation of stiffness versus alignment ease. The use of either three or four point support designs is essentially the same with adjusting screws and "spacer" tools used to provide canting. It is expected that canting in high quantity production will be accomplished using inverted assembly of a complete "wing" of the heliostat on a large tooling table with built-in mirror cants.

The free play and rotational flexibility of the structure and connections work together to produce minimum loads into the mirror module. Specific examples of this are:

- o The holes in the cross beam are oversize so the shoulder washers have a side free play of ± 0.030 inch. Also, the shoulder of these washers is approximately 0.055 inch thicker than the cross beam, thus allowing the side play and some rotational play when clamped.
- o The flange of the cross beam, the open section cross beam, and the small diameter steel are somewhat flexible from a rotational stiffness point of view. Therefore, we expect any loads induced by rotational misalignment to be small.
- o The most likely rotational misalignment would come from a twisting of the entire cross section of the cross beam or bending of the cross beam flange. Both these deformations will tend to put a moment directly into the mirror module stiffener about an axis parallel to the glass and perpendicular to the longitudinal axis of the stiffener. The hat section is very stiff in this direction and thus this type of loading will have minimal effects on mirror module stresses or deformations.

The main beam is shown in Figure 3-25. It consists of a 16-inch wide by 18-inch deep rectangular tube. The tube has end flanges for bolting each reflector assembly or wing and three pair of lugs for attachment to the drive units.

The pedestal is shown in Figure 3-26. It consists of a twin tapered circular tube of approximately 139 inches in length. A flange is welded to the top to provide for bolted attachment to the drive unit. The pedestal contains a motor access hole near the top and a provision for junction box attachment at

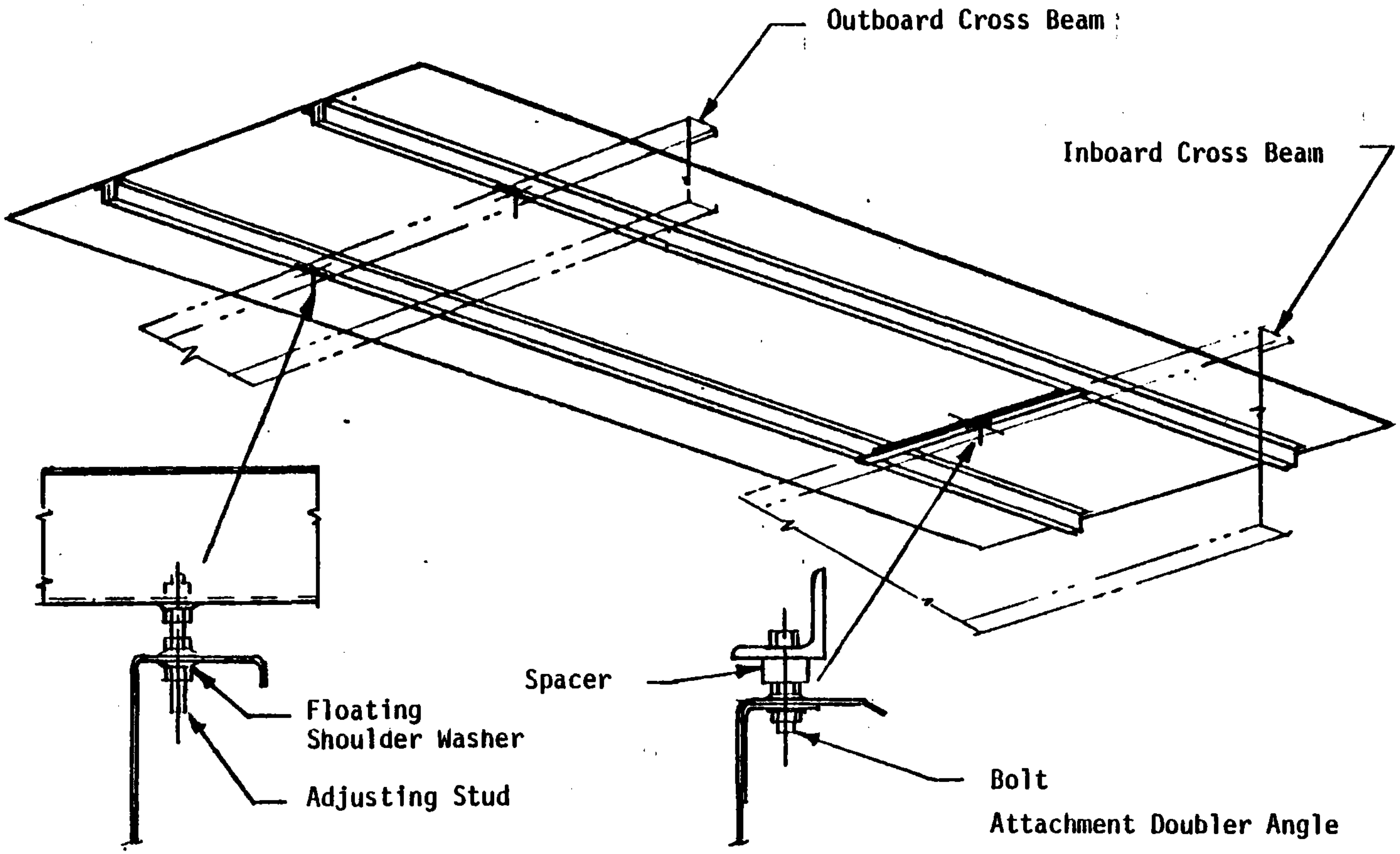

Figure 3-24. Mirror Module Mount Points

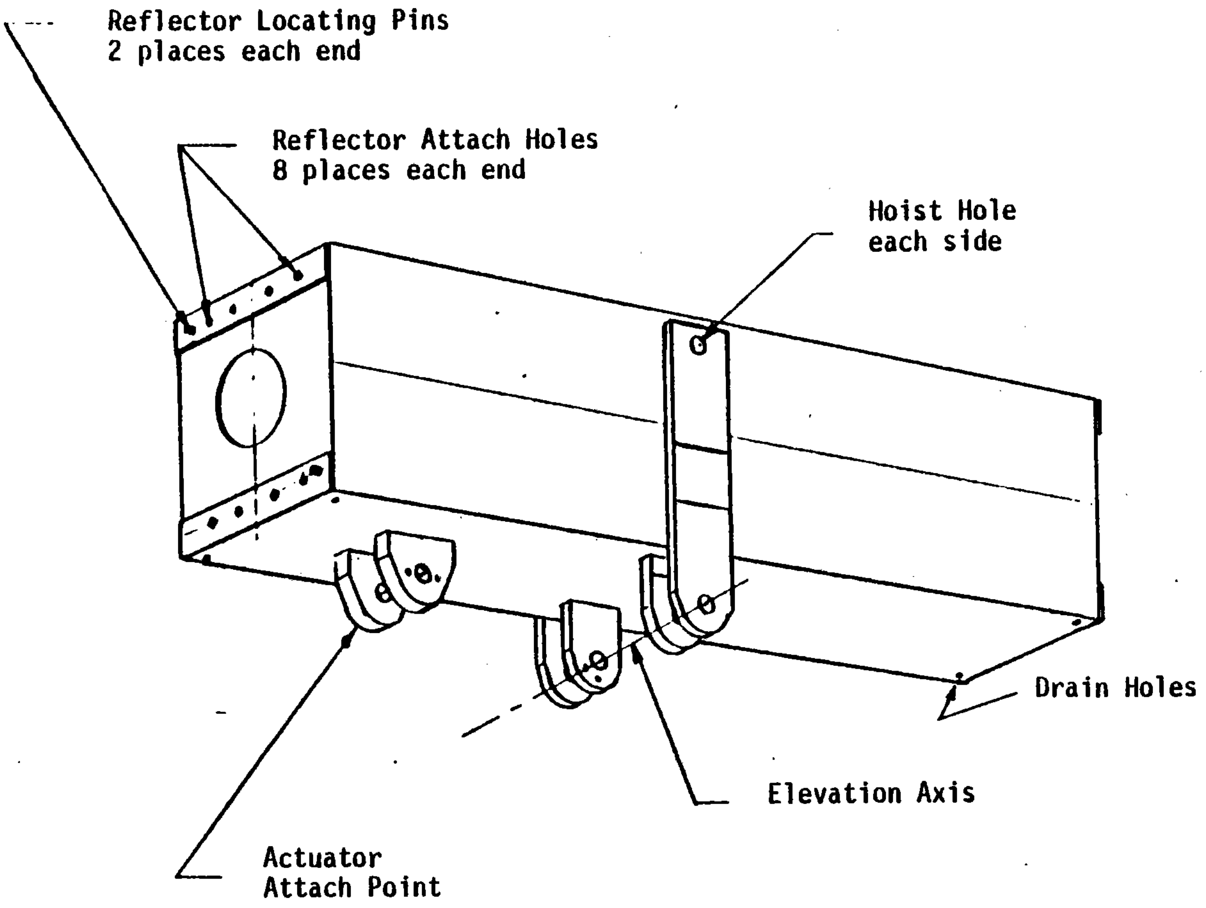

Figure 3-25. Main Beam Assembly

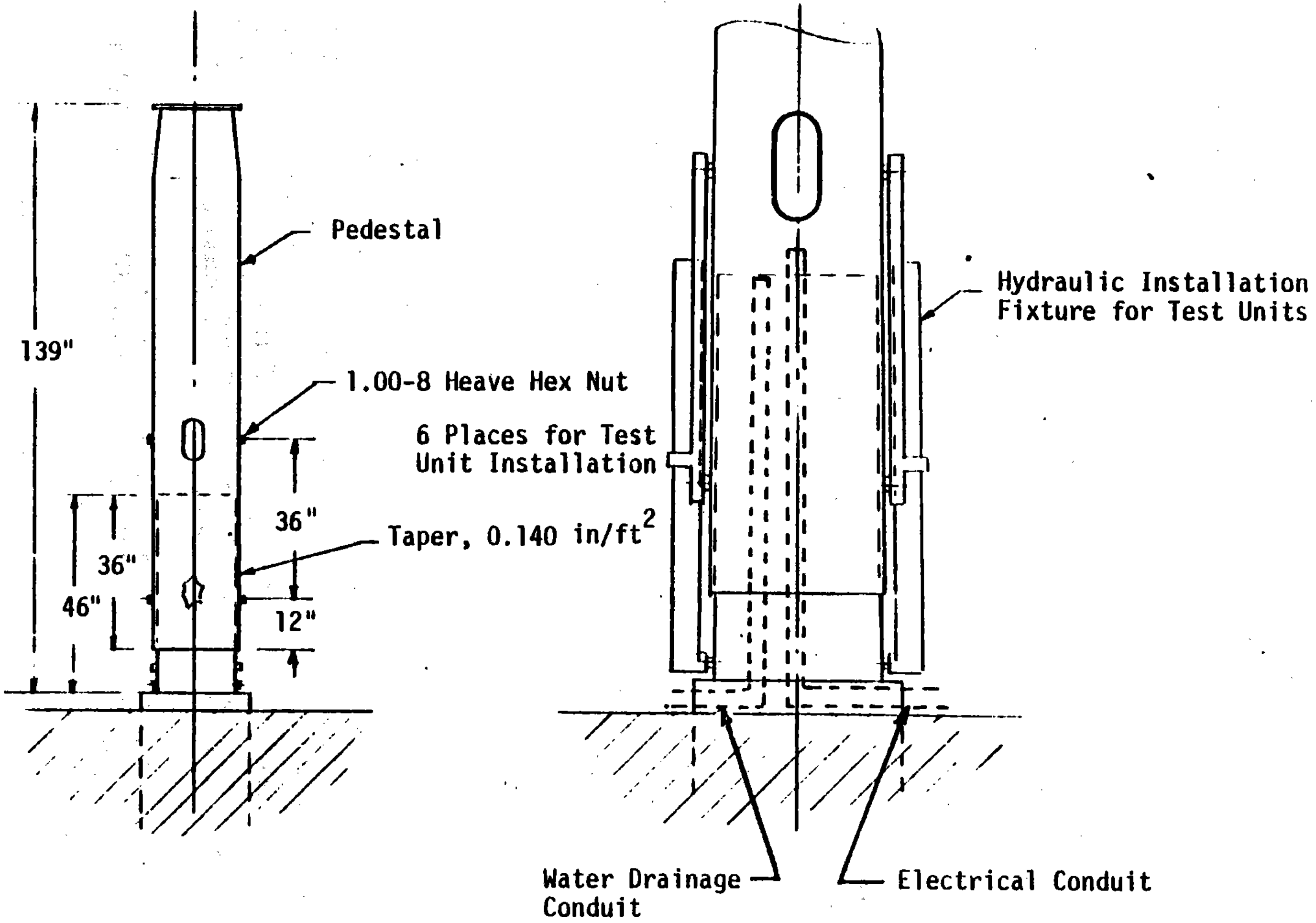

Figure 3-26. Pedestal/Installation

a height of five feet from the ground. The test units have six nuts which are provided to attach an installation fixture so that the proper loads can be applied during mating of the pedestal and foundation.

Figure 3-27 shows a typical foundation along with the requirements of the foundation to support the MDAC Second Generation heliostat.

3.2.2 Drive Design

3.2.2.1 Azimuth Drive (1D22494)

The azimuth drive is a separable sealed unit that is recessed into the top of the pedestal. Figure 3-28 is an illustration of this sealed unit. Expansion chambers are used to compensate for internal pressure fluctuations.

The circular spline portion of the harmonic drive provides the azimuth output rotation. It is supported by a wire race bearing which utilizes the circular spline as seats for the two inner wire races. The lower outer race seat is the flange that mates with the top of the pedestal. Shims are used between this flange and an upper retainer thus providing the proper spacing for the upper outer wire race.

Since the circular spline rotates, the flex spline portion of the harmonic drive is stationary and attached to the outer housing. Flexing is accomplished by a rotating three-lobe wave generator resulting in a reduction of 267:1. The turret bearing and harmonic drive are oil lubricated (Mobil 626). Filler blocks are used to reduce quantity of required oil which reduces cost and the adverse effects of thermal expansion. The oil can be added and level monitored through the port used to mount the upper expansion chamber. A drain port is provided near the base of the flex spline for unscheduled maintenance.

A hollow shaft driven by grease lubed (Alvania EP2) helicon gearing provides the input rotation to the wave generator. The helicon gear is keyed to the shaft and the pinion is an integral part of the drive motor shaft. The helicon reduction is 162:1. Grease and observation ports are provided at the gear level. The hollow shaft is utilized to route the electrical harness for the elevation motor, limit switches, and sensor through the center of the drive. An electrical proximity sensor and magnet are used to indicate revolutions of

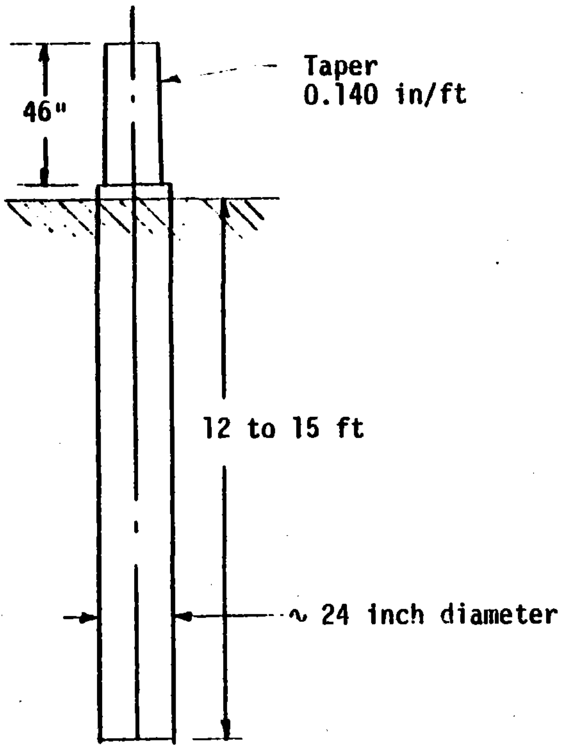

Typical Design

- o Vertical plumbness of tapered cone within ± 1.0°
- o Azimuth orientation of tapered cone within ± 3°
- o Satisfy performance deflection requirements for operating loads (at ground level)

  V = 1200 lb

  M = 200,000 in/lb
- o Satisfy plastic deflection and survival requirement for maximum loads (at ground level)

  V = 4100 lb

  M = 825,000 in/lb

Figure 3-27. Foundation Requirements

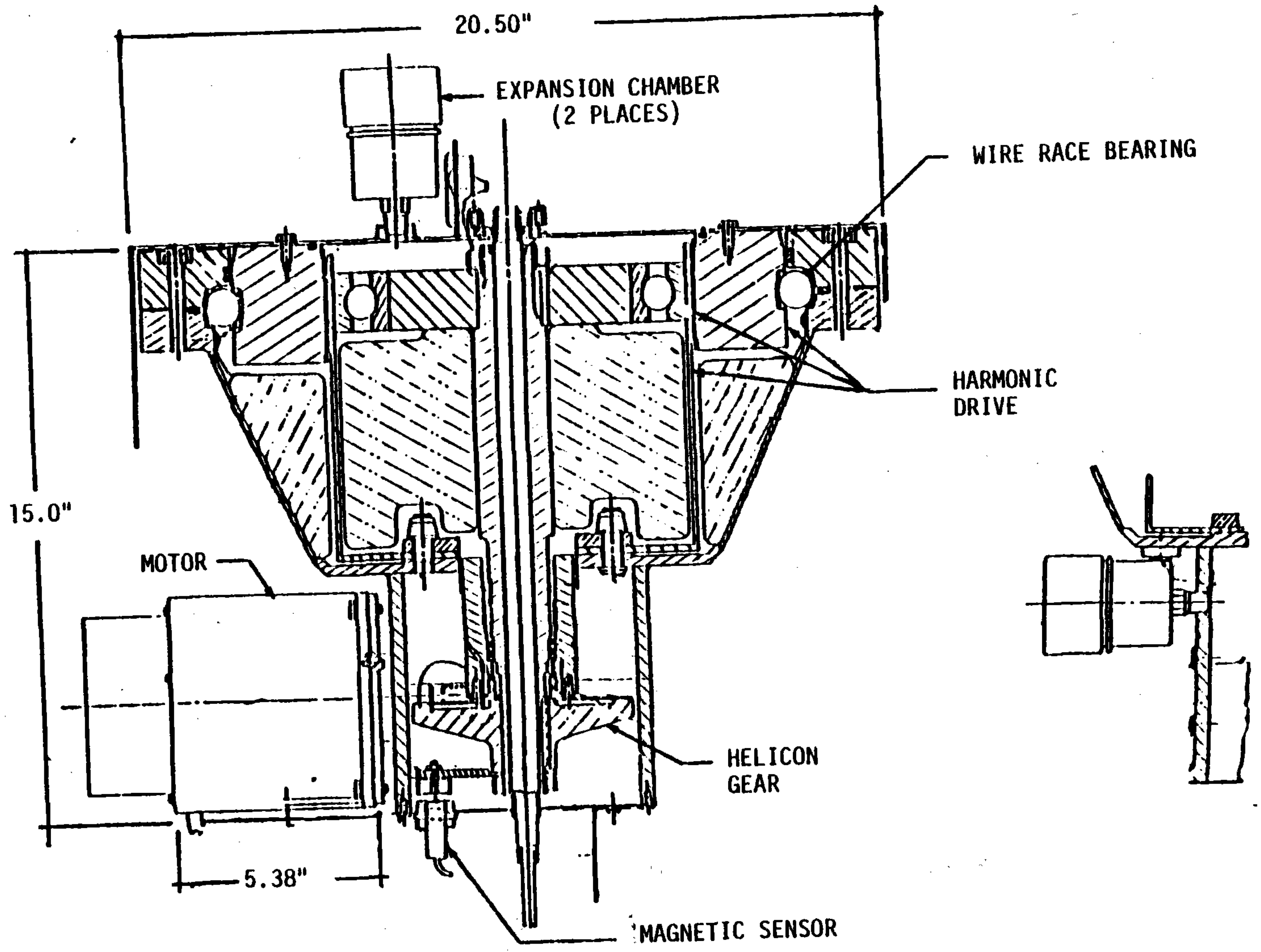

Figure 3-28. Azimuth Drive Assembly

the helicon gear. Another sensor mounted on the pedestal is used with a magnet on the azimuth cover to provide azimuth output rotation count. A motor mounted incremental encoder provides motor rotation count.

The azimuth drive does not require scheduled field maintenance during its projected 30 year life. Field adjustments are not required even with motor replacement. The drive motor is accessible through an opening in the side of the pedestal and is retained with a four bolt pattern. It can be driven manually by removing the incremental encoder cover and rotating the extended motor shaft.

3.2.2.2 Elevation Jack (1D22496)

The jack as shown in Figure 3-29 is also a sealed module and has an integral expansion chamber to compensate for pressure fluctuations. The output rod is chrome plated to resist corrosion and to provide a smooth interface for dual self lubricating support bushings. The same type of bushing is used at the trunnion block for interfacing with attaching trunnion pins.

The ball screw is configured with a traveling nut and 1/4 inch lead (four turns per inch of stroke). The base of the ball screw rod is supported by a set of preloaded tapered roller bearings and driven by the helicon gear set. The output gear is keyed to the rod and the pinion is integral with the motor shaft, as in the azimuth. The helicon reduction ratio is 106:1.

Motor replacement requires no adjustments. Helicon gear rotation is again sensed by a proximity switch and magnet.

3.2.2.3 Elevation Drive Unit (1D22475)

The elevation drive unit includes the interface support structure between the main beam and azimuth drive, the separate jack trunnion pins, the main elevation hinge pins, and the jack rod end attachment. Figure 3-30 illustrates this hardware. The bearings for the various pins utilize sealed self-lubricating sleeve type bearings. Each bearing has an integral rubber seal at each end of the sleeve to keep out contamination. A spherical bearing is used at one of the main beam hinge joints to react against side loads and to aid in alignment during beam attachment.

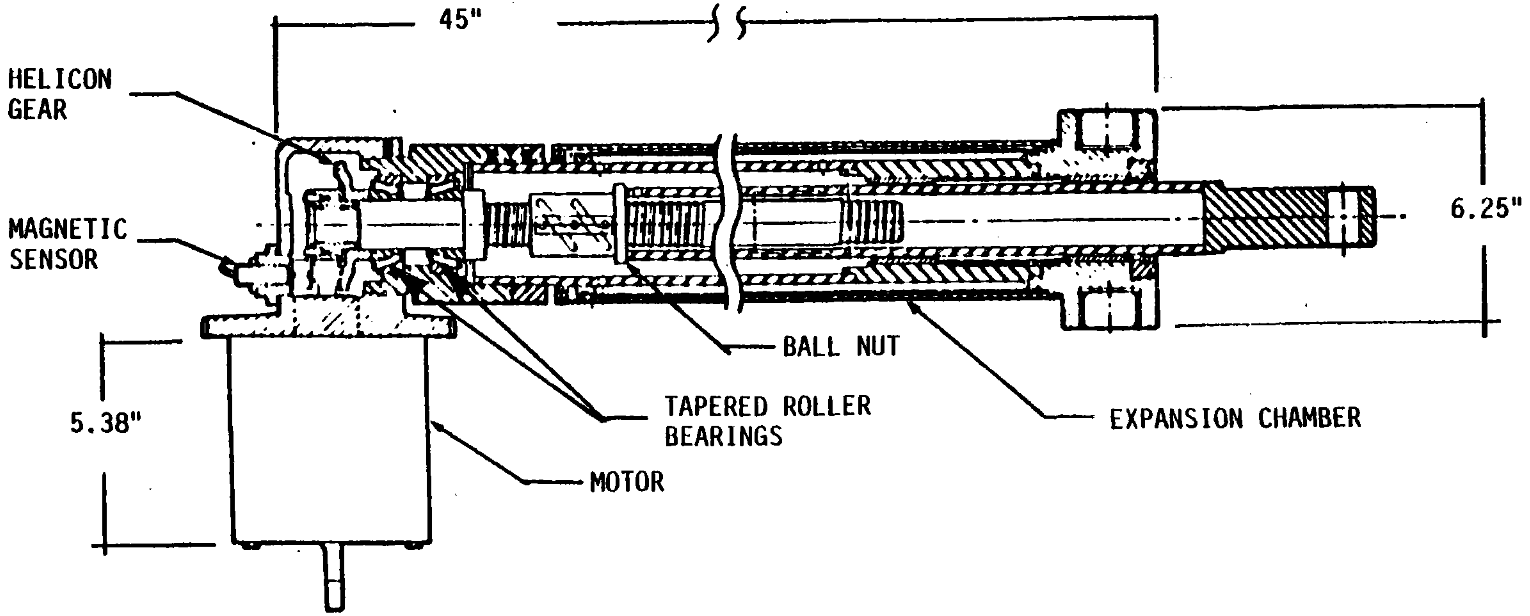

Figure 3-29. Elevation Jack/Drive Motor Assembly

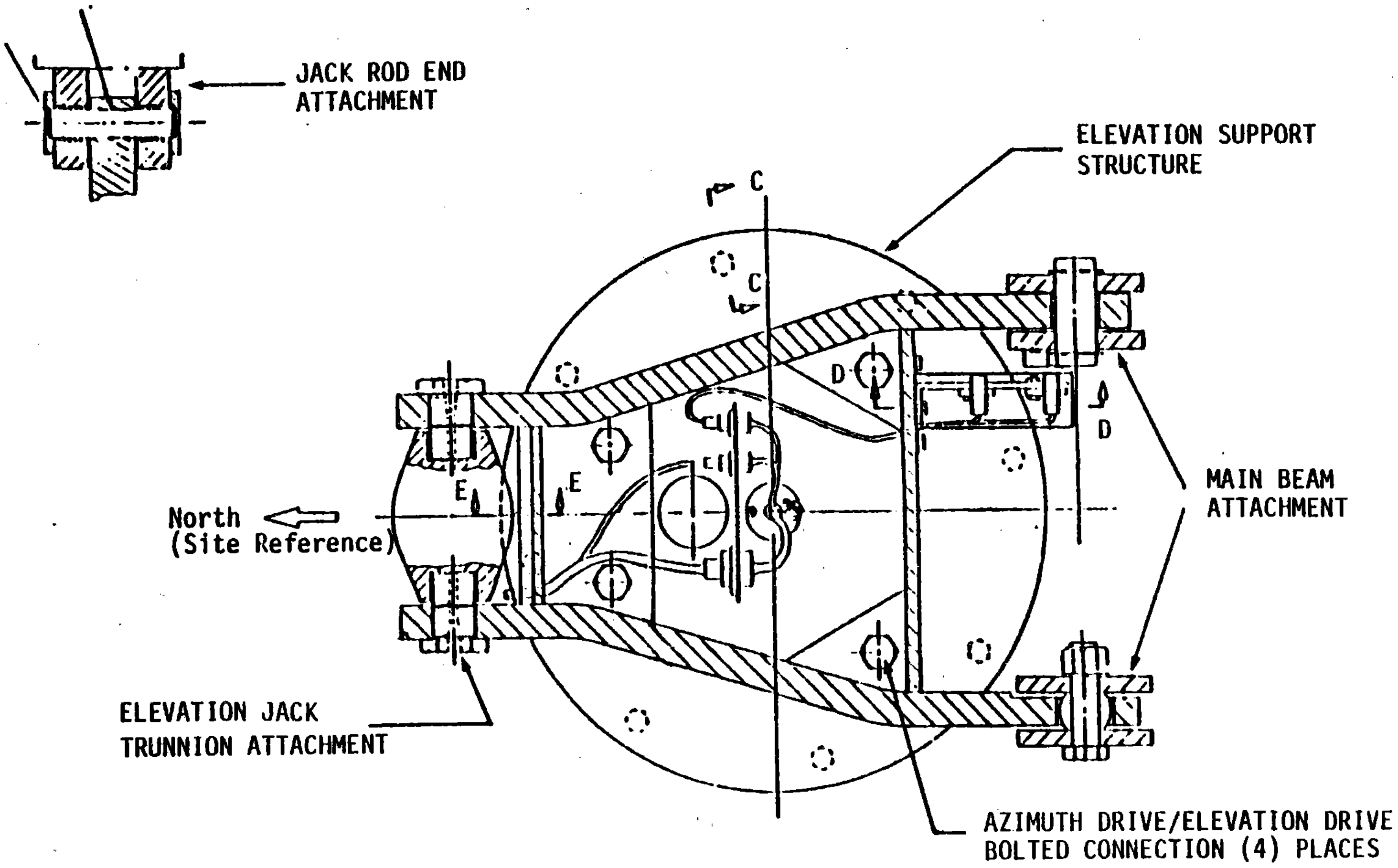

Figure 3-30. Elevation Drive Attachments

The support structure is anchored to the azimuth drive by a four bolt pattern. Removal of these bolts permits the removal of the entire elevation subsystem including the main beam without violating the sealed azimuth module.

3.2.2.4 Seals

The materials for the various seals throughout the drive have been selected primarily for resistance against weathering, oils and grease. The materials that fall into this category and that will provide the maximum life expectancy include viton, hypalon and urethane. Alternative materials have been used in some locations for the CRTF heliostats since use of the proper material would result in prohibitive lead times and cost. Table 3-19 indicates the correlation between usage and material for the current heliostats.

3.2.2.5 Drive Testing

The related drive tests that are included in this report involve the following:

- Azimuth harmonic drive capability test
- Vendor drive motor acceptance tests
- Wire race bearing test
- Jack acceptance tests
- Drive unit design evaluation test.

Only the harmonic drive and motor tests have been completed. The motor vendor data is in Appendix B.

3.2.2.5.1 Harmonic Drive Capability Test

The harmonic drive will ratchet (slip teeth) during operation if the torque load exceeds its capability. Although this is not a failure mode, it is desirable to avoid ratcheting since a full reference update (Paragraph 3.2.3.5) is required to realign the heliostat following such an occurrence. A structural or material failure has to occur before the drive will slip under static conditions. This test was conducted to determine the operational condition where ratcheting would occur. Torques were applied incrementally to the azimuth drive to obtain the ratchet data. The data indicated that ratcheting occurs repeatedly at 125,000 in-lbs operational torque but not at 103,000 in-lbs. Static loads were also applied at a given factor over and above the operational load to correspond to probable load relationships. No failures or deformations occurred with static loads up to 212,500 in-lbs.

Table 3-19
RUBBER MATERIALS FOR MDAC SECOND GENERATION HELIOSTAT DRIVE SYSTEM (CRTF HELIOSTATS)

Use	Component	Material
Azimuth Turret Bearing Static Seal	O-ring	Viton
Azimuth Turret Bearing Dynamic Seal	O-ring	Viton
Azimuth Cover Static Seal	O-ring	Viton
Azimuth Motor Static Seal	O-ring	Viton
Azimuth Wire Tube Dynamic Seal	Wiper Ring	Viton
Azimuth Harmonic Drive Shaft Dynamic Seal	Wiper Ring	Graphite-Teflon
Azimuth Expansion Chamber	Diaphragm	Viton
Elevation Jack Rod Dynamic Seal	Wiper Ring	Neoprene
Elevation Pivot Bearing Seals	Wiper Ring	Urethane
Elevation Expansion Chamber	Diaphragm	Neoprene
Elevation Housing Static Seal	O-ring	Viton
Elevation Motor Static Seal	O-ring	Viton
Elevation Magnetic Sensor Mount	O-ring	Viton
Azimuth Harmonic Drive Shaft Bearing	Bearing Grease Seals	Buna-N
Azimuth and Elevation Drive Motor Shaft Bearings	Bearing Grease Seals	Buna-N

Under the worst case stowage conditions involving adverse heliostat orientation and gust fronts to 50 mph, loads up to a maximum of 144,000 in-lbs can be encountered. This combination of events is a rare occurrence statistically. However, to avoid ratcheting of the azimuth drive, the loads may be reached statically by initiating azimuth travel to stow under these conditions only when the elevation angles are less than 45 degrees.

3.2.2.5.2 Drive Motor Tests

These tests were conducted by the motor vendor as a part of standard acceptance test procedures. A copy of the data transmitted to MDAC is included in Appendix B. The hardware data provided a good correlation with prior predicted computer simulation data thus lending confidence to the model being used. The following summary includes 1/4 and 1/3 HP hardware data, and model data for the higher start torque motor contemplated for elevation.

Motor Data at 208V	1/4 HP	1/3 HP	Higher Start Torque Motor (Computer Data)
Rated RPM	1774	1732	----
Torque at rated RPM (in-lbs)	9.2	12.2	----
Amps at rated RPM	1.1	1.4	1.4
Locked rotor torque (in-lbs)	37.5	41.8	63.0
Locked rotor amps	7.3	8.0	9.5

3.2.2.5.3 Wire Race Turret Bearing Test

The wire race bearing has not been used on previous heliostat designs, so development testing was intiated to determine its performance in this particular configuration. The objectives are:

- Check out assembly techniques.
- Determine the effect of bolt torques, shim sizing and overturning moments on the torque required to rotate the bearing.
- Determine the deflection and hysteresis in the bearing up to overturning moments corresponding with survival conditions.
- Life indications when cycled under overturning moments corresponding with maximum gravity loads.

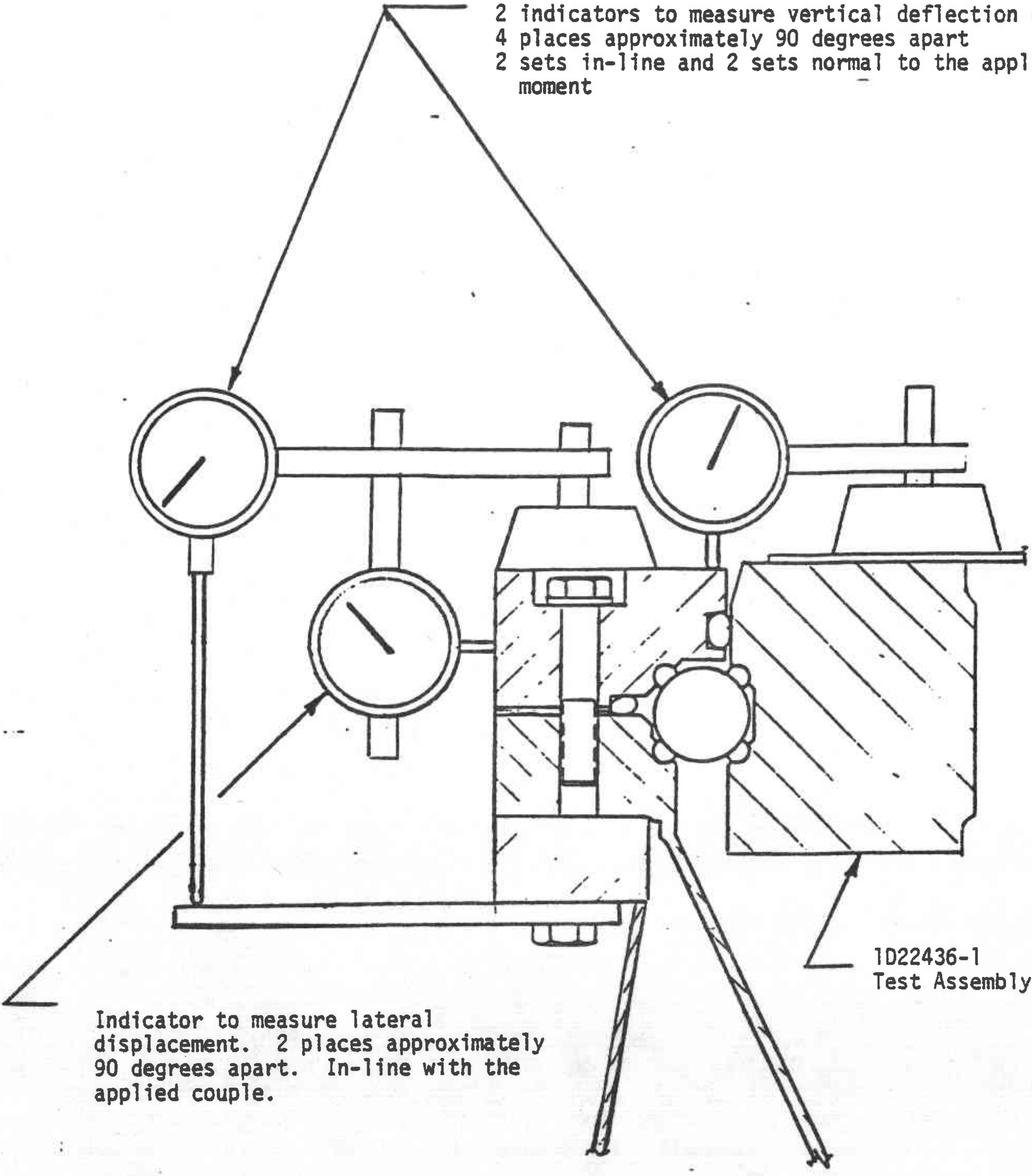

2 indicators to measure vertical deflection -
4 places approximately 90 degrees apart
2 sets in-line and 2 sets normal to the applied moment

1D22436-1
Test Assembly

Indicator to measure lateral displacement. 2 places approximately 90 degrees apart. In-line with the applied couple.

Figure 3-31. Dial Indicator Setup to Measure Deflection

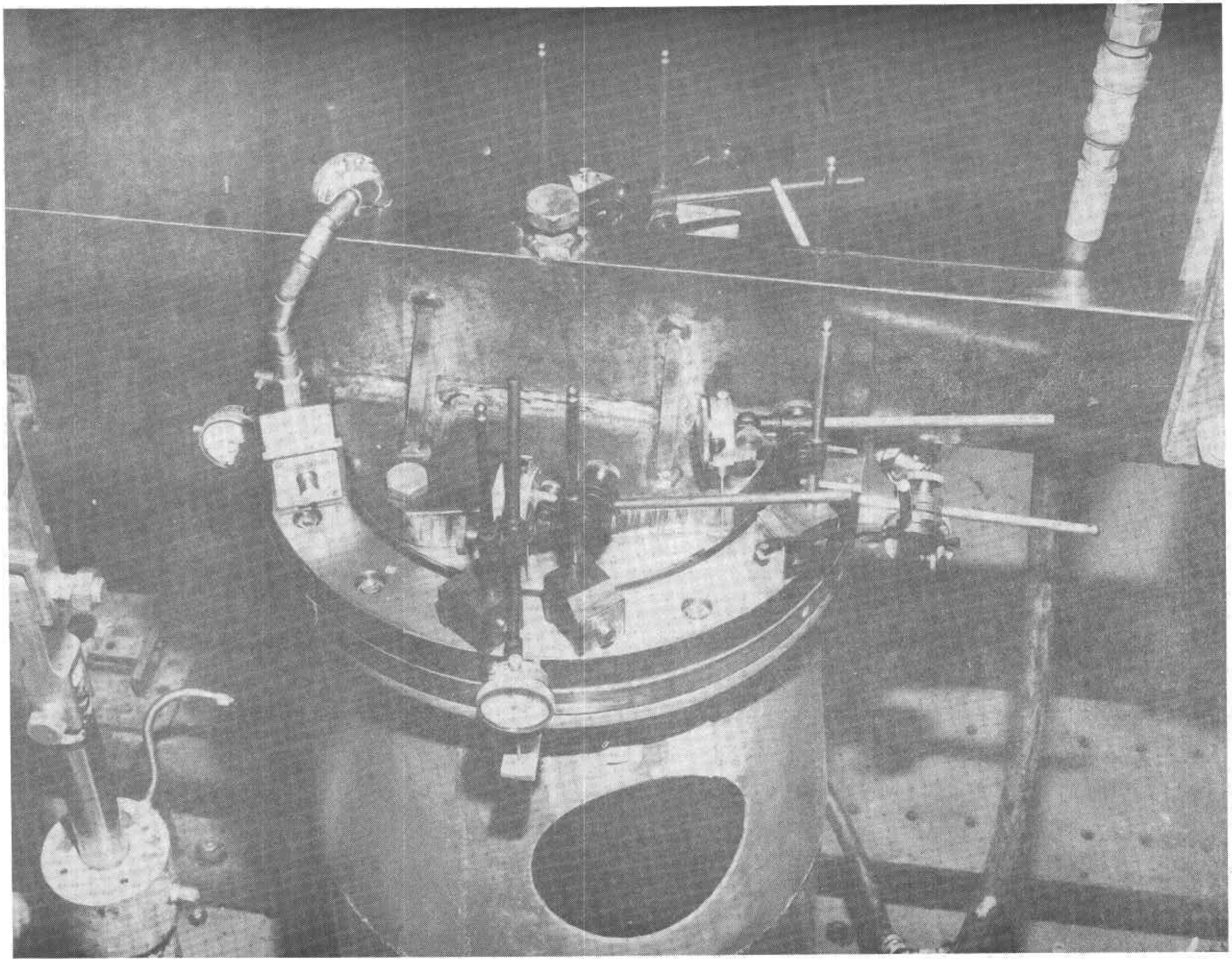

Figure 3-32. Wire Race Bearing Test

The tests are in progress and preliminary data indicates good performance. The backlash and compliance deflections appear to be reasonable with an easily definable shim thickness. Bearing torques are not excessive when assembled with the proper shim thickness. Figure 3-31 preceding shows a cross section of the bearing with indicators positioned to measure deflections during hysteresis testing. Figure 3-32 preceding is a photograph of the actual test setup.

3.2.3 Controls and Electrical Hardware Design

The major elements of the controls hardware are the HAC, HFC and HC. The HAC is located in the master control area. The HFC is located in a collector field in the data distribution interface assembly and is a proprietary design of MDAC. For 2nd Generation test demonstration purposes, the HFC electronics will be collocated with the HAC. The HC is located at each heliostat and is also a proprietary design of MDAC.

3.2.3.1 Electrical Installation and Interface

The electrical installation for Second Generation has been simplified over previous MDAC designs by the elimination of absolute encoders, the contactor box, the circuit breaker box, several wire harnesses, all but one limit switch, and conduit. Maintainability and field servicability have been improved by going to a lower pedestal controller box location, a hinged attachment for the box, color and/or size coding of connectors, wire harness service loops and judicious use of connectors, e.g., for jack removal. Reliability of the electrical system has also been improved by eliminating exposed wiring and reducing the number of connectors by one-half. Furthermore, with the protected wire scheme, a cost savings was realized inasmush as UV resistant insulation on wire costs five to ten times as much as conventional wire.

A typical facility interface with the Second Generation heliostat is shown in Figure 3-33. Three-phase, 208V ± 10%, 60 Hz power with a neutral and safety ground is required. For data communications, a twisted shield pair is required, # 18 AWG with less than 50 pf/ft nominal capacitance and limited to 2,000 ft.

3.2.3.2 HAC

The HAC for the test demonstration activity at CRTF will be a PDP 11/34 with 128K bytes of memory, floating point operation, a four line EIA RS232 serial interface and an RSX-11S operating system. Peripherals include a dual floppy disc (512K bytes), a 150 CPS printer and a color CRT. Figure 3-34 shows the configuration for CRTF.

POWER REQUIREMENTS

- 3 PHASE, 208V AC, 60 HZ, ± 10%
- NEUTRAL
- SAFETY GROUND
- 15 AMP SERVICE

COMMUNICATIONS REQUIREMENTS

- TWISTED SHIELDED PAIR
- #20 AWG
- ONE LINE FROM CONTROL ROOM TO EACH FOUNDATION

PULL BOX REQUIREMENTS

- 208V UTILITY OUTLET (5 WIRE)
- 110V UTILITY OUTLET (3 WIRE)
- ONE 3/4" KNOCKOUT
- TERMINAL BOARD INTERFACE

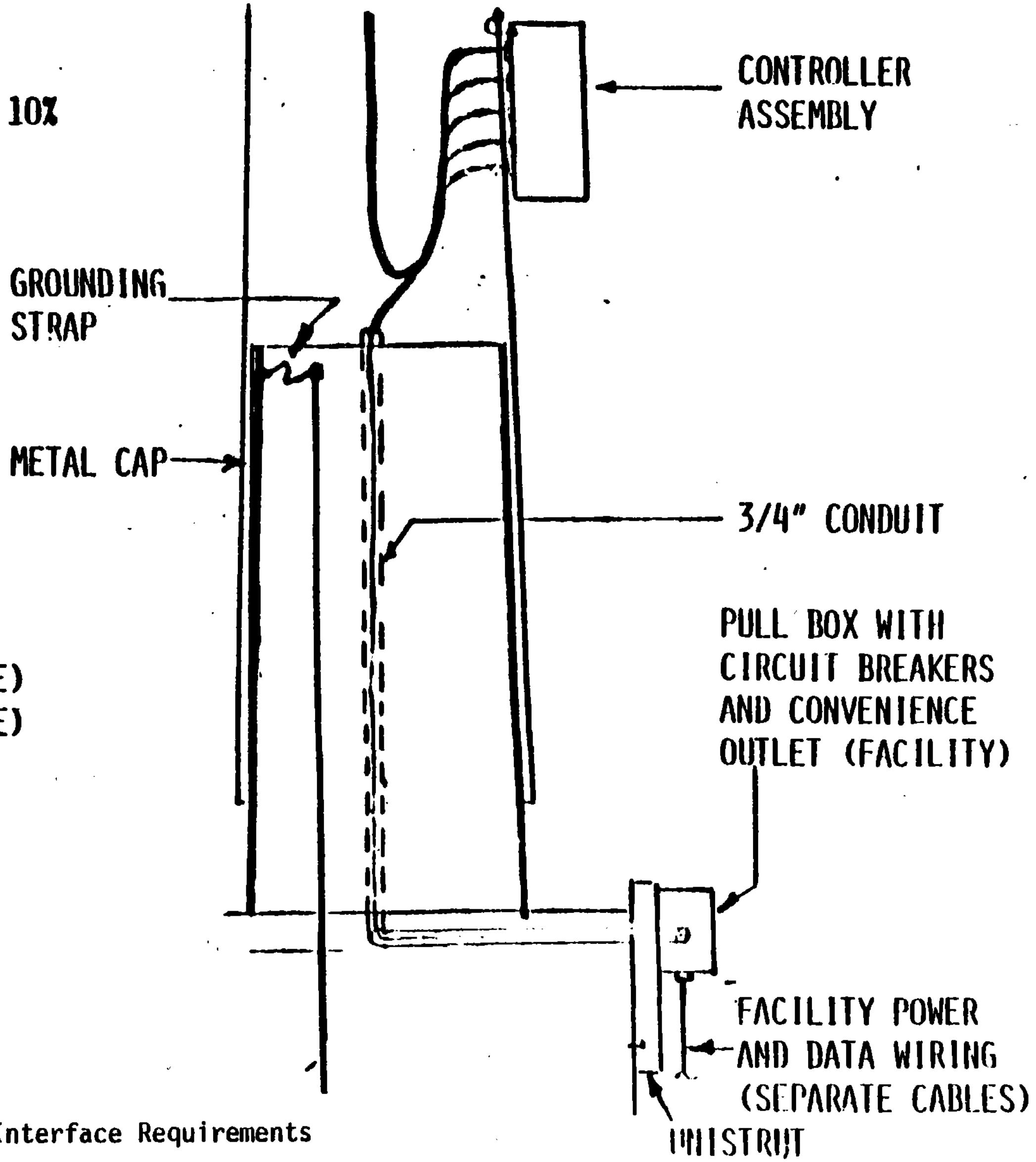

Figure 3-33. CRTF Electrical Interface Requirements

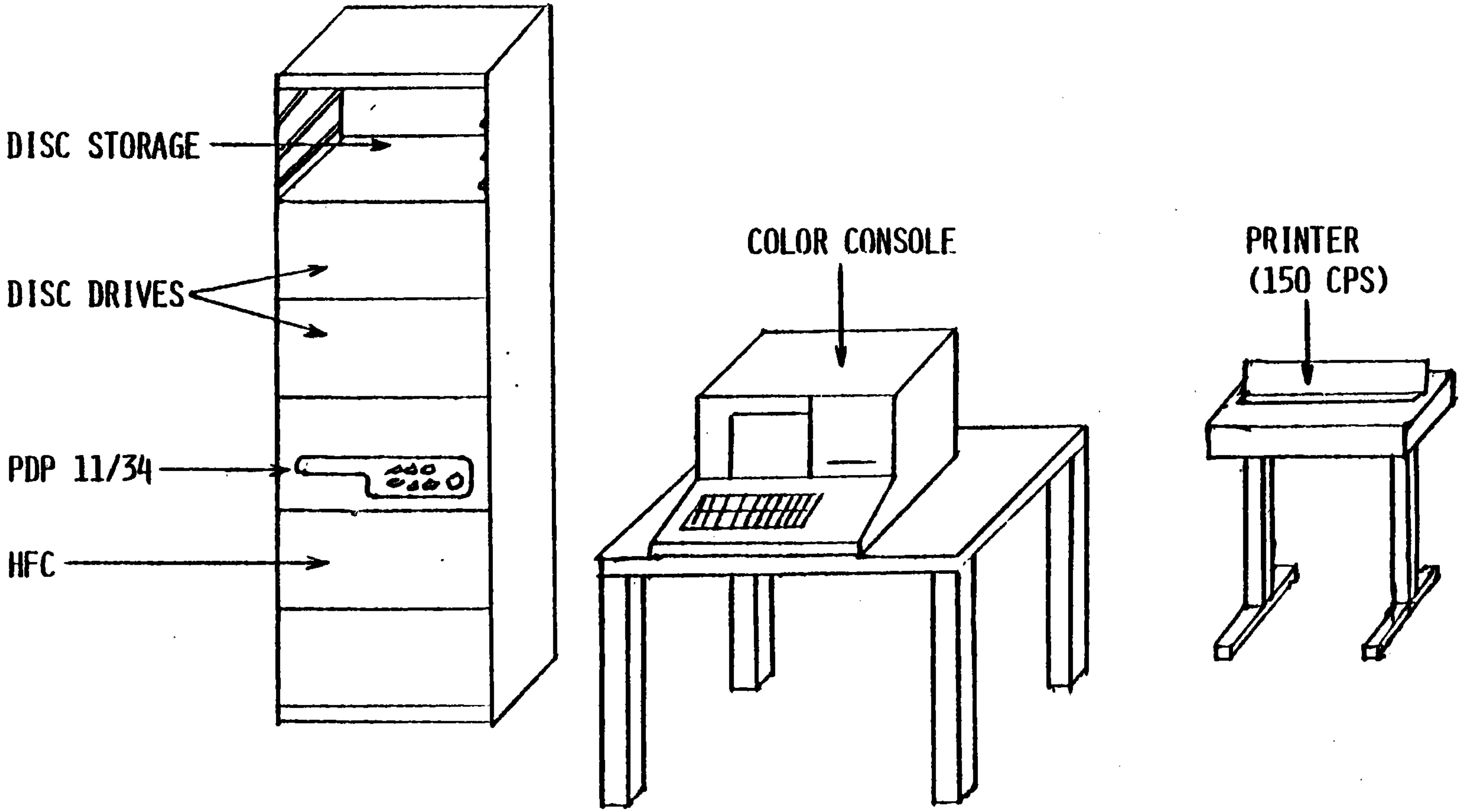

Figure 3-34. HAC and HFC Equipment Configuration for CRTF

3.2.3.3 HFC

The HFC's for Second Generation are located in the Data Distribution Centers (DDC's) which are strategically distributed in the collector field. Each DDC will contain up to eight HFC controllers providing control of up to 256 heliostats. The DDC will be a weather-proof enclosure mounted on a concrete slab. In addition to HFC circuit cards, it will contain 5 VDC and 12 VDC power supplies. DDC field locations will be optimized for minimum field wiring costs. At CRTF, the HFC will be collocated with the HAC.

The HFC circuit design is based on the 8085 Central Processing Unit (CPU). It operates at 3.072 MHz. Memory consists of 2K bytes of ultraviolet erasable PROM and 16K bytes RAM. Features include a direct memory access (DMA), an arithmetic processing unit (APU), an interrupt controller, and a real time counter. Communication with the HAC's and HC's is handled by 3 universal synchronous/asynchronous receiver/transmitters (USART's) which are linked to the communication lines by transceivers. A Field Programmable Logic Array (FPLA) is used for certain decoding. The rest of the IC's consists of various gates, buffers, decoders, flip-flops, and counters.

3.2.3.4 HC

The heliostat controller electronics includes all heliostat peculiar hardware; the controller assembly, incremental encoders, reference sensors, motors and wiring.

<u>Controller Assembly</u>

The controller assembly (Figure 3-35) is the heart of the HC electronics. The enclosure is an 18 x 12 x 8 inch welded steel NEMA 3 box. It is hinge-mounted on the pedestal and contains the following: HC processor circuit card, motor controller circuit card, mother board, 5 VDC power supply, contactors, contractors surge suppression network, and lightning surge arrestors. The Second Generation controller assembly has been improved relative to the Barstow Pilot Plant design by a reduction in parts count, refined packaging (heat sinks, wire routing, attachments, circuit card alignment), and power supply redesign to add a power dropout capability.

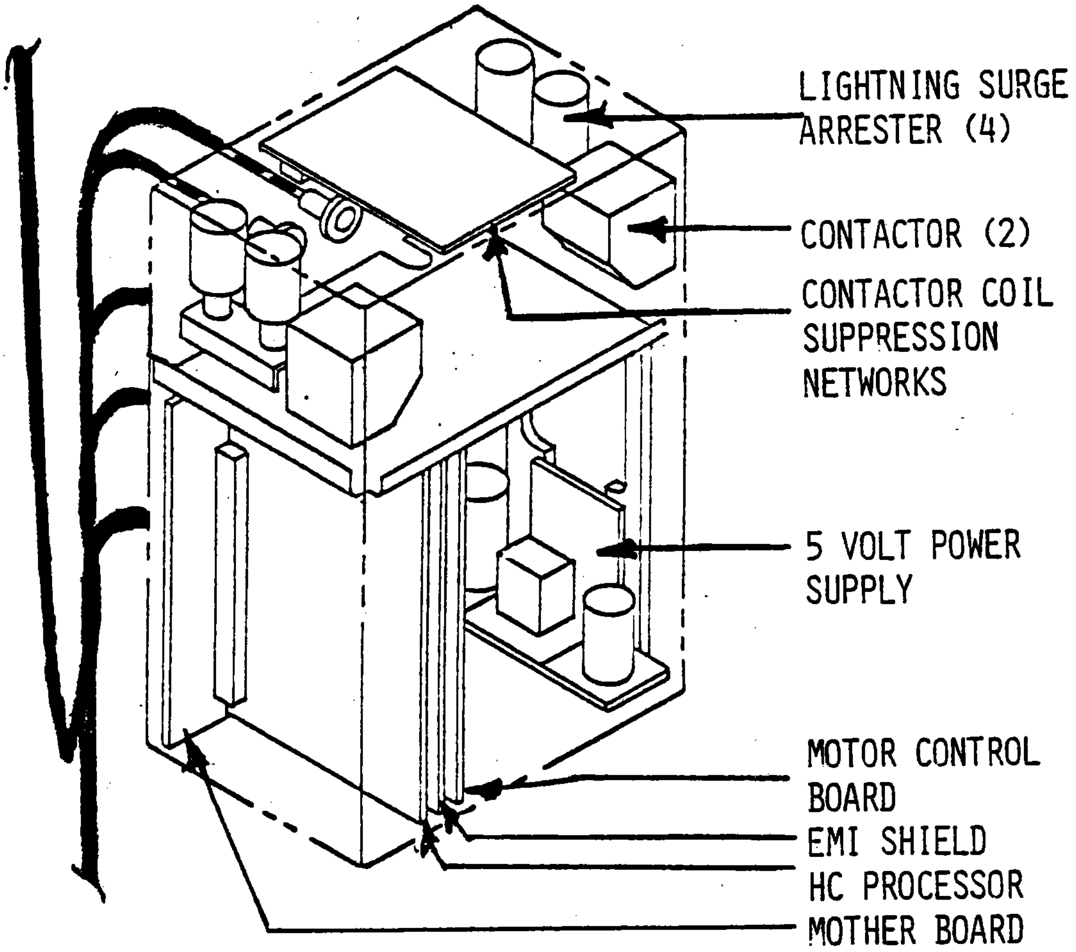

Figure 3-35. Controller Assembly, Second Generation

With the Second Generation design the previously used contactor box and circuit breaker box have been eliminated. Connectors for the controller assembly interface with the balance of the heliostat electronics and field wiring were selected for ease of maintenance and service considerations. The connectors also serve to segregate the box between DC (lower section) and AC (upper section) functions.

The HC processor circuit card is a 7 x 11-1/2 inch, two sided board with approximately 60 components. The layout of the board was based on automatic insertion equipment with wide circuit traces, trace spacing and pads to optimize yield. The processor is developed around the INTEL 8748, one chip microcomputer which contains 1K EPROM and 64 bytes of RAM. An 8755A EPROM is used during development for an additional 1K of EPROM. In production, the 8748/8755 will be replaced with an 8049 ROM.

In order to provide an automatic test capability, the circuit card for Second Generation includes a test connector and IC sockets for selected components, e.g., the microprocessor. Industrial grade IC components (or better) with an extended temperature capability to 85°C are baseline for the HC processor. In addition, all IC's are screened to MIL 883B and all passive components have an established failure history. These steps are considered necessary to maintain a reliable product in the environments anticipated for solar hardware.

The motor controller circuit card is also a 7 x 11-1/2 inch, two sided board with approximately 50 components. Circuit design is identical to that baselined for pilot plant production. This design has been under nearly daily use since September 1979 at SETF without incident. Motor control is achieved by TRIAC switching of three-phase 208V 60 cycle AC. TRIAC switching commands initiate at the HC processor with pulse transformer coupling on the motor controller circuit card. The motor controller has also been designed for automatic test equipment.

The mother board is a 6 x 11 inch, two sided circuit board. Interface of the HC processor and motor controller with each other and the balance of the controls hardware is provided by the mother board. Three phenolic alignment guides, one at each end and one in the middle of the board, have been used to ensure proper mating of the daughter/mother board connectors before pin engagement. There are no active components on the mother board, only connectors.

The 5 VDC power supply used by the controller is a commercial purchased part. Analysis, test and supplier discussions have determined that the power supply, as purchased, can tolerate the AC voltage overshoot requirements of the specification without modification. However, approximately 30,000 μf has been added to the power supply to accommodate the three cycle dropout requirements.

Contactors and lightning surge arrestors are also purchased parts located in the controller.

Lastly, a printed circuit card assembly has been added to the controller to accommodate resistor/capacitor surge suppression networks associated with contactor coils. A printed circuit card was selected as the packaging method for those components to reduce assembly costs.

Incremental Encoders

Two identical MDAC developed incremental encoders (Figure 3-36) are used on a heliostat, one on the elevation tracking motor and the other on the azimuth motor. The incremental encoder uses two magnetic sensors and a ferrous metal vane on a motor shaft to count motor turns for use by the HC processor. The Second Generation design uses the identical piece parts and circuit design as tested for the Barstow Pilot Plant. A significant packaging improvement has been achieved, however, by the replacement of a flexible printed circuit board with a standard flat board. The reliability of the incremental encoder has also been improved by the elimination of two connectors and the relocation of motor wires from underneath the encoder cover. The "breathable" packaging design of the encoder demonstrated in the Barstow Pilot Plant environmental tests at Point Mugu has been retained. It is planned that the incremental encoder and motor will be serviced as a unit; no field repair of the encoder itself is anticipated.

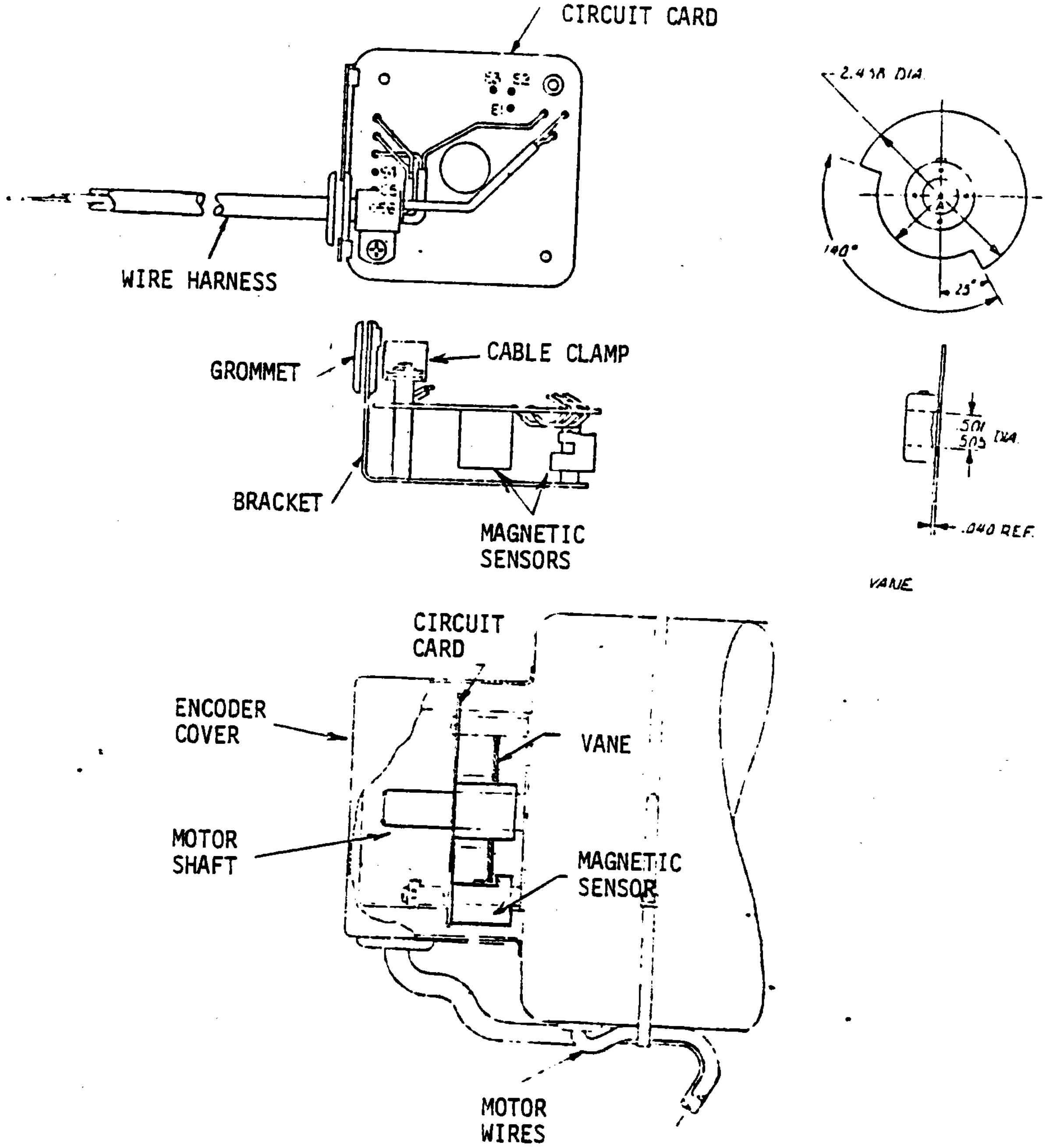

Figure 3-36. Incremental Encoder Assembly

Reference Sensors

Five position sensing proximity switches are required per heliostat to provide azimuth and elevation reference point detection. The sensors are purchased parts from Fifth Dimension, Inc., and replace the previously used absolute encoders. The sensor selected, type LC2P-1839, is a magnetically actuated mercury wetted sealed switch (see Figure 37). This device has a significant cost advantage over the absolute encoder approach while providing high reliability, mean cycles between failure exceeding 2×10^9 operations. The device is compatible with the control logic 5 VDC system and is field replaceable.

Motors

The azimuth and elevation motors are both AC motors manufactured by Emerson Electric, operating at 208V, 60 cycle, 3-phase, wye connected. The azimuth motor is 1/4 HP and the elevation motor is 1/3 HP. Both have a NEMA Type C torque/speed relationship.

Power requirements have been estimated for the Second Generation heliostat for the tracking, slew and stow modes. During track, approximately 35 watts (75V amps) of power is required per heliostat. (This estimate and all others include motors and electronics.) During slew, as in an emergency defocus operation, approximately 335 watts (500V amps) of power is required per heliostat. In this condition one motor is in continuous operation and one motor is pulsing for approximately 10 to 60 seconds. During stow, approximately 655 watts (930V amps) of power is required per heliostat. This is based on two motors in continuous operation. Since stow takes only 2 to 6 minutes to perform, it is anticipated that stowing of heliostats will be performed in groups (e.g., 2, 3, or 4) in order to minimize power demands. In a one year period a heliostat may use 175 KWHR of power assuming one unstow and one stow operation per day, a 10 hour tracking day and a 365 operating-day year.

The power requirements for defocus and emergency stow for a 50 MWe field for the MDAC heliostat are more system dependent than collector dependent. With the following field layout and requirement assumptions, defocus and stow power requirements are estimated as shown.

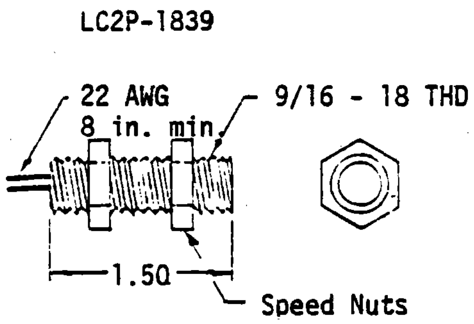

Figure 3-37. Reference Sensor

Emergency Defocus

Approximately 335 watts/heliostat is required to move a heliostat from target track to standby aimpoint track. Heliostats are commanded to the standby point in groups of three, separated by one second. For example:

Time (sec)	Commanded Heliostat
0.0 - 0.036	#1
0.036 - 0.072	#2
0.072 - 0.108	#3
0.108 - 1.108	--
1.108 - 1.144	#4
1.144 - 1.180	#5
1.180 - 1.216	#6, etc.

After 11.152 seconds, the HFC will have communicated with all 32 heliostats in the group. The power requirements, therefore, for a typical group will grow from 335 watts to a maximum of 32 x 335 watts or 10,720 watts.

The total power required by a 50 MWe field is not the number of heliostats per 50 MWe field x 335 watts. The modifying consideration is the variable time required by individual heliostats to get off target. For instance, a heliostat 1,000 meters away from a 20 meter^2 target, 200 meters above grade will take approximately 2.5 seconds to get off target. Under these conditions, some heliostats will achieve the standby aimpoint before others have even been addressed by the HFC. In fact, only nine heliostats in this group of thirty-two will be in the slew mode at any one time. The power demand for this group is reduced by approximately 72 percent, from 10,720 watts to a maximum of 3,015 watts. For heliostats closer in to the receiver tower; e.g., 250 meters; the time to move any one heliostat off target exceeds the time to communicate with all 32 heliostats. The power demand, therefore is 32 x 335 watts or 10,720 watts.

The total power required by a 50 MWe field depends on the field layout (north field only or surround field), the allowable number of seconds to get the whole field or a percentage of the field off target, and the location of the standby aimpoints (one, two or three ... receiver diameters away from receiver). A rough estimate for a surround field of 5,400 heliostats, a 20 meter^2 target 200 meters high, and a standby aimpoint one receiver diameter away from the target would be 790 KW where 75 percent of the heliostats would be off target in 20 seconds and all heliostats off in 30 seconds. If heliostats were further sequenced such that all heliostats were off target in 60 seconds, the power demand could be reduced to 300 KW.

Stow

The estimate of 655 watts per heliostat for stow (face up) is based upon continuous operation of both the azimuth and elevation motors. The stow operation takes from 2 to 6 minutes depending on initial heliostat orientation. To stow an entire field in less than 6 minutes would require 655 watts x number of heliostats per field. With a design modification to stow in elevation only (seemingly acceptable in an emergency high wind situation), the power demand can be reduced from 655 watts to 380 watts per heliostat. Further reduction can be achieved by stowing in groups. If, for instance, emergency power of 275 KW is provided for emergency defocus, the same power source could be used for stow. Approximately 725 heliostats would be stowed at once with the entire field being stowed in about 1/2 hour.

Transient Response

The above data are based upon motor running currents. Each heliostat does, in addition, have a starting transient of approximately 6 amps which decays to running load in about 5 AC cycles (80 msec). It is doubtful that this would be seen by the buss.

Wiring

There is essentially no exposed wiring on the Second Generation heliostat. Wiring from the controller assembly to the azimuth reference sensor, azimuth helicon sensor, azimuth motor and azimuth incremental encoder is done within the pedestal where it is protected from the environment, particularly ultraviolet and other damage. Connector terminations are used where appropriate for maintenance and are made on a bracket attached to the azimuth drive lube pan. Wiring which must reach the tracking jack and elevation sensors passes through the azimuth drive in a tube within a tube. All wires are clamped to the inner tube which turns with the azimuth drive eliminating any possibility of twisting wires within the tube. Connector terminations above the azimuth drive are also used where appropriate for maintenance and are also made on a bracket (Figures 3-38 and 3-39). Although connectors are still considered mandatory for a producible and maintainable heliostat, the Second Generation design uses only 11 connectors as opposed to 29 for the Barstow Pilot Plant design.

3.2.3.5 Software Design

The software for the Second Generation heliostat is based upon the MDAC Pilot Plant heliostat design.

The changes that are being made in the software are to accommodate a non-inverting heliostat, a new HAC computer, a new reference update scheme and simplification of the operator interface with the HAC. The last two changes will be discussed in some detail in this section.

Software Capabilities

Some of the general capabilities of the software are:

- HAC Control Capability - The HAC operator interface is designed for 1 HFC and 2 HC's, although the HAC data is designed for more.
- HAC External Interface - The HAC will not have any capability to interface with such things as master control, receiver, beam characterization or data acquisition system.
- HAC Backup - The HAC will consist of a single computer and will not have any logic for a backup computer.
- Stow Position - There will be a single stow command which will result in the heliostat going to a vertical position, mirror normal horizontal. If a horizontal stow position, face up, is desired, then the operator will have to use a gimbal command to position the heliostat in this position.

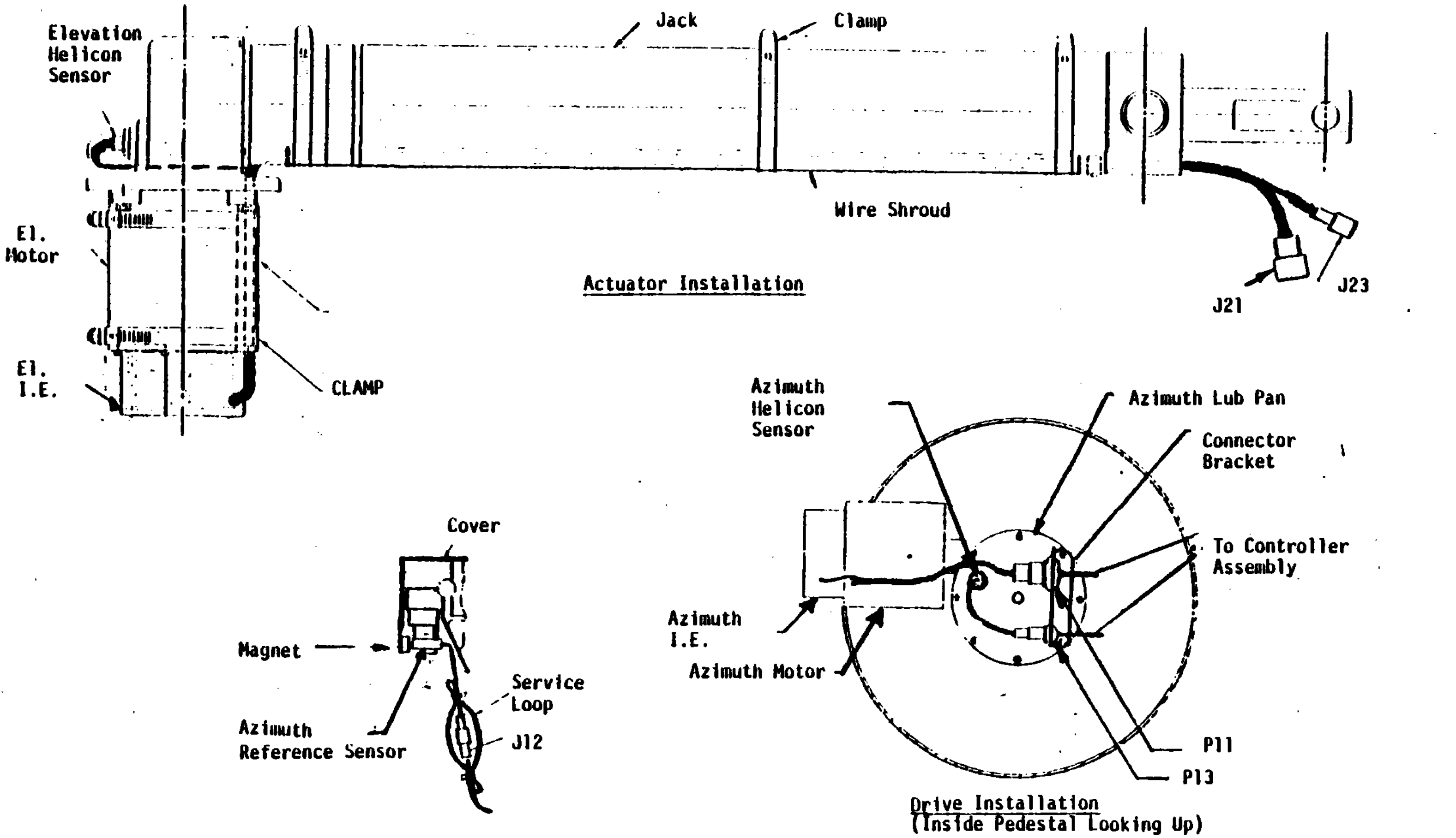

Actuator Installation

Drive Installation (Inside Pedestal Looking Up)

Figure 3-38. Elevation Jack and Azimuth Drive Electrical Installation

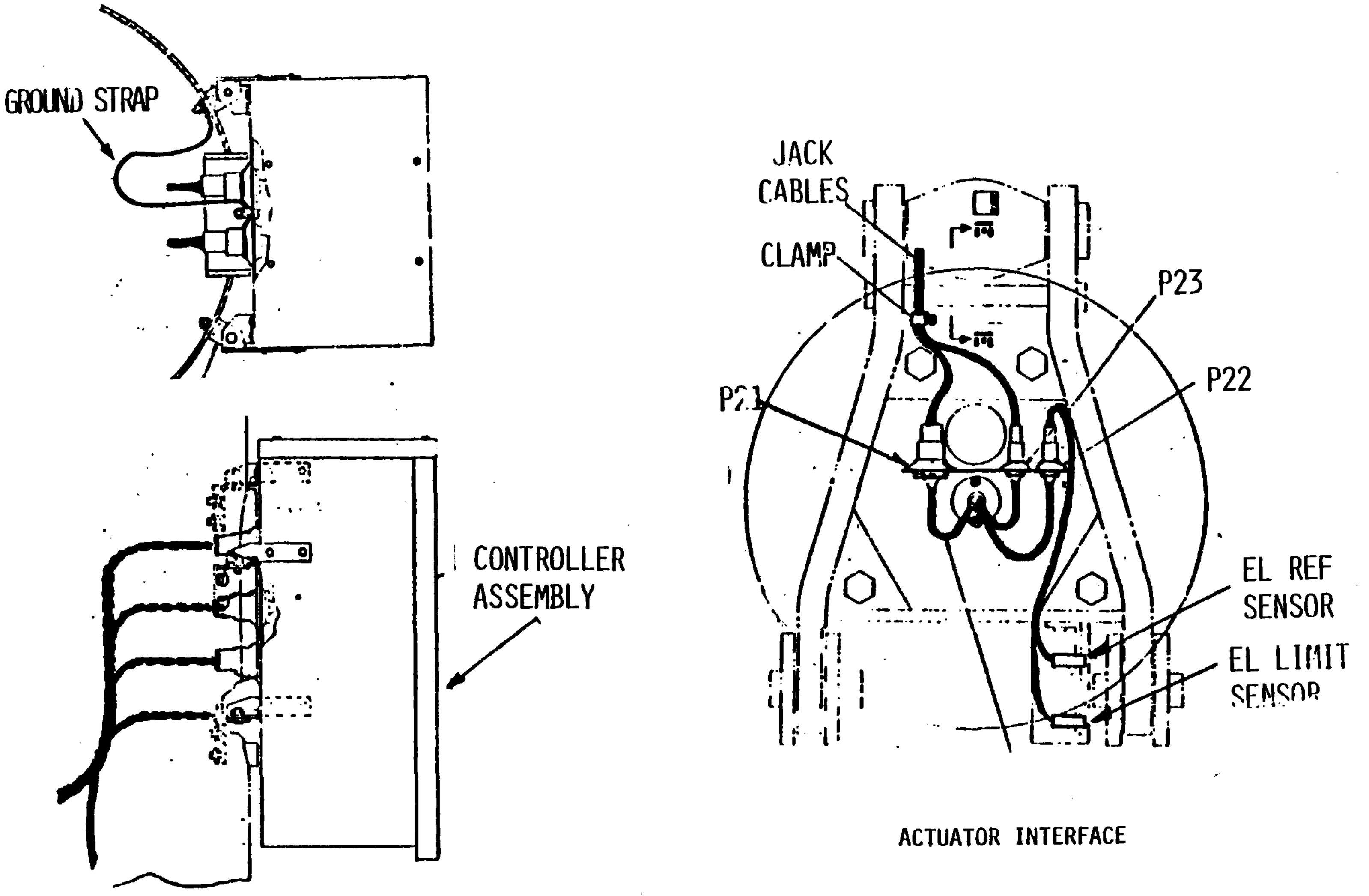

CONTROLLER INTERFACE

ACTUATOR INTERFACE

Figure 3-39. Heliostat Electrical Installation

- Beam Safety - In general, beam safety will be up to the operator. The HAC will not contain any beam safety logic such as keep out zones or mode change restrictions. Although an alarm will be printed out if a mode change request is made, that could be unsafe. After the alarm, the mode change is made but the operator can make a counter change at any time.

  The software will have a stow/unstow trajectory which the beam will follow when this mode is commanded. For a horizontal stow (mirror face-up), the operator will have to use gimbal angle commands. Beam safety will be up to the operator.

- Receiver Defocus - There is no special defocus command. The operator will have to command each heliostat to standby. The beam will be off the target in less than 15 seconds.

- Communication Loss - If communication between the HAC and HFC should go down, then the HFC will move the heliostats to standby and then move them to the stow position. The movement to a stow position will occur at different times so that the beams will not cross on the way to the stow position. This will occur for all heliostats that were in a track mode. Heliostats that were in a static position will maintain that position.

  If communication between the HFC and HC should go down and if rate commands were being used to control the heliostats, then the heliostat will continue moving until a gimbal limit is reached. If position commands were being used to control the HC, then the heliostat will maintain the current gimbal position. Position commands are used when the track rate is less than 0.01 turns/second.

- Operator Mode Commands - The basic operator commands for moving the heliostat are:

  - Receiver Beam Aimpointing - The control system will keep the beam at a point that has been defined as the receiver aimpoint.

  - Standby Beam Aimpointing - The control system will keep the beam at a point that has been defined as the standby aimpoint.

- Gimbal Position - The control system will move the heliostat to the commanded gimbal angles.
- Stow - The control system will move the heliostat from the standby aimpoint to a vertical stow position. The beam will be maintained on a defined trajectory.
- Unstow - The control system will move the heliostat from the stow position to the standby aimpoint. The beam will be maintained on a defined trajectory.

- Lifecycle - There are two lifecycle programs. Both programs take the heliostat from stow to standby to receiver to standby to stow. The first program does this in real time such that beam control is maintained, but only a short time is spent in the receiver track mode. The second program operates in unreal time such that one day of track is done in a few hours.
- Data Record - Upon request, the heliostat position (turns and gimbal angle), sun position, and beam error are printed. Alarms are printed out when they occur.

Reference Update

To achieve the beam pointing accuracy, the control system must know where it is in the inertial reference system in which the control equations are developed. In the event the power goes down to the heliostat, the HC will lose the reference position. The Second Generation control system will incorporate a reference update scheme that makes use of four magnetic sensors. Two sensors are involved in azimuth reference updating, and the other two for elevation reference updating. The locations of these sensors, as illustrated in Figure 3-40, are:

1. The elevation pivot point. This sensor is used in elevation reference updating. It is also used as a gimbal angle limit sensor, switching when the jack is fully extended.
2. The elevation jack helicon gear. This sensor is used in elevation reference updating.
3. The azimuth pedestal. This sensor is used in azimuth reference updating.

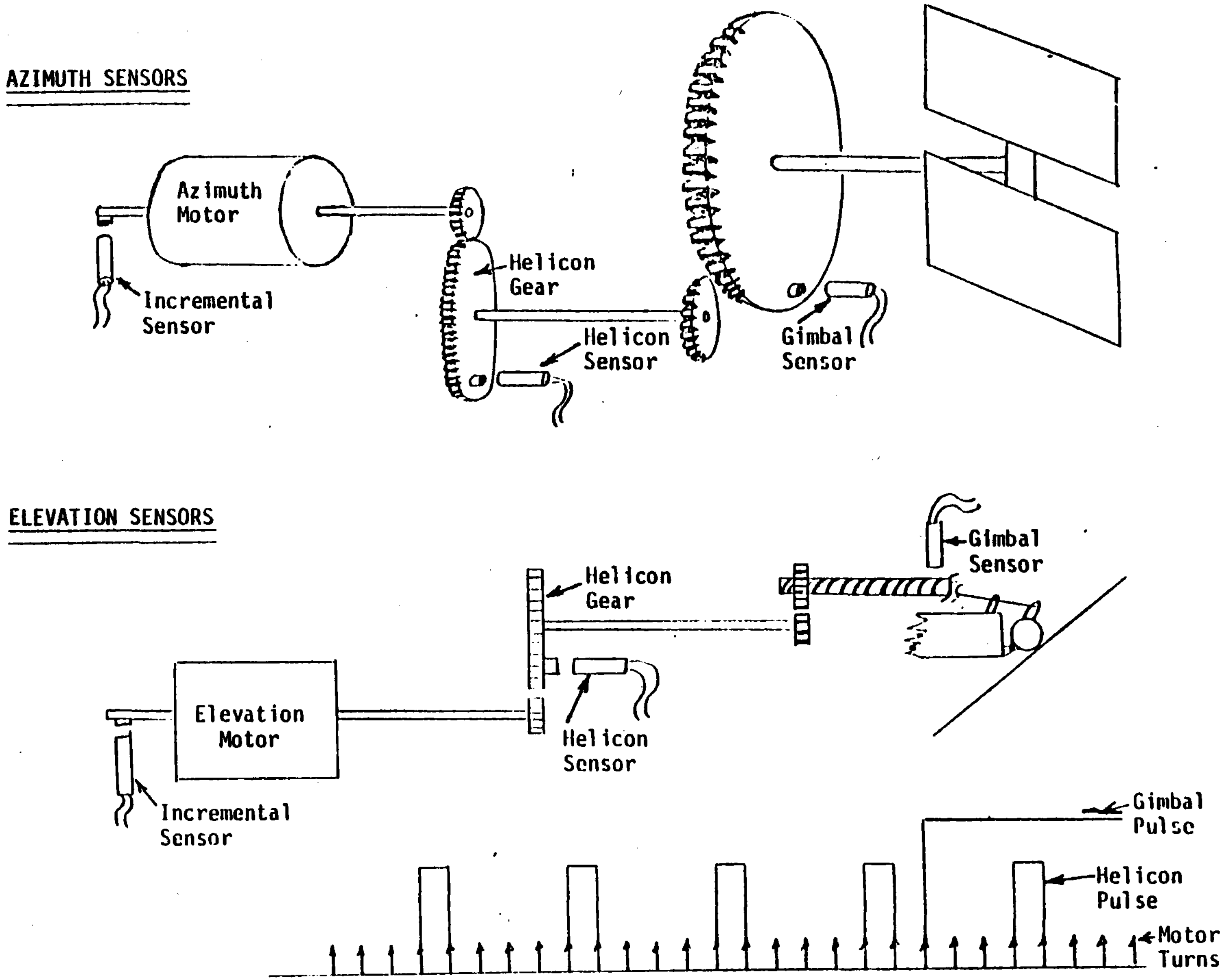
AZIMUTH SENSORS

ELEVATION SENSORS

Figure 3-40. Location of Control Reference Sensors

4. The azimuth drive helicon gear. This sensor is used in azimuth reference updating.

Except for the elevation pivot point sensors, these sensors do not play a role in the basic day-to-day control function of the heliostat. The reference update feature is only used after a power loss or at operator request. The purpose of the sensors is to provide a one bit absolute reference.

There are two types of reference updates that can be commanded. The first method, referred to as Mini Reference Update, does an update by moving the heliostat to the next helicon crossing. The sequence for the mini update for both azimuth and elevation channels is shown in Figure 3-41. This method requires some knowledge of heliostat position at the time of power failure.

For situations where both the HC and HFC had an unscheduled power failure or the heliostat was moved by other than a command from the HFC such as by maintenance personnel, a second method is used called Full Reference Update. In this method the heliostat is first rotated until the gimbal sensors are encountered, then it is moved to the reference helicon position. The basic steps are illustrated in Figure 3-42 for elevation and Figure 3-43 for azimuth.

Reference update will typically be of the mini update type and take between 90 and 240 seconds for completion. Full reference update, when required, will take between 1 and 8 minutes for completion depending on heliostat field location and time of day. The slew rate during reference update is 15°/minute.

3.2.3.6 Heliostat Track Alignment

The baseline track alignment scheme uses a beam centroid measurement device, such as a Beam Characterization System (BCS), to determine the orientation of the heliostat in inertial space. Alignment methods requiring extensive field operations are very costly. This system has been developed to minimize field operations. Three basic tasks must be performed:

1. Heliostat installation
2. Coarse track alignment
3. Fine track alignment.

The first alignment task is performed during heliostat installation on the foundation. The azimuth gimbal reference sensor is set to north within an accuracy of ± 3 degrees.

In the second task, course track alignment is done to enable the control system to direct the reflected beam to a target. This is done by first commanding the heliostat to move to the gimbal reference sensors. At this point an initial estimate is made of the elevation and azimuth reference position. The heliostat is then commanded to a standby aimpoint that is a long distance from the target aimpoint. A search mode is used to find the target. When the beam is on the target, the operator then moves the heliostat until the beam is at the target center. At this point a second estimate until the beam is made of the azimuth and elevation reference position. This estimate will be sufficient to allow the control system to keep the beam on the target or find the target the next time it is unstowed.

In the final step the beam is put on the target and the BCS is used to take measurements and calculate the beam centroid. This is done for CRTF at 1/2 hour intervals from early morning to late afternoon. Using these measurements, the errors in the heliostat orientation can be calculated. These error terms are then used by the HFC to determine the gimbal position which should be commanded in order to move the beam to the desired aimpoint. Some of the errors which will be determined are tilt of the foundation, pedestal and azimuth drive, reference errors, position location errors, azimuth drive pivot point errors, and mirror support pivot point errors.

3.2.3.7 Control Testing

Based on the specification requirements and previous Barstow Pilot Plant experience and testing, tests have been identified that will be performed on various hardware configurations to ensure that the Second Generation heliostat will meet performance requirements. A brief description of these tests is given in Table 3-20.

Table 3-20
DEFINITION OF SECOND GENERATION HELIOSTAT TESTS

HARDWARE TEST CONFIGURATION	TEST DESCRIPTION
Heliostat	1. Tracking Accuracy - Using the DIR, determine the beam point accuracy. Determine long term drift errors. Determine repeatability of tracking accuracy 5 days in a row. Determine accuracy repeatability when heliostat is stowed and unstowed before each DIR point is taken.
Heliostat	2. Beam Quality - Using the DIR, determine the beam shape and the 90% power contour. Take data at 8, 10, 12 and solar noon. Using the temperature and wind data, calculate theoretical contours, compare with measured data.
Heliostat	3. Operating Mode Test - Observe heliostat response to operating modes. Measure time to achieve mode changes.
Heliostat	4. Mini-Life Cycle - Life cycle heliostat up to 360 mini-life cycles.
Heliostat	5. Startup Test - Turn power off to HC and go through first the mini-reference update and then repeat with full update. Simulate HFC/HC communication loss, power down HC, power down both HC and HFC, move heliostat while HFC/HC communication down and power down.
Heliostat	6. Elevation Transfer Function Test - Using inclinometer, measure the gravitational bending from top of pedestal to earth and from mirror surface to ground. Measure elevation angle as a function of motor turns.
Heliostat	7. Gimbal Angle Test - Demonstrate all required gimbal angles. Demonstrate gimbal limits on heliostat and in alarm system.
Heliostat	8. Singularity Test - Determine stability during singularity transition. Determine singularity resolution time and beam error as a function of time.
Components	9. Temperature Test - Controller assembly through temperature survival temperature range. The controller will be in operation at different points during test to verify performance.
Heliostat & Components	10. Power Consumption Test - Static and dynamic power requirements include stow and track requirements for different locations in the field.
	11. HAC/HFC/HC Jack Bench Test - Checkout of reference update software. Determine accuracy and repeatability of reference update under no load and full load.

Table 3-20
DEFINITION OF SECOND GENERATION HELIOSTAT TESTS
(Continued)

HARDWARE TEST CONFIGURATION	TEST DESCRIPTION
Components	12. Noise Test - Determine noise level critical areas. 13. HC Dynamic Response - Determine the response of the HC control system to different control pulses. Run three different elevation angles and up and down direction at each angle. 14. Power Transient - Test the controller box for power dropout and overshoot requirement.

Section 4

AUTOMATED MIRROR INSPECTION TECHNIQUES

4.1 OBJECTIVES

This study was conducted to assess the technical feasibility and potential cost savings of a variety of automated mirror inspection techniques. It can be assumed that some method of mirror inspection must be used to resolve production problems and reduce rework, scrap, and field realignment costs. However, existing methods, usually employing optical laboratory setups with lasers, height gages and transits, dial indicators, or precision accelerometers are relatively time consuming and do not appear to be practical except for inspection of a limited percentage of heliostats. Automated inspection of all heliostat mirrors with the methods investigated here has the potential for not only reducing production costs, but more importantly, appears to substantially reduce the costs of mirror alignment in the field and improve the overall field performance by optimum siting of each heliostat.

Included in this study was effort to (1) evaluate which of the candidate techniques best meets the requirements and (2) determine the system costs and savings. Concepts proposed include:

(1) Adjacent Image Monitoring ("Zebra Board").
Reflected patterns are evaluated in terms of actual versus theoretical scenes (i.e., line widths, angles, etc.).

(2) Reflected Beam Image
A reflected beam displayed on a screen is evaluated for intensity distribution, beam shape, etc., as with the basic Digital Image Radiometer (DIR) technique used with heliostat field evaluation.

(3) Parallel Light Beams
Reflected beam spot locations on a screen are evaluated.

(4) Reflected Point Source Viewing
Images of distant spots (point light sources, etc.) are viewed principally to determine mirror cant angles.

(5) Focused Reflected Beam at twice the mirror focal length (f).
Parabolic mirrors are evaluated by viewing the focused beam at 2f from a radiant light source at 2f.

(6) View of Image at 2f
The reflected image in a parabolic mirror of an object at 2f is viewed to assess slope errors.

(7) Lambertian Screen
General evaluation parameters (reflectivity, size, configuration and integrity) are evaluated by viewing the images of a lambertian screen as seen in mirror modules.

(8) Uniform Light Panel
General evaluation parameters are determined by methods similar to those used for the lambertian screen technique except various spectral distributions are used to more accurately evaluate reflectivity and surface contamination.

4.2 TECHNIQUES

The inspection parameters considered include overall surface flatness and curvature, "waviness" or small scale slope errors, cant angle, focal length, reflectivity, surface contamination, configuration, size, and integrity.

The techniques evaluated for this study are capable of evaluating mirrors for all of the above parameters. These potential techniques are an outgrowth of earlier development efforts with the MDAC DIR. The DIR utilizes computer controlled video data acquisition and various calibration techniques to determine the intensity distribution, net power, and other optical evaluation parameters of reflected heliostat beams. The DIR approach was emphasized in this study because it has the capability of meeting the inspection parameter requirements with high data acquisition rates, accuracy, versatility, and low cost. Furthermore, two operational systems are available at MDAC with hardware and software which are useful in performing preliminary evaluation tests of candidate techniques.

4.3 RESULTS

The analyses and tests conducted to date show that all of the above techniques can meet the expected requirements for accuracy. Selection of preferred techniques depends more on such practical issues as time and cost associated with mirror module or reflector panel setup and positioning and hardware costs for the inspection station. Although results have not been sufficiently evaluated for a firm recommendation, it appears that use of adjacent image monitoring will be a relatively simple method for determining mirror "waviness" (i.e., small scale slope deviations) for essentially flat mirrors; parabolic mirrors of relatively short focal length can be evaluated easily by both methods (5) and (6), with method (5) being more practical for general inspection purposes since mirror positioning tolerances give wider latitude. Overall inspection parameters (reflectivity, size, configuration, and integrity) can be evaluated by various techniques similar to those of methods (7) and (8). The other techniques also hold promise. For example, method (4) may be practical for workers adjusting mirror module cant angles in the factory or in the field since slight module position changes result in easily observable shifts in the reflected image, and could be observed on a monitor. Computer generated values of corrective shim thickness or adjustment fixture values are also feasible.

Preliminary benefit/cost analyses indicate that DIR automated inspection of all mirrors is justified. For example, assuming a heliostat factory production rate of 25,000 heliostats/year, cost savings were estimated for the following four areas:

Reduction of Reflector Panel Scrap	\$ 325,000
Reduction of Reflector Panel Rework	\$ 58,666
Improvement in Field Performance by Optimum Heliostat Location	\$1,170,000
Reduction in Field Canting of Mirror Modules	\$4,000,000

These data indicate that inspection of all heliostats with various DIR techniques has the potential for reducing overall heliostat costs by approximately $\$4.40/m^2$ or $\$5.5x10^6$/year for a production rate of 25,000 heliostats/year.

4.4 STATUS

A more detailed discussion of results achieved to date is presented in a final report "Automated Mirror Inspection" (MDC G8663) which covers the initial phases of general requirements, initial optical analyses and tests, and preliminary cost analysis.

This completes the development activity for the inspection techniques in this program.

Section 5

HELIOSTAT INSTALLATION AND CHECKOUT

The design and production of the Second Generation Heliostat facilitates field installation. At-site assembly is confined to the mating of major subassemblies. This involves setting the pedestal - drive unit - main beam on the foundation, attaching the reflector subassemblies to the main beam and hooking field cables to the heliostat controller.

In the following subsections, the installation process design, applicable to both the test units and production, is described.

5.1 CENTRAL RECEIVER TEST FACILITY (CRTF) PROTOTYPE HELIOSTATS

Two test heliostats are to be delivered to the CRTF, assembled, installed and operationally checked out. They will then be turned over to Sandia Laboratories for evaluation tests.

5.1.1 Hardware Description

The following items will be shipped to the CRTF from the MDAC Huntington Beach facility and suppliers.

A. 2 Each, Interface Cone Assembly

This cone, shown in Figure 5-1, is cast onto the foundation and interfaces with the pedestal.

B. 2 Each, 1D22475-1, Drive Unit - Pedestal - Main Beam Assembly

This item supports and positions the reflector. It is an assembly consisting of the pedestal, azimuth drive, elevation drive, the reflector main beam, the heliostat controller, sensors and electric wiring. During factory assembly these components are mated together and checked operationally. The drive positions are set at design points so that initial operation of the heliostat can be safely controlled, while being

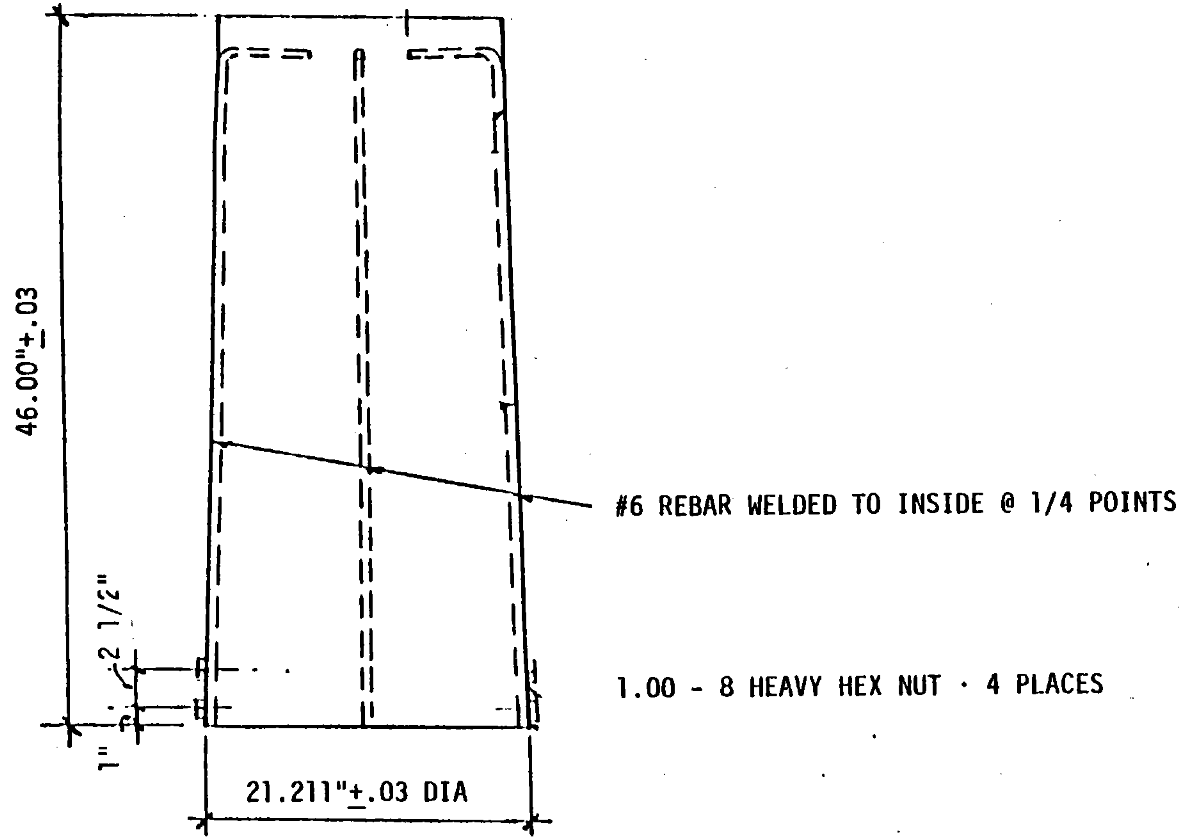

Figure 5-1. Interface Cone Assembly

brought up to the target for alignment. This item interfaces with the foundation, the reflector assemblies, and field data and power cabling.

C. 4 Each, 1D22456-1, Reflector Assembly

This item is the mirrored reflector used to beam solar energy onto the receiver. It is made up of seven laminated mirrors attached to a steel support structure. Two reflector assemblies interface with the main beam.

D. 1 Each, Heliostat Array Controller

A cabinet containing a DEC computer and a heliostat field controller is provided, along with software packages for heliostat control. These items are provided on a loan basis.

5.1.2 Transportation and Handling

The hardware described in Section 5.1.1 will be transported to the CRTF in MDC trucks. Since production support equipment is not available, handling of these large items will be accomplished using slings and fixtures developed for the test units. The reflector assemblies are shipped in a vertical position and are rotated 90° for mating with the main beam. This translation will require either a special loading-transportation fixture or a special hoisting sling which can accommodate the translation. Selection of the method to be used is in process.

5.1.3 Assembly, Installation and Checkout

Following receipt of the hardware at the CRTF, MDAC will install, checkout and align the two heliostats.

The flow of this process is illustrated in the functional flow block diagram presented in Figure 5-2.

During installation of the foundations at CRTF, MDAC will provide quality assurance verification.

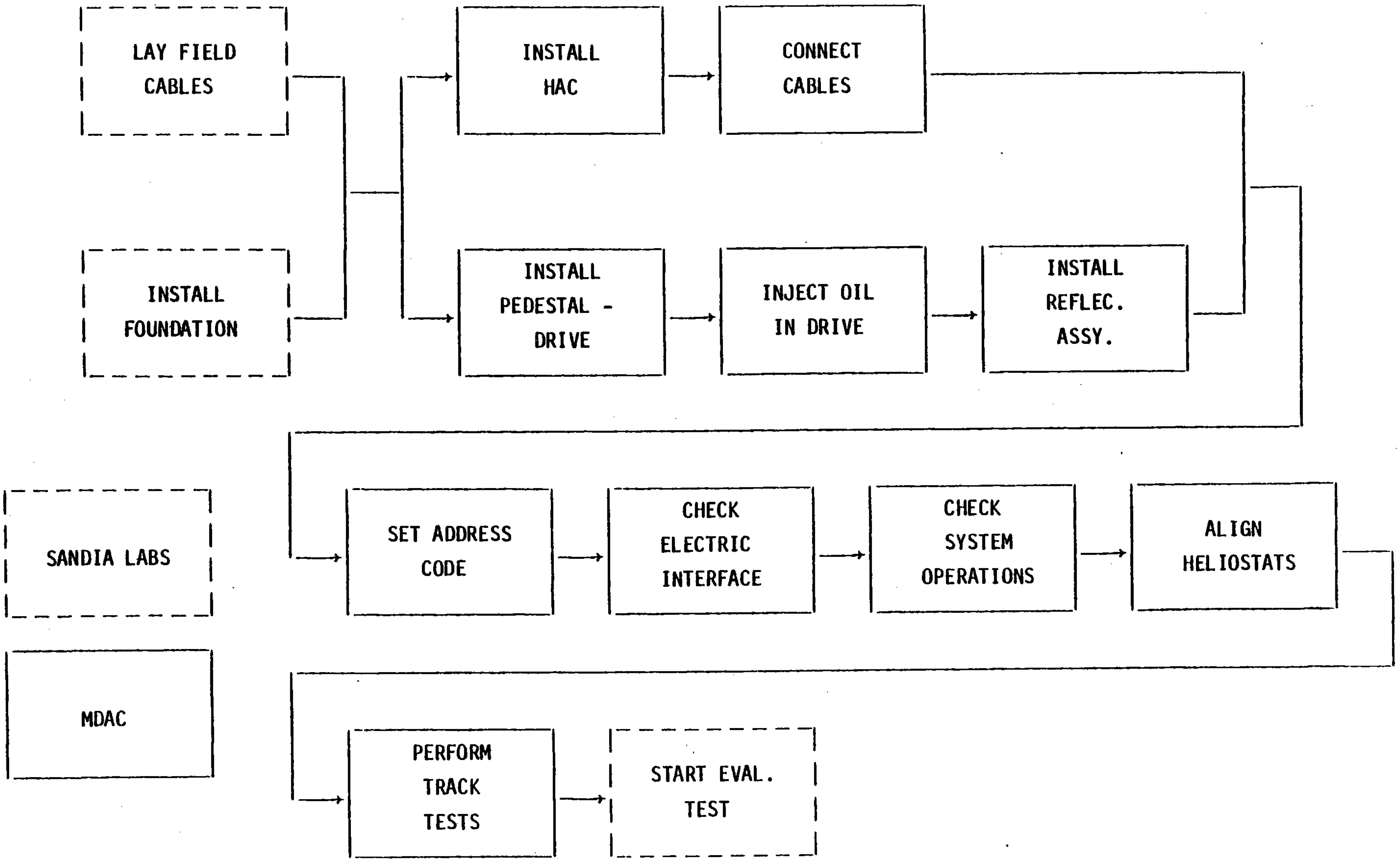

Figure 5-2. Prototype Heliostat Assembly, Installation, Checkout and Alignment Flow

Heliostat installation will be performed by Sandia technicians under MDAC supervision. This includes installing the HAC in the CRTF control room, connecting power and control cables and check out the operation of the heliostat and HAC. Following this, heliostat alignment with the target and BCS will be accomplished under the direction of the control engineer. Prior to turnover of the completed test installation, a series of heliostat tracking tests will be performed to further verify that the subsystem is fully operational.

5.2 PRODUCTION INSTALLATION AND CHECKOUT CONCEPTUAL DESIGN

The heliostat installation concept is to assemble the heliostat in the field from major elements which have been constructed and checked out in the factory. This concept, which is based on the prototype study and the current heliostat design, provides the benefits of factory assembly in the form of high accuracy and efficiency and simplifies the field installation by minimizing tasks which must be performed in the field.

5.2.1 Task Description

Using the assumption that surveying, grading and facilities construction are part of the overall plant erection activities, installation and checkout tasks for the heliostat field are categorized as:

A. Mechanical Installation

B. Electrical Installation

C. Heliostat Alignment and Checkout.

Completion of these tasks provides the initial operational capability of the collector subsystem. At this point, the field can be safely operated under the control of the HAC in a stand-alone mode and is ready to be integrated with the other plant subsystems. Descriptions of the tasks are provided in the following subsections.

5.2.1.1 Mechanical Installation Tasks

A. Foundation Installation - The foundation will be formed in place by drilling holes approximately 2 ft in diameter x 15 ft deep, installing a prefabricated rebar cage with a tapered form, both of which extend approximately 4 ft above grade, and filling the cage and the form with concrete. The rebar cage and the tapered form are welded together at the factory and brought to the site on a standard flatbed vehicle.

Subassembly	Dimensions (Approx.)	Weight (Approx.)	Special Operation
Rebar Cage with Tapered Form	21-1/4 in. dia. x 19 ft long	382 Lbs	Vert within 1°

B. Drive Unit - Pedestal - Main Beam - These units will be assembled and checked out at the factory, and delivered to the site on flatbed trailers, with 12 on each trailer. The drive units will be placed over the tapered foundation and loaded with 3,000 pounds of force; they will then be vibrated to ensure proper seating.

Subassembly	Dimensions (Approx.)	Weight (Approx.)	Special Operation
Drive Unit - Pedestal - Main Beam	21-1/4 in. dia. x 167-1/2 in. long	1,311 Lbs	Positioned within 3° to north-south and 1° vertical

C. Reflector Assembly - These units consist of seven identical laminated mirrors assembled on a support structure. Two reflector panels will be bolted to the main beam of the drive unit and form the heliostat reflective unit.

Subassembly	Dimensions (Approx.)	Weight (Approx.)	Special Operation
Reflector Assembly	28-1/2 ft long x 132 in. wide x 23 in. deep	2,216 Lbs	Positioning accomplished by jig drilled alignment holes

D. Harmonic Drive Oiling - During assembly, the moving parts of the harmonic drive are lubricated with a light coating of grease. This is adequate protection during operation of the drive during production assembly and checkout. The task of filling the harmonic drive housing with oil is performed in the field after the drive - pedestal - main beam assembly is installed on the foundation. Delaying the task until this time protects the wave generator bearing from contamination during transportation and handling.

Filling the harmonic drive housing with oil is done through the mounting hole of the upper expansion chamber. The expansion chamber is removed and oil is injected through the mounting hole until the oil level rises to approximately 0.250 inch above the wave generator upper surface. The expansion chamber is then replaced.

5.2.1.2 Electrical Installation Tasks

A. Heliostat Field Interface Connections - Field power and data cables terminate in a facility junction box located adjacent to the heliostat. The interface connection task requires pulling the heliostat cable assembly, which is plugged into the heliostat controller, through the conduit in the foundation, and terminating the power and data wires in the facility junction box.

B. Set Heliostat Address Code - Each heliostat in the field has a unique address for data and communication which must be set after the heliostat is installed on its foundation. This task requires opening the heliostat controller box and adjusting the DIP switch mounted on the processor board. The DIP is set in accordance with the master field layout plan so that each heliostat address code corresponds with the surveyed coordinates of the heliostat.

5.2.1.3 Heliostat Alignment and Checkout Tasks

A. Alignment - The heliostat alignment task, as described in Section 3.2.3.6, is also used for the 50 MWe field heliostats. For the larger field, four BCS cameras are used simultaneously to quickly align large groups of heliostats on a daily basis.

B. Checkout - Operational checkout of the heliostats, including proper response to HFC commands, is accomplished as part of the alignment task. This approach is feasible because of the complete operational checkout each heliostat is subjected to at the factory. A very small percent of heliostats could exhibit anomalies during alignment; however, the cost savings realized by eliminating a separate checkout task is expected to outweigh the cost of repair of consequential damage.

5.2.2 Resources Requirements

A study was undertaken to determine the best method of allocating personnel and special equipment to sites for installation and checkout (I&C) activities at production rates of 50,000 heliostats per year for 10 years.

These groundrules were used during the study:

- Production rate is satisfied by the installation schedule; e.g., no significant backlogs or surpluses of heliostat subassemblies at the site. This requires a daily installation average rate of 208 units.
- 5,600 heliostats per field.
- 40-hour weeks; 48 weeks per year.
- Work at four sites simultaneously.
- All sites to be within a 400 mile radius of the production facility.

The approach used was to determine resources for one site needed to absorb its share of the factory daily output, i.e.,

$$\frac{\text{208 Heliostats}}{\text{4 Sites}} = \text{52 Per Day}$$

The resultant resource allocation is shown in Table 5-1. The table also identifies the tasks and provides the estimated elapsed time needed to complete one cycle of each task. An effective work day of seven hours was used, with the estimated task time, to calculate the number of units needed. Because resources come in units, the results provide an excess capability at site, which is considered adequate to compensate for delays caused by weather and equipment breakdown.

Table 5-1

INSTALLATION AND CHECKOUT RESOURCE ALLOCATION

Task No.	Time/Heliostat	Resource Allocation
1. Pedestal Excavation, Iron and Concrete	30 min/heliostat	Furnished by Subcontractor
2. Drive Unit Installation	18 min/heliostat	3 Pedestal/Drive Assy. Installation Equipment 3 Installation Equipment Operators 3 Millwrights 3 Laborers
3. Reflector Panel Installation	21 min/heliostat	3 Reflector Panel Assy. Installation Equipment 3 Installation Equipment Operators 3 Hi-Lift Forklifts 3 Forklift Operators 6 Millwrights 6 Laborers
4. Connect, Check & Close Out	15 min/heliostat	2 Electricians 2 Laborers 2 Test Sets
5. Align Heliostat	10 min/heliostat	1 Controls Engineer (Also requires BCS Support)

5.2.2.1 Special Equipment

Two items of special equipment are needed to support this conceptual design of the installation and checkout process. One is a highly specalized mobile item of equipment used to unload, translate and install the pedestal - drive - main beam subassembly. The other item will consist of a large, mobile grapple used to lift, translate, and position the reflector assembly for attachment to the main beam. The initial concept of the pedestal machine is shown in Figure 5-3.

5.2.2.2 Special Facilities

At the present stage of development, no dedicated special facilities have been identified to support I&C activities. Certainly there will be requirements, but they may well be in the nature of added loads on existing plant construction facilities; e.g., medical, sanitary, locker rooms and food preparation.

5.2.3 Task Sequences and Time Estimates

The resource allocation, as shown in Table 5-1, supports absorption of the factory output. The sequential flow of I&C tasks would be as shown in Figure 5-4, which also presents the number of work days needed to complete I&C of 5,600 heliostats. No allowance has been made for delays in I&C caused by weather and equipment breakdown because, as allocated, the resources for installation of the heliostat subassemblies provide a capability greater than the factory output of 52 units per day. Also, lost time can be made up by applying extended work days and work weeks.

Plant construction schedules are expected to be unique to each site. Where these schedules permit, the installation of heliostat foundations should be completed prior to start of heliostat installation. This would reduce traffic congestion at the site.

5.2.4 Site Activities Support Requirements

A certain amount of common support is required for the I&C activities. While not necessarily limited to the following, site support requirements include:

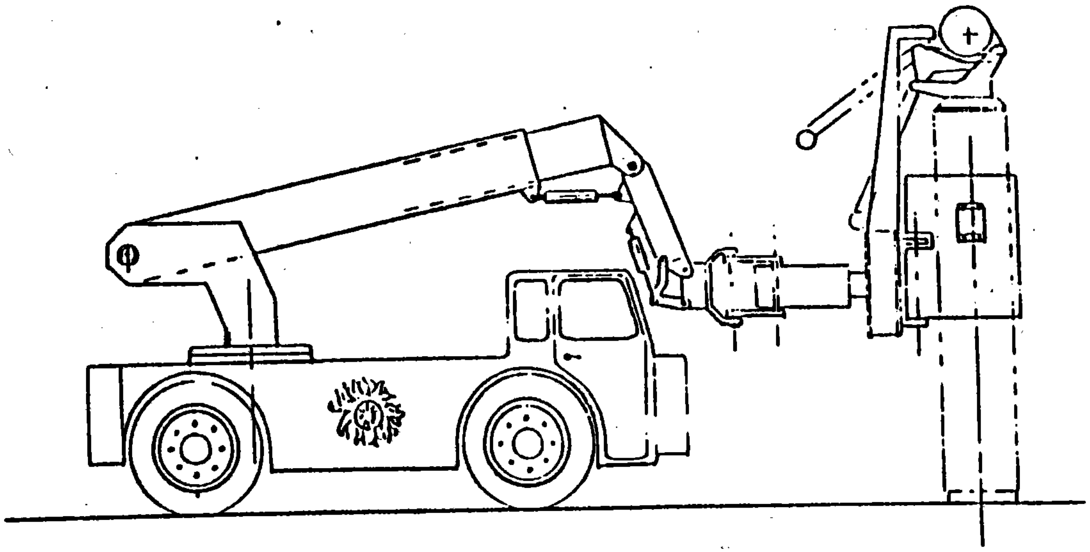

Figure 5-3. Pedestal Installation Machine

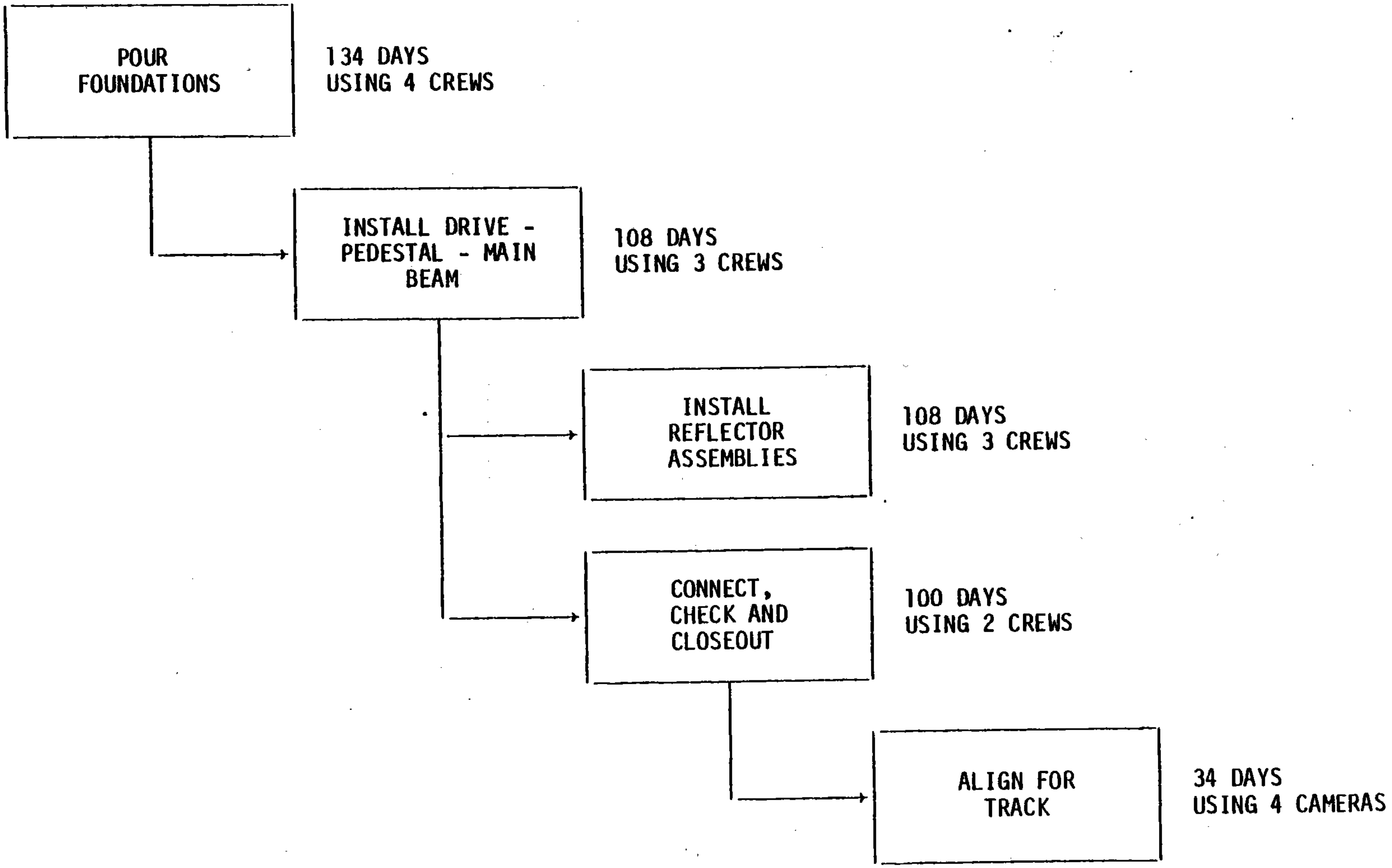

Figure 5-4. Heliostat Installation Task Flow

o Site Manager	1
o Assistant Site Manager	1
o Material Accountability Clerk	1
o Inspector	2
o Field Engineer	1
o Rework Capability	
- Millwright	AR
- Electrician	AR
-	AR
- Equipment Operator	AR
- Mobile Crane	AR
- Forklift	AR
- Truck	AR
- Mobile Highlift Work Stand	AR

Since the need to rework installed equipment will be sporadic, a dedicated rework capability is not justified. This function could be performed by the I&C contractor or by a local maintenance subcontractor. In either case, any work performed would be on a call basis.

5.2.5 Preliminary Transportation Plan

The plan presented here covers the transport of heliostat subassemblies from the production facility to the construction sites. Because the availability of rail transportation is as yet unknown, the plan only considers highway truck transportation. The basis for the information presented in this subsection is the movement of the hardware required for one site, 5,600 heliostats.

The concept for transportation of heliostat subassemblies is to pick up a loaded trailer at the factory with a prime mover, haul the trailer to site, position the loaded trailer adjacent to the work area, pick up an empty trailer and return to the factory. This approach eliminates the need for intermediate handling and storage at the site. Transportation requirements are summarized in Table 5-2 and are based on the following:

A. Reflector Assembly	104 Per Day
B. Drive Unit - Pedestal - Main Beam	52 Per Day
C. Weighted Mean Round Trip Distance	288 Miles
D. Average Round Trip Time	10 Hours

Since the data in Table 5-2 are based on Items C and D preceding, the number of prime movers and trailers needed to serve a specific site will vary with the location of the site within the 400 miles radius from the production facility.

5.2.6 Trade Study

The major I&C trade study accomplished under this contract relates to the economics of the heliostat reflector assembly transportation and production. The options studied were:

A. Produce (assemble) the item at a centralized production facility and transport the assembly to site.

B. Transport the component parts to site and assemble the item in a site located facility.

The conclusion reached is that it is more economical to use Option A.

Details of the trade study are included in Table 5-3. The study and resultant cost figures are based on a 30 year production run with an annual output of 50,000 units.

TABLE 5-2

TRANSPORTATION SUMMARY

Item	Unit Pack	Units Per Truck	Loads Per Day	Loads Per Site
Drive Unit - Pedestal - Main Beam	1	12	4.4	467
Reflector Assembly	4	1	26	2,800

Table 5-3

COST STUDY

OBJECTIVE:	IDENTIFY LOW COST CONCEPT FOR SECOND GENERATION HELIOSTAT REFLECTOR ASSEMBLY PRODUCTION
OPTIONS:	A. ACCOMPLISH TASKS IN A CENTRALIZED PRODUCTION FACILITY.
	B. ACCOMPLISH TASKS IN SITE LOCATED FACILITIES.
DATA SOURCES:	1. TRANSPORTATION COSTS - MDC (LONG BEACH) TRANSPORTATION DEPARTMENT.
	2. FACILITIES AND LABOR COSTS - SERI REPORT TR-8043-1

FACTORS	OPTION A	OPTION B
DIRECT LABOR	$ 19,980,000	$ 22,970,000
FACILITIES	1,911,000	36,036,600
TRANSPORTATION	128,775,000	101,556,085
PACKAGING	5,506,400	16,019,000
RECRUIT & TRAIN LOCAL PRODUCTION WORKERS	N/A	570,240
TOTAL	$156,172,400	$177,151,985
DIFFERENCE		20,979,585

Section 6

HELIOSTAT MAINTENANCE

Heliostat maintenance support is directed toward two primary objectives: (1) achieving and maintaining specified system availability and (2) providing the necessary support with minimum expenditures for labor and materials. Because of the large quantity of heliostats in the collector subsystem and a basic design which does not rely primarily on maintenance to achieve system availability, there is little risk that the required availability will not be satisfied. This permits consideration of support concepts with reduced concern that they will affect system availability.

In the following the current maintenance process design is described for the production program.

During hardware design there has been a continuous evaluation of maintainability characteristics. The goals set for the maintainability program include the elimination of scheduled heliostat maintenance requirements and the reduction of the mean time to repair (MTTR). The MDAC heliostat design fulfills these goals by requiring: no periodic lubrication, having no limited life items, and having no critical failure modes. Failure rates for heliostat components were extracted from standard reliability data sources, which justifies a high level of confidence in their accuracy. During the verification process, any deficiencies noted in either hardware design or maintenance concepts will be corrected through design changes or improved maintenance processes. All electrical and mechanical elements of the heliostat have been developed conservatively so that failure rates are inherently low.

The initial maintenance requirements were determined by a hardware analysis to identify significant components for maintenance and related maintenance tasks.

6.1 MAINTENANCE CONCEPT

Restoration of inoperable heliostats to active status is accomplished under the following maintenance concepts. Standard mechanical and electronic skills are adequate to perform the maintenance tasks required for the heliostat. Maintenance activities are categorized as:

A. On-equipment maintenance.

B. Off-equipment on-site repair.

C. Off-site repair.

Category A includes:

- o Removal and replacement of line replaceable items* (LRU).
- o Adjustments to mirror module positioning.
- o Washing reflectors.
- o Minor structure repair.
- o Minor electric cable repair.

Category B includes:

- o Bench repair of LRU.
- o Test and recertification of LRU.

Category C consists of Category B tasks accomplished at a suppliers facility or a centralized repair facility.

Recycle time for LRU is estimated as:

- o 1 week for on-site repair.
- o 4 weeks for off-site

The maintenance concept includes a spares philosophy as described in the following.

---

*An LRU is an assemblage of parts which is to be replaced as a unit in the event of a failure of any part in the unit.

Repairable LRU's, upon failure, are removed from the system, placed in the repair cycle, and subsequently returned to spare stock inventory. Initial spares quantity for these items is the sum of the pipeline quantity and a 30-day contingency supply. The pipeline quantity is equal to the maximum number of items in the repair pipeline at any given time and is based on the failure rate and the repair cycle time. The 30-day contingency quantity is equal to the number of predicted failures in a 30-day period, and provides a cushion of the event of delays in repair or delivery, as well as providing for a non-linear failure rate, over time. The initial spares quantity will be procured and stocked at the appropriate repair location when the first year of operation begins.

The discard factor represents the number of failures which result in the LRU being discarded instead of repaired, primarily due to extensive damage. The product of the total number of failures per year and the discard factor equals the number of replacement LRU's to be procured at the beginning of the second and subsequent years.

Application of this spares approach is considered suitable for stable operations of an established plant. Because of the infant mortality of LRU during startup and checkout of new plants, a buffer stock of spares will most likely be required to support the first two or three plants put into operation. The spares summary, Table 6-1, does not include a buffer stock. Also not included are the initial spare items of the non-repairable components and piece parts needed to support heliostat maintenance. A list of recommended spares to replace discard items will be furnished in the final report.

The quantities shown in Table 6-1 are the results of calculations using the predicted failure rate, the number of units in the field, the operating time per year and the repair cycle time.

6.2 TASK DESCRIPTIONS

The heliostat design is such that there are no requirements for scheduled maintenance other than washing the reflector, during the life of the hardware.

Table 6-1
SPARES SUMMARY REPAIRABLE ITEMS

Component	*Annual Demand	Repair Location	Pipeline Qty.	30 Day Cont. Qty.	Initial Spares Qty.	Discard Factor	Annual Rep. Spares
Heliostat Controller	441	On-Site	8	37	45	0.01	5
Azimuth Drive	55	Off-Site	6	6	12	0.03	2
Elevation Jack	51	Off-Site	4	4	8	0.07	4
Drive Motor	**84	On-Site	8	7	15	0.1	9
CCA Processor	41	Off-Site	4	4	8	0.3	12
CCA Motor Controller	118	Off-Site	10	10	20	0.3	35
Incremental Encoder	50	On-Site	7	4	11	0.05	3

*Annual demand equates to predicted failures per year.

**Motor demand is based on a Frequency of Repair of 2.24 x 10^{-6}. Annual demand in excess of 84 (see Table 6-3) is caused by incremental encoder malfunctions. Encoders are spared separately.

However, because of safety considerations and established service requirements, special support equipment will require periodic servicing and recertification. Also, heliostat reflector washing is, for the moment, considered to be a periodic requirement. It is expected that operational experience may determine that washing should be accomplished only in response to "on-condition" requirements. Depending on site environmental conditions, the "on-condition" requirements could range from no requirement to wash, to a continuous washing cycle.

To be consistent with the preceding, the heliostat task descriptions that follow are separated into corrective maintenance and scheduled maintenance.

6.2.1 Corrective Maintenance Tasks

Under the maintenance concept described in Section 6.1, corrective maintenance tasks fall under all three categories; i.e.,

A. On-equipment maintenance.

B. Off-equipment on-site repair.

C. Off-equipment off-site repair.

Most of the Category A tasks for the MDAC heliostat consist of removing and replacing a malfunctioning or discrepant LRU. Some minor repair-in-place activities on the structure and electric wiring items are expected. Maintenance tasks identified as Category A are listed in Table 6.2, along with their predicted frequency, predicted MTTR, and estimated manhour requirements.

Since Categories B and C tasks are similar, except for the repair location, both categories are listed in Table 6-3. Further overlapping of the two categories is unavoidable because a minor repair may be done on-site, while a major repair or overhaul of the same item is done in an off-site facility. The nature and extent of such overlapping will be determined at each site over a period of time.

Table 6-2

PREDICTED MAINTENANCE SUMMARY (Category A)

Component	Fail Rate (10^{-6})	Operating Time	Population	Annual Failures	MTTR	Men to Repair	MMH to Repair	MMH Per Year
Heliostat Controller	23.678	3326	5600	441	1.3	2	2.6	1146.6
Pedestal	0.11	7884	5600	5	1.0	2	2.0	10.0
Mirror Module	0.1	7884	78400	67	2.0	3	6.0	402.0
Support Structure	0.12	7884	5600	5	1.5	2	3.0	15.0
Azimuth Drive	2.94	3326	5600	55	4.0	5	20.0	1100.0
Elevation Jack	2.73	3326	5600	51	2.2	2	4.4	224.4
Drive Motor	3.59	3326	11200	134	1.7	2	3.4	455.6
Position Sensor	1.133	3326	28000	106	2.1	2	4.2	445.2
				Total Annual MMH (Category a)				3798.8

MTTR - Mean Time to Repair

MMH - Maintenance Manhours

Table 6-3

PREDICTED MAINTENANCE SUMMARY (Category B & C)

Component	Fail Rate (10^{-6})	Operating Time	Population	Annual Failures	MTTR	Men to Repair	MMH to Repair	MMH Per Year
Heliostat Controller	23.678	3326	5600	441	3.5	1.0	3.5	1543.5
Azimuth Drive	2.94	3326	5600	55	5.5	1.3	7.15	393.3
Elevation Jack	2.73	3326	5600	51	3.6	1.2	4.32	220.3
Drive Motor	3.59	3326	11200	134	2.5	1.0	2.5	335.0
Circuit Card Assembly, Processor	2.2	3326	5600	41	3.5	1.0	3.5	143.5
Circuit Card Assembly, Motor Control	6.32	3326	5600	118	3.5	1.0	3.5	413.0
Incremental Encoder	1.35	3326	11200	50	2.5	1.0	2.5	125.0
Total Annual MMH (Category b & c)								3173.6

MTTR - Mean Time to Repair

MMH - Maintenance Manhours

6.2.2 Scheduled Maintenance

For scheduled maintenance, all tasks except heliostat reflector washing are Category B. These Category B tasks only require standard practices for proofload, vehicle servicing, and electric/electronic check, adjustment and recertification.

Reflector washing, Category A, is a major activity in the process of maintaining heliostat energy output. For now, the predicted frequency of cleaning a specific heliostat is once per month. A review of various studies on methods and procedures applicable to heliostat reflector washing resulted in the selection of the following approach as acceptable for both an economic and a technical basis.

In the cleaning procedure, two trucks with spray heads move continuously across the field at approximately 1 foot per second. The lead truck sprays the acidic washing solution on the heliostat as it passes. The second truck lags about one minute (two heliostats) behind the lead truck to allow for soak time (Figure 6-1). The lag truck sprays the heliostat with dionized water to rinse off the cleaning solution to complete the task. Runoff is not collected and falls on the ground except in those locations where prohibited by statute.

The frequency of reflector cleaning is very site-dependent, seasonal, and weather-dependent. MDAC has chosen a one-month interval for cleaning as perhaps representative of long-term average cleaning rates. The MDAC 1 fps spray-soak method has been selected for manhour and cost projections.

Cost Projections

Conditions

A. Use 2 trucks
B. Trucks sized for 480 heliostats per load.
C. One man per truck
D. Complete 1 heliostat per minute average
E. One hour needed for truck refill except where not allowed by local load

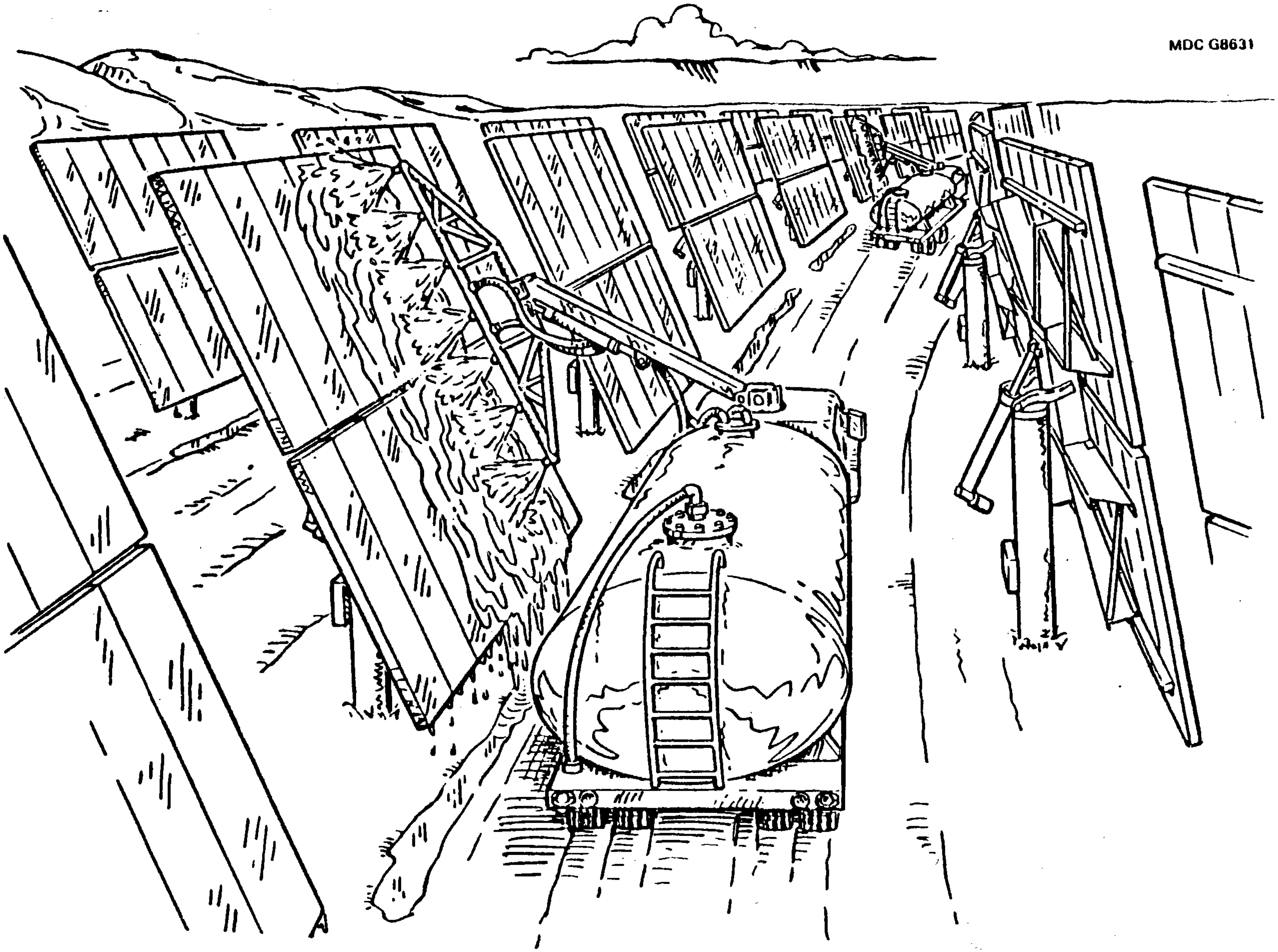

Figure 6-1. Reflector Washing Equipment

Calculations

5600 Hel. ÷ 60 per hour = 93.33 hours

$\frac{\text{5600 Hel. x 1 hour}}{\text{480 Per Load}}$ = 11.67 hours

Elapsed Time 105 hours

2 men x 105 hours = 210 hours/month

12 months x 210 hours = 2520 hours/year

Scheduled maintenance requirements are summarized in Table 6-4.

6.2.3 Facilities Requirements

The maintenance concept applied to a 50 MWe size field of heliostats generates the need for dedicated facilities at the site. The functions assigned to these facilities are: (1) storage of maintenance support spares and material and (2) repair of discrepant LRU. These requirements must be included in the architectural plans of each site, either as a separate maintenance building or as an allocation of space in a common purpose building. A tentative floor plan is provided in Figure 6-2.

6.2.3.1 Storage Facilities

Based on the quantity of spares recommended for maintenance support, an area of approximately 2000 ft^2 is required for storage. This area needs to be furnished with a minimum of:

A. Industrial lighting

B. Potable water (could be bottled water)

C. Adequate electric outlets - 110V 60 Hz, 3 wire

D. Parts racks

E. Parts bins

F. Washing and toilet facilities (or easy access to such facilities)

Table 6-4

SCHEDULED MAINTENANCE SUMMARY

Component	Quantity	Task	Frequency	Manhours Per Task	Manhours Per Year
Support Equipment					
Handling sling, mirror	2	Load/Test Recertification	Annually	1	2
Control unit, portable	5	Inspect and Service	Annually	2	10
Heliostat Reflector	5600	Wash	30 days	210 (Field)	2520
				Total	2532

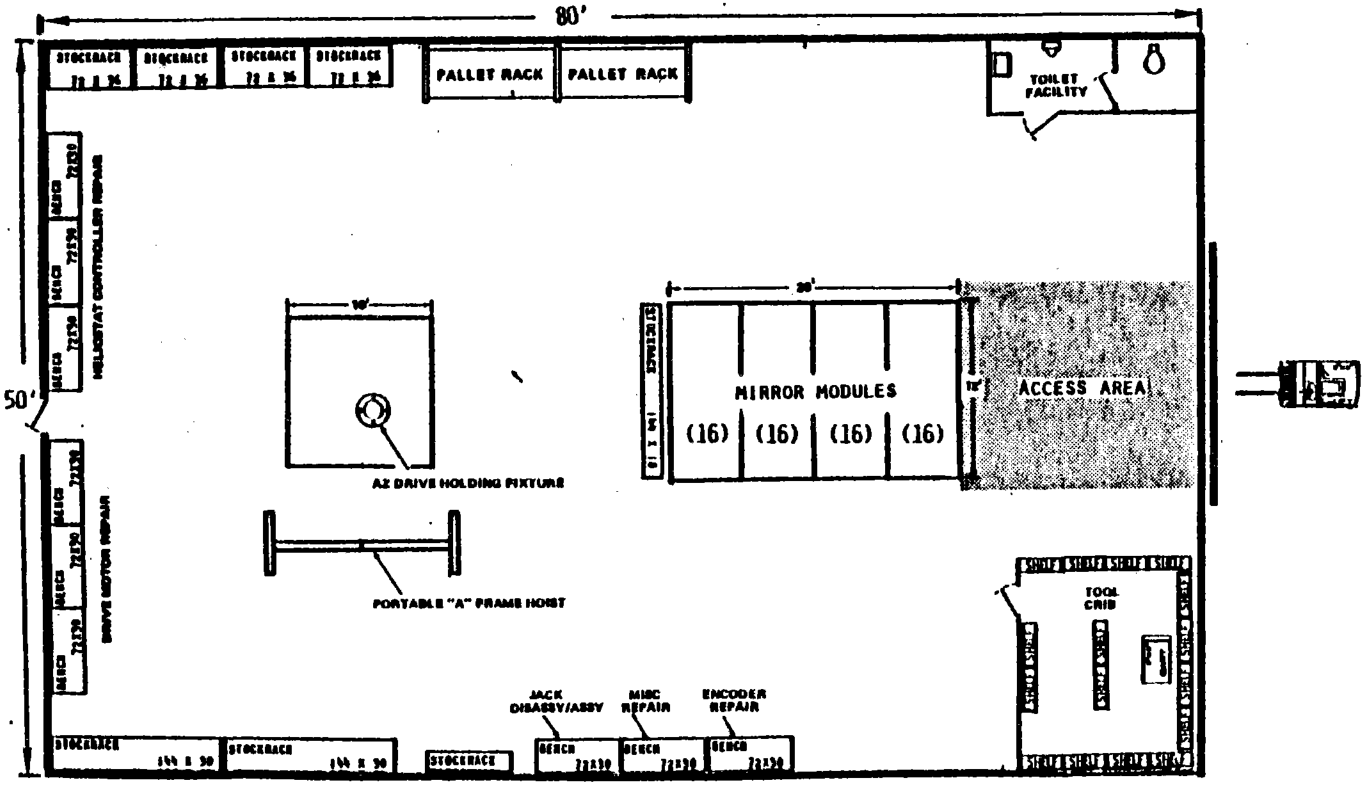

Figure 6-2. Heliostat Maintenance and Storage Area

G. Loading dock

H. Service door to loading dock

I. Air conditioning (if needed for work environment for personnel). (Material stored in this facility does not require environmental control).

The storage area should be collocated with the maintenance area so that repair technicians have immediate access to the support material stored there.

6.2.3.2 Maintenance Facilities

The facilities needed to house and support the repair activities are determined by both the nature and the frequency of the LRU repairs. Only one special fixture is required and it is a support fixture needed to hold the azimuth drive during preparation of the unit for shipment and installation. The other LRU can be disassembled, inspected, reassembled and tested on standard work benches. Maintenance requirements are included in Figure 6-2.

The azimuth drive weight, approximately 330 pounds, precludes manual lifting of the unit. However, a permanently installed hoist is not recommended. The cost of such a device cannot be justified by the need to lift one item. Instead, use of a mobile, hand operated, hoist or jib crane is considered adequate.

The maintenance area needs to be furnished with a minimum of:

A. Industrial lighting

B. Potable water

C. Convenience electric outlets 110V 60 Hz 3-wire.

D. Electric power for drive motor operation
    208 V 3-phase, 60 Hz, 5 wire or 4 wire and safety

E. Washing and toilet facilities (can be common with storage facility)

F. Azimuth drive holding fixture

G. Work benches

H. Air conditioning (as necessary to maintain a comfortable work environment)

I. Tool crib for secure storage of shop tools and test equipment.

The maintenance requirements of a total 50 MWe solar plant will encompass additional facility requirements to those described in this report. Therefore, overall planning may result in a combined maintenance facility designed to service all plant subsystems.

6.2.4 Support Equipment

The support equipment identified for heliostat maintenance use falls into two categories: (1) special equipment and tools and (2) commercial equipment and tools. Most items in the commercial category should have common usage in the support of heliostat and other subsystem maintenance activities. Special items of equipment and tools are designed by MDAC for specific use during heliostat maintenance. The design of these items, other than reflector washing equipment, is in work and will be completed shortly. The design of the washing equipment is not a part of this contract.

The support equipment and tools identified for use during Category A, on-equipment maintenance, are listed in Table 6-5. Shop repair equipment and tools needed to support Category B, off-equipment on-site maintenance, will be furnished in the final report.

Table 6-5

SUPPORT EQUIPMENT SUMMARY

I. Commercial Items

Item	Use
1. Mobile Crane 10 Ton, with standard rigging	Remove and hold heliostat reflector during removal and replacement of azimuth drive.
2. Forklift with hoisting adapter	Remove and replace azimuth drive.
3. Hydra-Set, 2-1/2 Ton	Precise positioning of reflector during reinstallation on the azimuth drive.
4. Pick-up Truck	General.
5. Wyler Minilevel	Measurement of mirror module cant angle.
6. Oil Injector	Fill azimuth drive housing with oil.

II. Special Items

Item	Use
1. *Portable Control Unit	Fault isolation and control of an individual heliostat.
2. Service Link Kit	Stabilize heliostat reflector during removal and replacement of elevation jack.
3. Jack Adjustment Tool	Set elevation jack extension to a design point for initial track calibration.
4. Clinometer Mount	Provide interface between clinometer or minilevel and main beam reference point.
5. Hoisting Tool, Azimuth Drive	Remove and replace azimuth drive.

*Current design is for a less sophisticated Manual Control Box for immediate use.

Table 6-5

(Continued)

Item	Use
6. Hoisting Tool, Reflector/ Support Assembly	Remove and replace reflector/support assembly during azimuth drive change out.
7. Tool, Panel Leveling	Measure mirror module cant angle. Used in conjunction with Wyler mini-level.
8. Sling, Mirror Module Lifting.	Remove and replace mirror module.

Appendix A
STRUCTURAL TESTING

Appendix A includes three sections. The first section is MDAC's mirror module test plan. This in turn contains four elements: the environmental exposure tests, the thermal distortion test, the thermal cycle test, and the hail impact tests. Of these, the first three will be undertaken in the near future; the latter is complete and its results are detailed. The second section addresses the justification for deleting the previously planned reflector support structure test. The last section of Appendix A presents the results of MDAC's adhesive laminating development testing.

MIRROR MODULE TESTING

The Second Generation heliostat design is required to conform to the Collector Subsystem requirements. That document specifies the environmental conditions which must be survived and the performance which must be delivered. The mirror module, which is a thin 48 x 132 inches second-surface silvered glass mirror laminated to a thicker glass backlight with two full length stringers for support and sealed edges for protection,is a critical component. The mirror module must survive the rigors of a desert type environment for a design life of 30 years. In addition, the mirror module must maintain acceptable beam quality throughout a wide range of temperature and gravity conditions.

The objectives of the mirror module test are to demonstrate the following:

1. The Environmental Exposure Tests will demonstrate that the mirror modules can survive long term exposure to typical desert and marine environments.
2. The Thermal Distortion Test and Cold Water Shock Test will demonstrate that the curvature changes experienced at operational temperature extremes due to the differential expansion or contraction of the steel and glass components will provide cost effective performance. It will also demonstrate that cold water sprayed on a hot mirror module will not cause damage.
3. The Thermal Cycle Tests will demonstrate that the mirror module is unaffected by repeated exposure to cycling between anticipated temperature extremes.

4. The Hail Impact Tests will demonstrate the capability of the mirror module to survive severe hailstorm conditions without damage.

The test specimen shall be a 1D22462 mirror module. Three test specimens are required, one for the desert exposure test, one for the marine exposure test, and one which will be used for both the thermal distortion and the thermal cycle test. A subscale mirror module (4 x 4 feet with two stringers 28 inches apart) will be used for the hail impact tests. Two specimens are required, one with a 0.093 float glass mirror laminated to a 0.188 backlite, and one with a 0.060 fusion glass mirror laminated to a 0.188 backlite.

TEST CONDITIONS

Environment Exposure Tests

1. General
   a. Test Location
      1) Desert exposure - One mirror module will be exposed to a desert environment at Fort Irwin, California.
      2) Marine Exposure - One mirror module will be exposed to a marine environment at MDAC's Solar Energy Test Facility at Huntington Beach, California.
   b. Test Setup - The mirror module will be attached to an exposure rack through the mirror module's three attachment points. The mirror surface shall be horizontal ± 10 degrees and facing upwards.
   c. Instrumentation - A Wyler mini-level shall be used to measure slope data at the locations shown in Figure A-1.

2. Environmental Conditions
   The mirror modules will be exposed to the natural weather conditions at the two test locations.

3. Failure Criteria
   The mirror modules will be considered to have successfully completed testing if both the desert and marine exposure produce no visual evidence of damage or degradation to the test specimen.

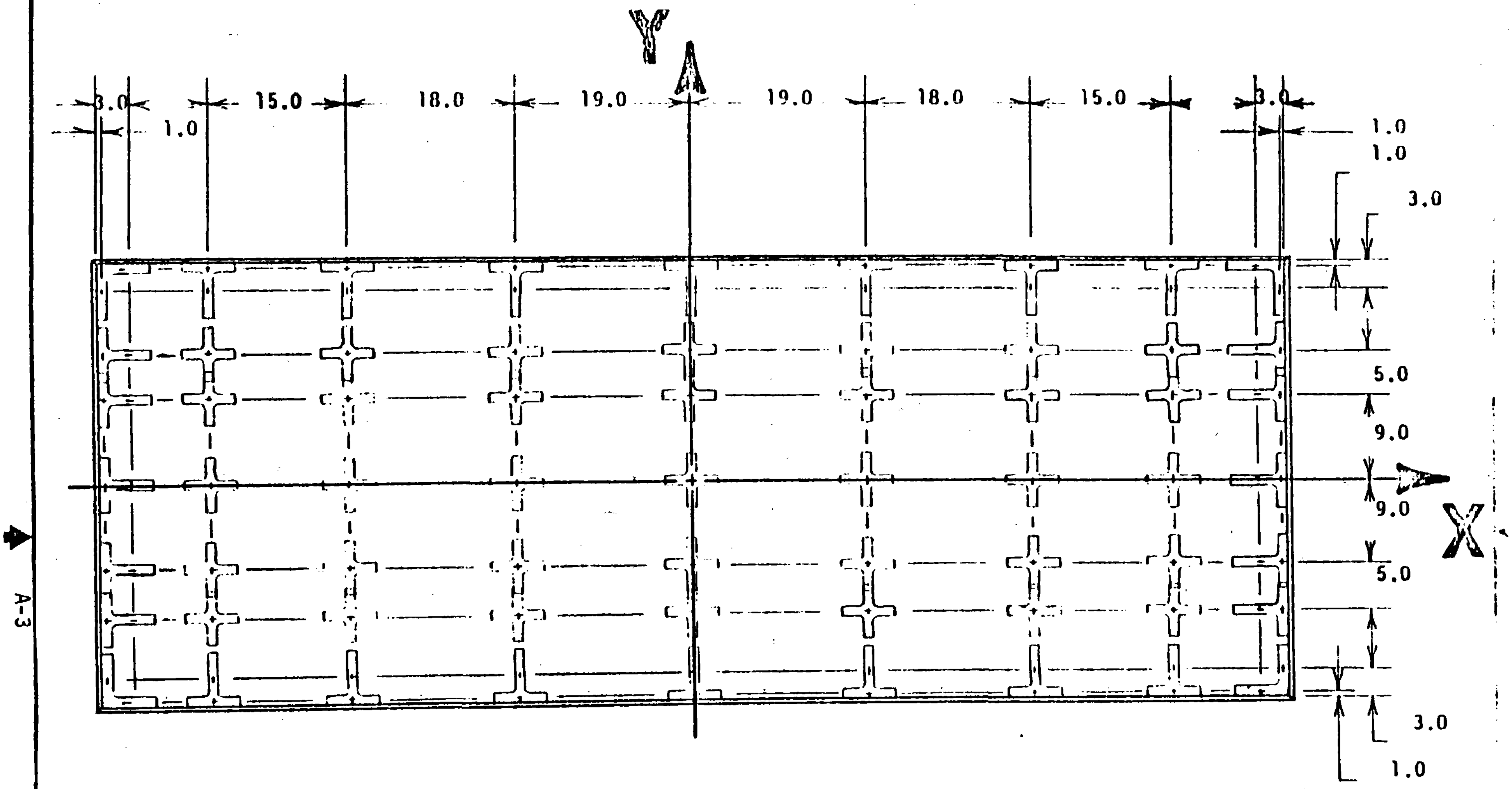

Figure A-1. Slope Measurement Locations

MCDONNELL DOUGLAS ASTRONAUTICS CO.
HUNTINGTON BEACH CALIF
MCDONNELL DOUGLAS

SIZE	CODE IDENT NO	DRAWING NO.
A	18355	IT54042

SCALE	REV	SHEET 2.6

Thermal Distortion Test and Cold Water Shock Test

1. General
   a. Test Location - This test will be conducted at the Structures and Environments Laboratory, Building 30, of MDAC's Huntington Beach facility.
   b. Test Setup - A mirror module will be set up within an environmental chamber capable of providing the conditions required. The module shall be supported at its three attachment points, but not restrained from expansion. A means of leveling the mirror module must be provided so that the center point can be adjusted to a level position prior to taking slope data at each temperature required.
   c. Instrumentation - A Wyler mini-lever shall be used to measure slope data at the locations shown in Figure A-1.
   d. Data Reduction - Slope data in milliradians versus position will be provided for the two mirror module axes, along the length and along the width, for each temperature condition.
2. Environmental Conditions

   The chamber will be operated to obtain temperatures of 77°F, 32°F, and 122°F. Slope measurements of the mirror module will be made at each temperature after the chamber temperature has been maintained at the test temperature for a minimum of one hour. Upon conclusion of the slope measurements at 122°F, five gallons of cold water at 60°F shall be thrown onto the mirror module surface.
3. Failure Criteria

   The test will be considered successful if:
   a. The slope measurements are in good agreement with NASTRAN predictions, and
   b. No visible damage occurs from the cold water shock.

Thermal Cycle Test

1. General
   a. Test location and test setup are the same as the thermal distortion test and cold water shock test.
   b. Instrumentation shall consist of the temperature versus time readout of the chamber.

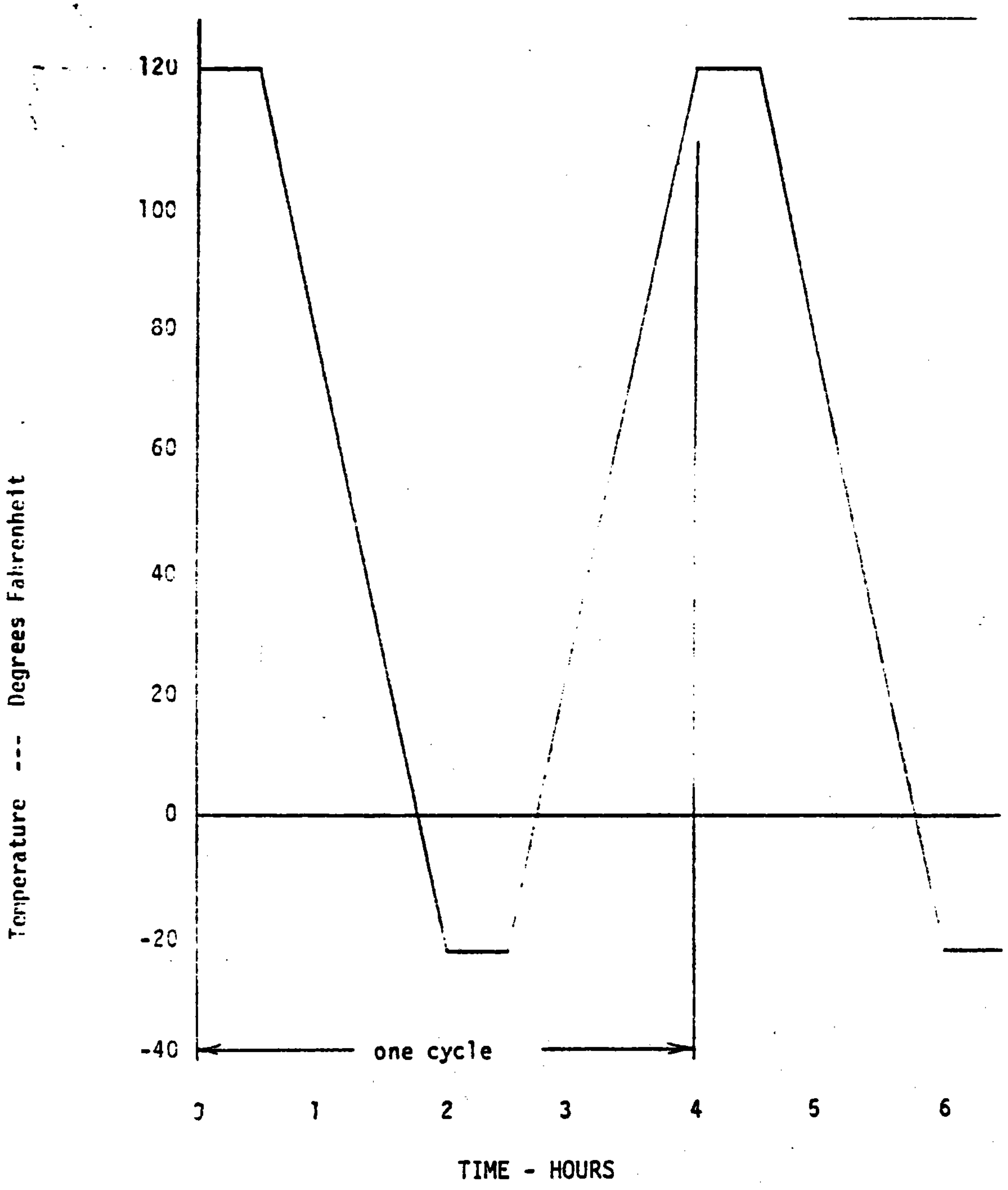

Figure A-2 Thermal Cycle Test - Temperature Cycle

MCDONNELL DOUGLAS ASTRONAUTICS CO.
HUNTINGTON BEACH, CALIF.
MCDONNELL DOUGLAS

SIZE	CODE IDENT NO.	DRAWING NO.
A	18355	1T54042

SCALE
REV
SHEET 2.8

60-0213 1A02 (06 AUG 71)

2. Environmental Conditions

The temperature shall be varied from -22°F to +122°F within the chamber and held at those extremes for one half hour. Six cycles or more per day are required for a two week period. The mirror module should be inspected every other day for any indications of damage. See Figure A-2.

3. Failure Criteria

The test will be considered successful if at the end of the 84+ cycles over the two week test period, no visible evidence of damage or deterioration of the mirror module can be found.

Hail Impact Tests

1. General
   a. Test Location - These tests will be conducted in the Photoelastic Laboratory, Building 22 of MDAC's Huntington Beach facility.
   b. Test Setup - The test specimen will be supported vertically in front of MDAC's hail cannon by the stringers and/or the panel edge remote from the selected impact location.
   c. Instrumentation - Each of two backlited photodiodes positioned three inches apart will be connected to one trace of a Tektronix Model 555 dual beam oscilloscope equipped with a Polaroid camera to record the time of passage of the simulated hail stone. The hailstone velocity is then determined by dividing the time in seconds into 0.25 foot to obtain the velocity in feet per second.

2. Test Conditions

One inch diameter hail stones are simulated by one inch diameter ice spheres maintained at 20°F until loaded into the hail cannon. These will be fired at the test specimen at 75 ft/sec in order to impact it at various locations as shown in Figure A-3.

3. Failure Criteria

The test will be considered successful if no visible damage occurs from the 75 ft/sec hail.

4. Results

The two test specimens were each fabricated with four edge treatments along their perimeter. Both panels were impacted at the interior locations at 75 ft/sec with only one failure occurring in the 0.093 mirror. A repeat

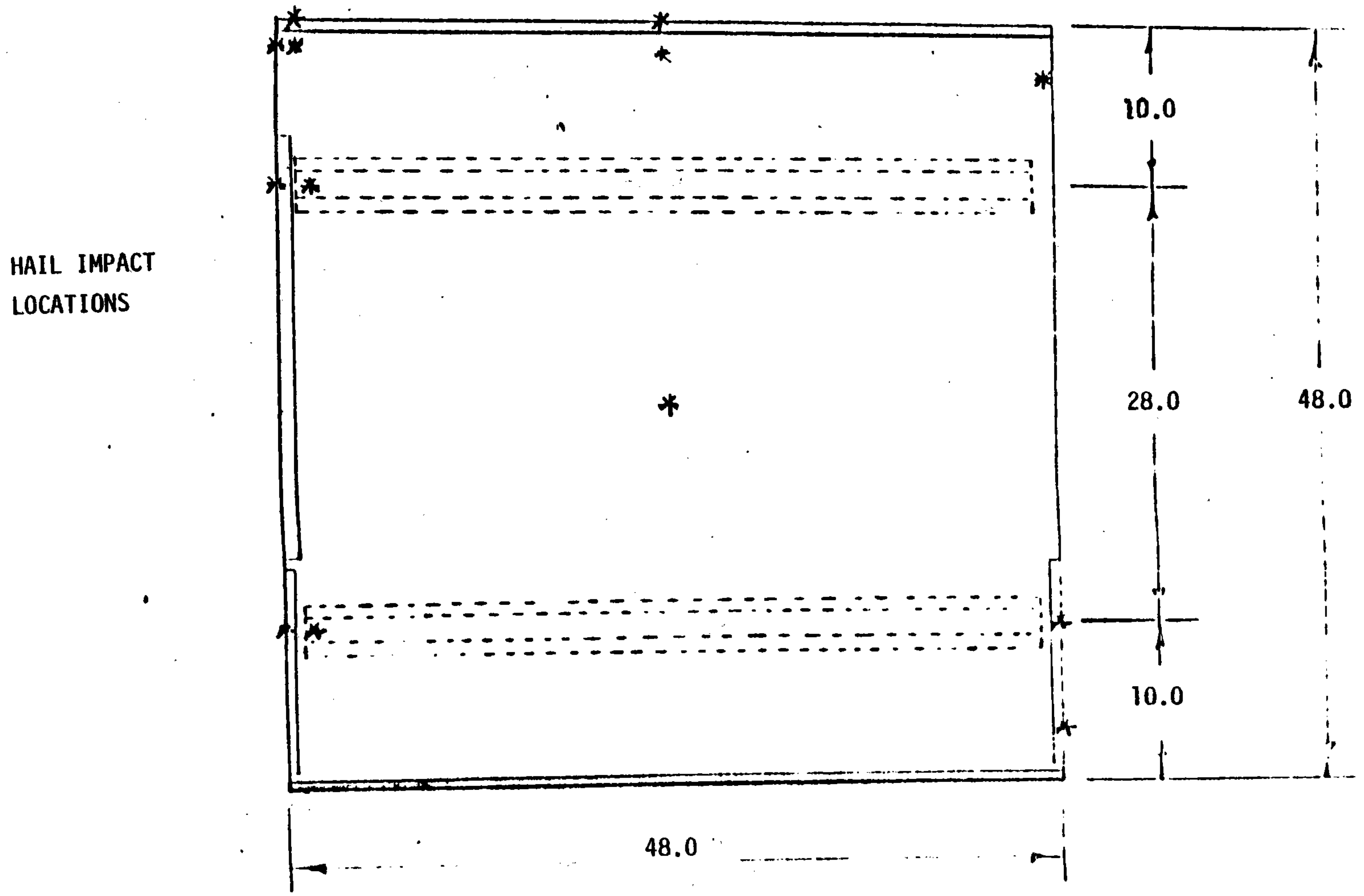

Figure A-3. Hail Impact Test

strike at a similar location did not induce a failure. The four edge treatments were also subjected to hail impact. The edge treatments tested were a bare edge, a metal edge member with silicone and butyl sealant, an aluminum tape covered butyl sealant, and a silicone rubber edge member bonded with a silicone adhesive. The bare edge inadvertently came as two types, one with the 0.060 mirror extending past the 0.188 backlite by about 0.10 inch, and, on the opposite side of the panel the 0.188 backlite extending past the 0.060 mirror. This afforded the opportunity to obtain additional information, so both of those edge conditions were tested. The metal edge seal was undamaged by the 75 ft/sec hail impact. The aluminum tape experienced failure in the glass and tears in the aluminum which could provide a moisture leak path to the edge. The rubber edge strip was unable to protect the overhung front edge and received indentations which increased with repeated impacts on the undercut front edge; however, the indentations subsequently recovered. The overhung bare edge was broken by the hail, but the undercut edge survived intact. Both of the panels were struck from the backlite side without damage.

In summary, the metal edge seal and a bare edge with the thin sheet even with or cut back from the edge can survive the 75 ft/sec hail condition. The aluminum tape and rubber edge seal are unacceptable.

In addition to testing at the specification requirements, the panels were tested at a higher velocity of 100 ft/sec. No damage occurred on the 0.093 mirror specimen. One failure under the metal edge seal occurred on the 0.060 mirror; however, three repeats of the test could not reproduce the failure.

REFLECTOR SUPPORT STRUCTURE TEST

This test was deleted from the test program to reduce costs. It was selected as having a low risk of failure for the following reasons:

1. Performance
    a. Overall Stiffness - High confidence in analysis and available margin with specification performance requirement.

   b. Joint Stiffness - Difficult analysis with accuracy of ±50 percent; however, total is only about 10 percent of the overall structural stiffness.

2. Strength and Stability
   a. Conservative wind load approach.
   b. Stability margins based on allowables of 50 percent of critical.
   c. Adequate margins on reduced allowables.
   d. Critical spot welded joint not present on prototype hardware.

ADHESIVE LAMINATING TEST RESULTS

Introduction

Low cost bonding procedures were developed using sprayed polyurethane adhesive and mating the mirror module components by pressurization as they pass through a set of pinch rollers. The mirror module is allowed to cure on a flat table until the adhesive has enough strength so that the mirror may be moved without any damage to the bond or distortion of the reflected image.

Galvanized steel stringers were bonded to the back of the mirror module; these maintained the flatness or added curvature as required.

Edge members were used to protect the mirror-backlite bond from degradation due to edge corrosion.

Objective

Fabrication of full-sized mirror modules, 48 x 132 inches, using 3/32 inch mirrors with exposed copper backing and 3/16 inch float glass backlite, bonded together with 1XB3507 polyurethane adhesive using pinch rollers for bond pressurization.

The 1XB3504-1 adhesive was evaluated for viscosity and spraying process properties. Adhesion properties, tensile strength, shear strength, shear modulus and the effects of aging on these properties were evaluated.

The stringer adhesive, EC3532, will be evaluated for adhesion to glass and galvanized steel using lap shear and tensile strength coupons.

Edge seal evaluation was done using a cyclic test chamber exposing the mirror modules to 10°F to 140°F, 60 to 100 percent relative humidity, and ultra violet radiation.

Processes will be developed to incorporate adding concave curvature to the mirror side to improve reflective image-efficiency.

Procedures will be written into a process document with all the pertinent details to produce production quality mirror modules.

Requirements

Mirror module components, mirror and glass backlites, shall meet flatness requirements, as determined by scatterometer measurements and reflected images.

The bonded mirror modules, with bonded stringers and edge members, shall meet reflected image requirements.

The edge members shall provide a seal against degradation for a period of 30 years for mirror-backlite bond.

Engineering adhesive material and process requirements for the selected adhesive is compared to the glass laminating industry's polyvinyl butyral film material in Figure A-4.

Methodology

Many chemical types of adhesives were evaluated. Adhesives have different types of curing and processing characteristics, such as hot melts, ultra violet curing, the application of one component on each faying surface, as well as the typical two component mixed adhesives. These adhesives were subjected to seven-day tests at 140°F to determine their mirror compatibility, as shown in Figures A-5 and A-6. Other tests such as tensile block strength and compressive shear strength were for selected candidate adhesive against the copper plated mirror surface, as shown in Figure A-7. Only two adhesives, 1XA3504-1 polyurethane and the XB2464 ultra violet epoxy curing, developed acceptable strengths and showed no corrosion effects.

SELECTED CANDIDATE ADHESIVES

PHYSICAL PROPERTIES AT RT	ENGINEERING REQUIREMENTS	POLYVINYLBUTYRAL MONSANTO SR10	POLYURETHANE 3M 1XA3504-1
FLATWISE TENSILE STR.	400 PSI	998 PSI AVG (AUTOCLAVED) 626 PSI AVG (PINCH ROLLED)	801 PSI AVG.
SCREEN PEEL STR.	NONE	8.0 PIW	3.8 PIW
SHEAR MODULUS (DOUBLE LAP)	25 PSI	115 PSI AVG. TAN @ 25#	1492 PSI AVG. TAN @ 100#
SHEAR STRENGTH (SINGLE LAPS)	400 PSI	442 PSI AVG.	656 PSI AVG.
COMPRESSIVE STR. (SINGLE LAP)	400 PSI	693 PSI AVG.	1102 PSI AVG.
PROCESS CHARACTERISTICS			
1. APPLICATION	100% COVERAGE	LAYUP DRY FILM	SPRAY MIXED ADH.
2. CURE TIME	≈ 15 MINUTES	METHOD (A) AUTOCLAVE ≈ 2 HRS. (B) PINCH ROLL ONLY @ 220°F ≈ 2 MINUTES	≈ 15 MINUTES
3. LAMINATING PROCESS	ANY METHOD RESULTING IN GOOD IMAGE; NO SHADOWS OR BRIGHT SPOTS	METHOD (A) AUTOCLAVE ≈ 200 PSI (B) PINCH ROLL ≈ 80 PSI	PINCH ROLL ≈ 1-2 PSI CURED ON MICRO FLAT TABLE

Figure A-4. Selected Candidate Adhesives

COMPATIBILITY AND AGING EFFECTS OF COPPER PLATED SILVERED MIRRORS ON ADHESIVE BONDS

III - COMPATIBILITY OF ADHESIVES AND COPPER IN 140°F ENVIRONMENT

7-DAY EXPOSURE RESULTS

ADHESIVES	AG + CU + PAINT .050 SANDIA MIRROR	AG ONLY	AG + CU-20 MIN	AG + CU AMB COND	AG + CU N_2 PURGED
<u>IN CIRCULATING OVEN</u>					
1XA3504-1 (3M P.U.)	NO EFFECT	NO EFFECT	NO EFFECT	NO EFFECT	NO EFFECT
GR529-18 (G.E. SILICONE)	NO EFFECT	NO EFFECT	NO EFFECT	NO EFFECT	NO EFFECT
3227-6 (HUGHSON ACRY)	----	----	AG LIFTED OFF GLASS	-----	----
B2464 (3M U.V. EPOXY)	NO EFFECT	NO EFFECT	---	NO EFFECT	NO EFFECT
6AM (W.R. GRACE H.V. EPOXY)	NO EFFECT	NO EFFECT	---	NO EFFECT	NO EFFECT
Y12-384 (SWIFT HOT MELT)	NO EFFECT		---	NO EFFECT	NO EFFECT
LR 100-225 (HYSOL ACRYLIC)	NO EFFECT	CORROSION - 24 HRS.	---	CORROSION IN 24 HRS.	CORRODED
227-179-1 (DESOTO U.V. EPOXY)	NO EFFECT	NO EFFECT	---	NO EFFECT	NO EFFECT

Figure A-5. Compatability and Aging Effects of Copper Plated Silvered Mirrors on Adhesive Bonds

COMPATIBILITY AND AGING EFFECTS OF COPPER PLATED SILVERED MIRRORS ON ADHESIVE BONDS

III - COMPATIBILITY OF ADHESIVES AND COPPER IN 140°F ENVIRONMENT (CONTINUED)

7-DAY EXPOSURE RESULTS

ADHESIVES	AG + CU + PAINT .050 SANDIA MIRROR	AG ONLY	AG + CU-20 MIN	AG + CU AMB COND	AG + CU N_2 PURGED
<u>IN SEALED BAG PLUS OVEN</u>					
1XA-3504-1	NO EFFECT	NO EFFECT	NO EFFECT	NO EFFECT	NO EFFECT
SR529-18	NO EFFECT	NO EFFECT	NO EFFECT	NO EFFECT	NO EFFECT
3227-6	---	---	AG LIFTED OFF GLASS	---	---
B2464	CORROSION ONE SPOT	NO EFFECT	---	SOME AG LIFTED OFF GLASS	ONE EDGE AG LIFTING
16AM	NO EFFECT	NO EFFECT	---	NO EFFECT	NO EFFECT

Figure A-6. Compatability and Aging Effects of Copper Plated Silvered Mirrors on Adhesive Bonds

COMPATIBILITY AND AGING EFFECTS OF COPPER PLATED SILVERED MIRRORS ON ADHESIVE BONDS

I - EFFECTS OF AGING PLATED COPPER ON ADHESIVE BOND STRENGTHS

ADHESIVE MFG & TYPE	COPPER PLATING SEQUENCE	COMPRESSIVE PSI	SHEAR STR. FAILURE	TENSILE PSI	BLOCK STR. FAILURE	COMMENTS
1XA3504-1 3M-POLYURETHANE	CU PLATED-20 MIN.	AVG 1223	100% AG-GLASS	AVG 1052	100% GLASS	INDICATES SOME LOSS OF ADHESION TO UNPURGED AGED CU
	CU STORED-AMB. COND.	973	75% ADH. CU.-25% GLASS	800	60% ADH-CU.	
	CU STORED N_2 PURGE	1231	100% ADH-GLASS	---	30% AG-GLASS 10% ADH-GLASS	
SR 529-18 G.E.-SILICONE	CU PLATED-20 MIN.	AVG 173	100% COH.	AVG 378	ADH-GLASS-CU	NO EFFECT ON ADH. TO AGED
	CU STORED-AMB. COND.	230	100% COH.	*171	100% COH.	*SOLVENTS TRAPPED IN BOND
	CU STORED N_2 PURGE	237	100% COH.	*130	100% COH.	*ON TENSILE COUPONS
B3327-G HUGHSON-ACRYLIC	CU PLATED-20 MIN.	AVG 4000	NO FAILURE	AVG 516	100% AG-GLASS	ACRYLIC ADHESIVE ATTACKING CU + AG.
XB2464 3M U.V. EPOXY	CU STORED-AMB. COND.	AVG 873	100% ADH-CU	AVG 905	75% ADH-CU 25% AG-GLASS	INDICATES SOME LOSS OF ADHESION TO UNPURGED AGED CU
	CU STORED N_2 PURGE	1203	100% ADH-CU	716	40% ADH-CU 60% ADH-GLASS	
LR-100-225 HYSOL-ACRYLIC	CU STORED-AMB. COND.	Avg 210	100% COH	AVG 699	50% COH 50% ADH-CU	ACRYLIC ADHESIVE ATTACKING CU + AG
	CU STORED N_2 PURGE	110	100% COH	695	60% COH 40% ADH-CU	COH FAILURES NOT ATTRIBUTABLE CU ADH.
16 AM W.R.GRACE U.V. EPOXY	CU STORED-AMB. COND.	FAILED DURING CLEANUP TO GLASS		AVG 375	100% ADH-GLASS	POOR ADHESION TO GLASS
	CU STORED N_2 PURGE	" "	"	357	100% ADH-GLASS	
CVV LOCTITE-ANAROBIC N PRIMER	CU STORED-AMB. COND.	AVG 502	100% ADH-GLASS	AVG 865	100% ADH-GLASS	CORROSION TO CU OCCURRING
	CU STORED N_2 PURGE	---	---	780	100% ADH-GLASS	

Figure A-7. Compatability and Aging Effects of Copper Plated Silvered Mirrors on Adhesive Bonds

DESERT EXPOSURE

38 DAYS - FORT IRWIN - GOLD STONE

SAMPLES - EACH CANDIDATE ADHESIVE WAS USED TO LAMINATE TWO 5" x 5" MIRROR MODULES

(A) ONE LAMINATED MIRROR HAD NO EDGE MEMBERS

(B) ONE LAMINATED MIRROR HAD A GALVANIZED STEEL U-CHANNEL EDGE MEMBER WITH A POLYISOBUTYLENE INNER SEAL AND A SILICONE OUTER SEAL.

ADHESIVE	MIRRORING CONDITION					
	SILVER & COPPER-20 MIN.		SILVER & COPPER-AMB. COND.		SILVER & COPPER-N_2	
	NO EDGE MEMBER	EDGE MEMBER	NO EDGE MEMBER	EDGE MEMBER	NO EDGE MEMBER	EDGE MEMBER
1XA-3504-1 (3M P.U.)	NO EFFECT	NO EFFECT	NO EFFECT	NO EFFECT	CORROSION IN VOID AREA	NO EFFECT
SR529-18 (G.E. SILICONE)	NO EFFECT	NO EFFECT	CORROSION	NO EFFECT	CORROSION	CORROSION
XB2464 (3M U.V. EPOXY)	---	---	EDGE CORROSION	NO EFFECT	---	---
16 AM (W.R.G. U.V. EPOXY)	---	---	CORROSION	NO EFFECT	---	---
227-179-2 (U.V. EPOXY)	---	---	CORROSION	NO EFFECT	---	---
SR10 (MONSANTO PVB) PINCH ROLLED)	NO EFFECT	NO EFFECT	---	---	---	---
SR10 (MONSANTO PVB AUTOCLAVED)	NO EFFECT	NO EFFECT	---	---	---	---
H.B. 636-47 (P.U.)	---	---	NO EFFECT	NO EFFECT	---	---

Figure A-8. Desert Exposure 38 Days - Fort Irwin - Gold Stone

EFFECT OF BOND PRESSURE ON IMAGE

ADHESIVE	PRESSURE APPLIED	RESULTS
1. SR10 PVB ADHESIVE	PINCH ROLL ONLY - 80 PSI	ACCEPTABLE IMAGE
	AUTOCLAVED - 200 PSI	ACCEPTABLE IMAGE
2. 1XA-3504-1 ADHESIVE	PINCH ROLLED - 30 PSI	POOR IMAGE
	1 1/2 ± 1/2 PSI VACUUM	POOR IMAGE
	BACKLITE WEIGHT ONLY	ACCEPTABLE IMAGE (VOIDS)
	1-2 PSI APPLIED BY ROLLER ON MICROFLAT TABLE	ACCEPTABLE IMAGE
	PINCH ROLLED - 1-2 PSI	MARGINAL IMAGE

- TALC FILLER IN 1XA-3504-1 ADHESIVE PRODUCES PRESSURE SPOTS THAT 1XA-3504-2 ADHESIVE (NO TALC FILLER) SHOULD ELIMINATE

Figure A-9. Effect of Bond Pressure on Image

WEATHEROMETER TESTING
30-DAY TEST

PANEL DESCRIPTION: 10" X 14" LAMINATED MIRRORS WITH AND WITHOUT EDGE MEMBERS

- O NINE PANELS ARE BEING TESTED USING THIS WEATHEROMETER CYCLE.

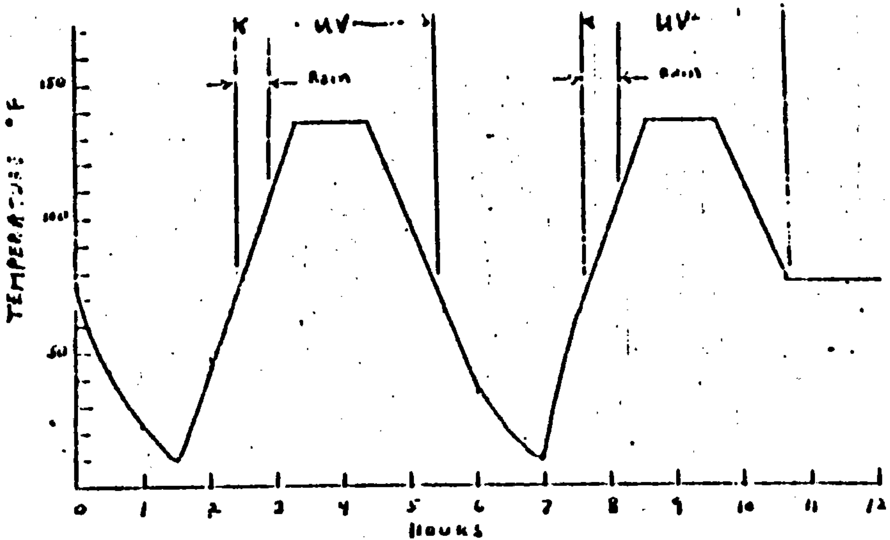

- O TEMPERATURE RANGE
  - 10°F TO 135°F
- O UV RADIATION
  - O 500 $\mu W/CM^2$ AVERAGE
  - O DURATION 12 HOURS/DAY
  - O MAX. INTENSITY AT WAVELENGTH OF 365 NM
- O RELATIVE HUMIDITY
  - O GREATER THAN 85%
- O WATER SPRAY
  - O 1.12 GAL/MIN OVER 16 SQ. FT.
  - O DURATION 2 HOURS/DAY

Figure A-10. Weatherometer Testing 30 Day Test

		RESULTS
1.	1/8" MIRROR-COPPER/1/4" FLOAT BACKLITE - SR10 PVB ADHESIVE AUTOCLAVED - GALVANIZED EDGE MEMBER	NO EFFECT
2.	1/8"MIRROR-COPPER/1/4" FLOAT BACKLITE - SR10 PVB ADHESIVE AUTOCLAVED - NO EDGE MEMBER	COPPER CORROSION AT EDGES
3.	1/8" MIRROR-COPPER/1/4" FLOAT BACKLITE - SR10 PVB ADHESIVE PINCH ROLLED - GALVANIZED EDGE MEMBER	NO EFFECT
4.	1/8" MIRROR-COPPER/1/4" FLOAT BACKLITE - SR10 PVB ADHESIVE PINCH ROLLED - NO EDGE MEMBER	CORROSION AT EDGE
5.	1/8" MIRROR-COPPER/1/4" FLOAT BACKLITE - SR10 PVB ADHESIVE AUTOCLAVED - SILICONE EDGE MEMBER	NO EFFECT
6.	1/8" MIRROR-COPPER/1/4" FLOAT BACKLITE - SR10 PVB ADHESIVE PINCH ROLLED - SILICONE EDGE MEMBER	NO EFFECT
7.	1/8" MIRROR-COPPER/1/4" FLOAT BACKLITE - 1XA-3504-2 - NO EDGE MEMBER	CORROSION AT EDGE AND IN ADHESIVE
8.	1/8" MIRROR-COPPER/1/4" FLOAT BACKLITE - 1XA-3504-2 - GALVANIZED EDGE MEMBER	NO EFFECT
9.	1/8" MIRROR-COPPER/1/4" FLOAT BACKLITE - 1XA-3504-2 - SILICONE EDGE SEAL	NO EFFECT

Figure A-11. Weatherometer Testing - 30-Day Test

EDGE MEMBERS FOR 2ND GENERATION MIRROR MODULES

MATERIAL	CONFIGURATION	ADVANTAGES	DISADVANTAGES
1. GALVANIZED STEEL (FOUR PIECES + FOUR CORNERS)	U-CHANNEL 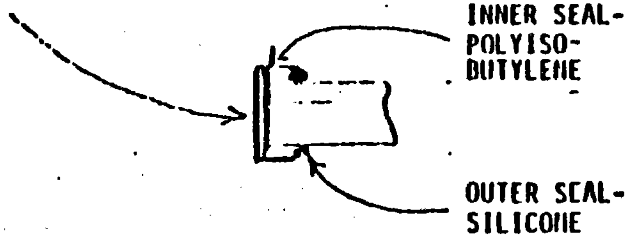	PROVEN SEALING CAPABILITIES	ASSEMBLY OF FOUR EDGES AND FOUR CORNERS REQUIRED
2. SILICONE RUBBER (ONE PIECE)	U-CHANNEL 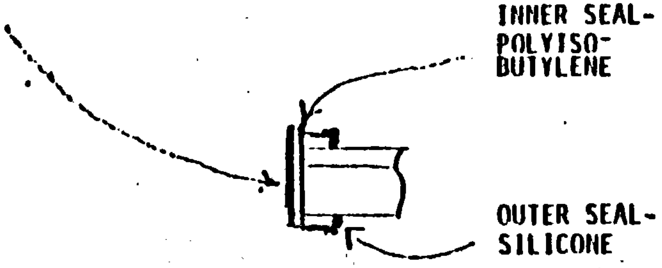	MINIMAL ASSEMBLY TIME - SNAPS ON AROUND PERIPHERY OF PANEL	HIGHER MATERIAL COSTS

Figure A-12. Edge Members For 2nd Generation Mirror Modules

Table A-1

Desert Aging - Mirror Laminates

6" x 6" Specimens	Faying Surfaces	Adhesives	Backlite Thickness	Edge Seal	Location	Exposure	Results
#1 Ag + Cu laminated mirror (14 day Amb stored)*	Cu - glass	P.U. 1XA3504-1 adhesive (large voids)	(1/4")	(butyl silicone galv. steel)	Fort Irwin	9 mos.	Corrosion in area of voids
#1A - Ag + Cu laminated mirror (14 day amb. stored)	Cu - glass	P.U. 1XA3504-1 adhesive (large voids)	(1/4")	None	Fort Irwin	9 mos.	Edge corrosion
#4 - Ag + Cu (20 min. Cu storage)	CU - glass	P.U. 1XA3504-1 (voids)	(1/4") (1/4")	(butyl silicone galv. steel)	Fort Irwin	9 mos.	1/4 of panel resulted in corrosion of mirror
#4A - Ag + Cu (20 min Cu storage)	Cu - glass	P.U. 1XA3504-1 (voids)	(1/4")	None	Fort Irwin	9 mos.	Edge corrosion & void corrosion
#6 - Ag + Cu laminated mirror (20 min. Cu storage)	Cu - glass	PVB SR10 Autoclaved	(1/4")	(butyl silicone galv. steel)	Fort Irwin	9 mos.	Edge corrosion of Cu
6A - Ag + Cu laminated mirror (20 min.) (Cu storage)	Cu - glass	PVB SR10 autoclaved	(1/4")	None	Fort Irwin	9 mos.	Edge corrosion of Cu and interior corrosion
#7 Ag + Cu laminated mirror (20 min. Cu storage)	Cu - glass	PVB SR10 pinch rolled	(1/4")	(butyl silicone galv. steel)	Fort Irwin	9 mos.	Cu corrosion
#7A Ag + Cu laminated mirror (20 min. Cu storage)	Cu - glass	PVB SR10 pinch rolled	(1/4")	None	Fort Irwin	9 mos.	Cu corrosion
#11 Ag only laminated mirror (20 min. storage)	Ag - glass	PVB SR10 pinch rolled	(1/4")	(butyl silicone galv. steel)	Fort Irwin	9 mos.	Air voids growing
#11A Ag only laminated mirror (20 min. storage)	Ag - glass	PVB SR10 pinch rolled	(1/4")	None	Fort Irwin	9 mos.	Edge corrosion Air voids growing

Table A-1 (Cont'd)

6" x 6" Specimens	Faying Surfaces	Adhesives	Backlite Thickness	Edge Seal	Location	Exposure	Results
#12 Ag only laminated mirror (20 min. storage)	Ag - glass	PVB SR10 autoclaved	(1/4")	(butyl silicone galv. steel)	Fort Irwin	9 mos	Edge corrosion
#12A Ag only laminated mirror (20 min. storage)	Ag - glass	PVB SR10 autoclaved	(1/4")	None	Fort Irwin	9 mos.	One small spot of corrosion + edge corrosion
#14 Ag + Cu laminated mirror (14 day N_2 purge)	Cu - glass	P.U. 1XA3504 (voids)	(1/4")	(butyl silicone galv. steel)	Fort Irwin	9 mos.	Corrosion in voids
66-4 Ag + Cu + mirror backing paint - gray	Gray - glass mirror backing paint	PVB SR10 autoclaved	(1/4")	None	Fort Irwin	36 mos.	1" edge discolorati of paint. Air bubbles in PVB
65-21 Ag + Cu + mirror backing paint - gray	Gray mirror - glass backing paint PPG VC 44409 7 - gm/ft^2	PVB SR10 autoclaved	(1/4")	None	China Lake	36 mos.	1/2" gray paint discoloration
65-13 Ag + Cu + mirror backing paint	Gray mirror backing paint - glass	PVB Monsanto Saflex 10 autoclaved	(1/4")	None	China Lake	36 mos.	3/4" gray paint discoloration

* Storage time of bare copper before bonding mirror.

Conclusions:

1. Good edge seals required for any laminating adhesive.
2. Panels bonded with 1XA3507, when exposed to desert environment, resulted in mirror corrosion where voids extended to edge of bondline, even with good edge seals.
3. Copper and silver faying surfaces do show corrosion in shorter periods of time when exposed to desert environment, than mirrors with backing paint.
4. Gray mirror backing paint shows edge discoloration, but with an adequate seal would result in the service over a 30-year period.

Initial 38-day desert exposure of some of the selected candidate adhesives showed very quickly that there were compatibility problems between the mirrored surfaces and adhesives (Figure A-8).

After all initial screening had been completed, the 1XA3504-1 adhesive was selected as the most likely candidate for laminating mirrors to backlites. The industry standard method of laminating mirrors using PVB film was also selected as a control and also candidate method. Different methods of pressure applications were evaluated on these materials in the lamination and bonding of mirror modules (Figure A-9). Accelerated weatherometer testing of the two candidate materials with and without selected edge members were completed (Figures A-10 and A-11).

The two selected edge seals, silicone rubber and a galvanized steel edge member, were used in testing the laminated mirrors in different environments (Figure A-12).

Long term desert aging of the two selected laminating adhesive was done, and the results are shown in Table A-1. The conclusions drawn are as follows:

1. Good edge seals are required.
2. Mirror backing paint is better than copper alone in a corrosive atmosphere.
3. Voids in 1XA3504-1 adhesive resulted in mirror corrosion.

APPENDIX B

VENDOR DRIVE MOTOR TEST DATA

Figures B-1 and B-2 indicate actual test data on the azimuth 1/4 HP motor and 1/3 HP elevation motor. The data was obtained during acceptance testing by the motor vendor. It correlated closely with predicted computer model performance.

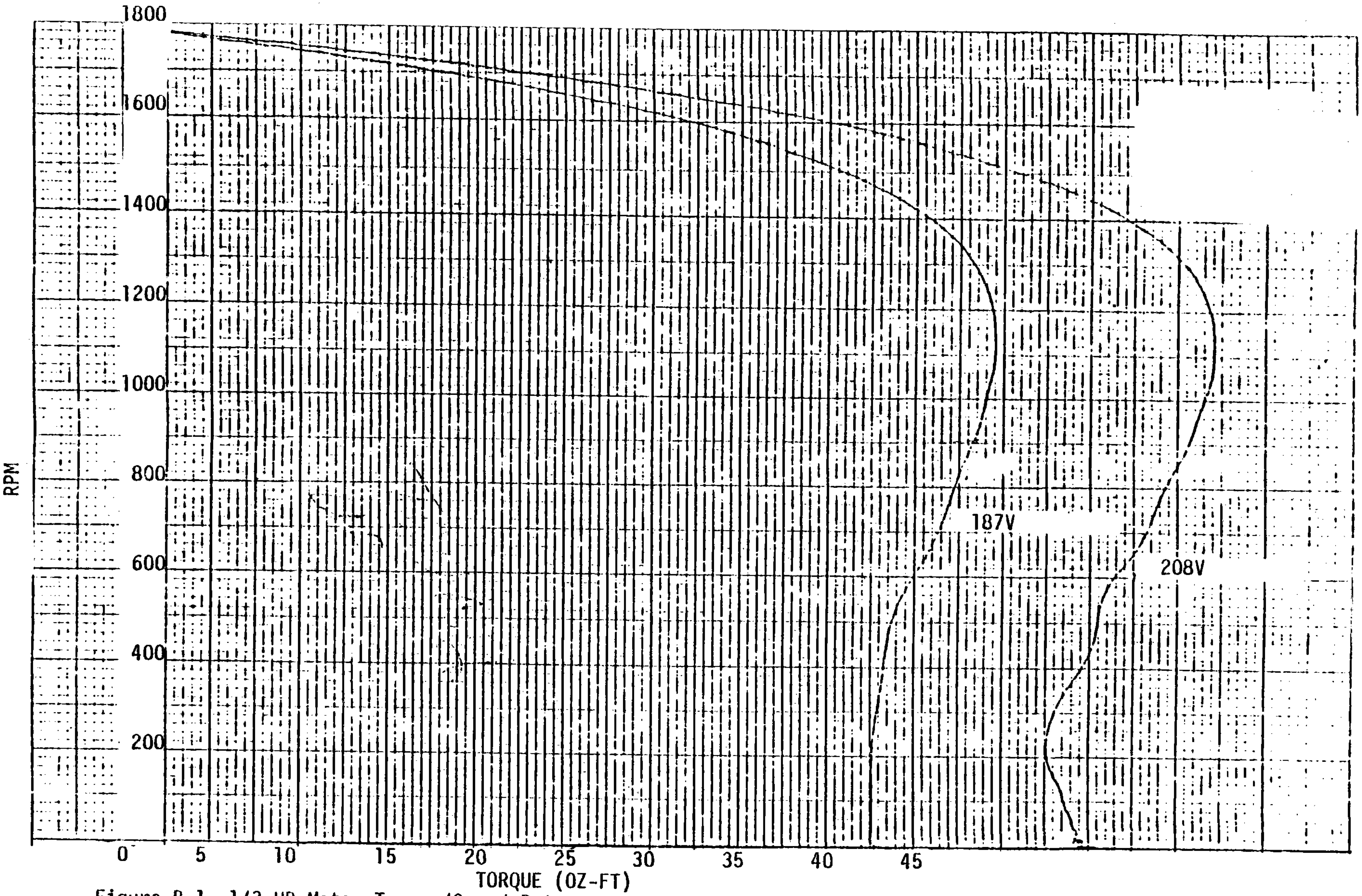

Figure B-1. 1/3 HP Motor Torque/Speed Data

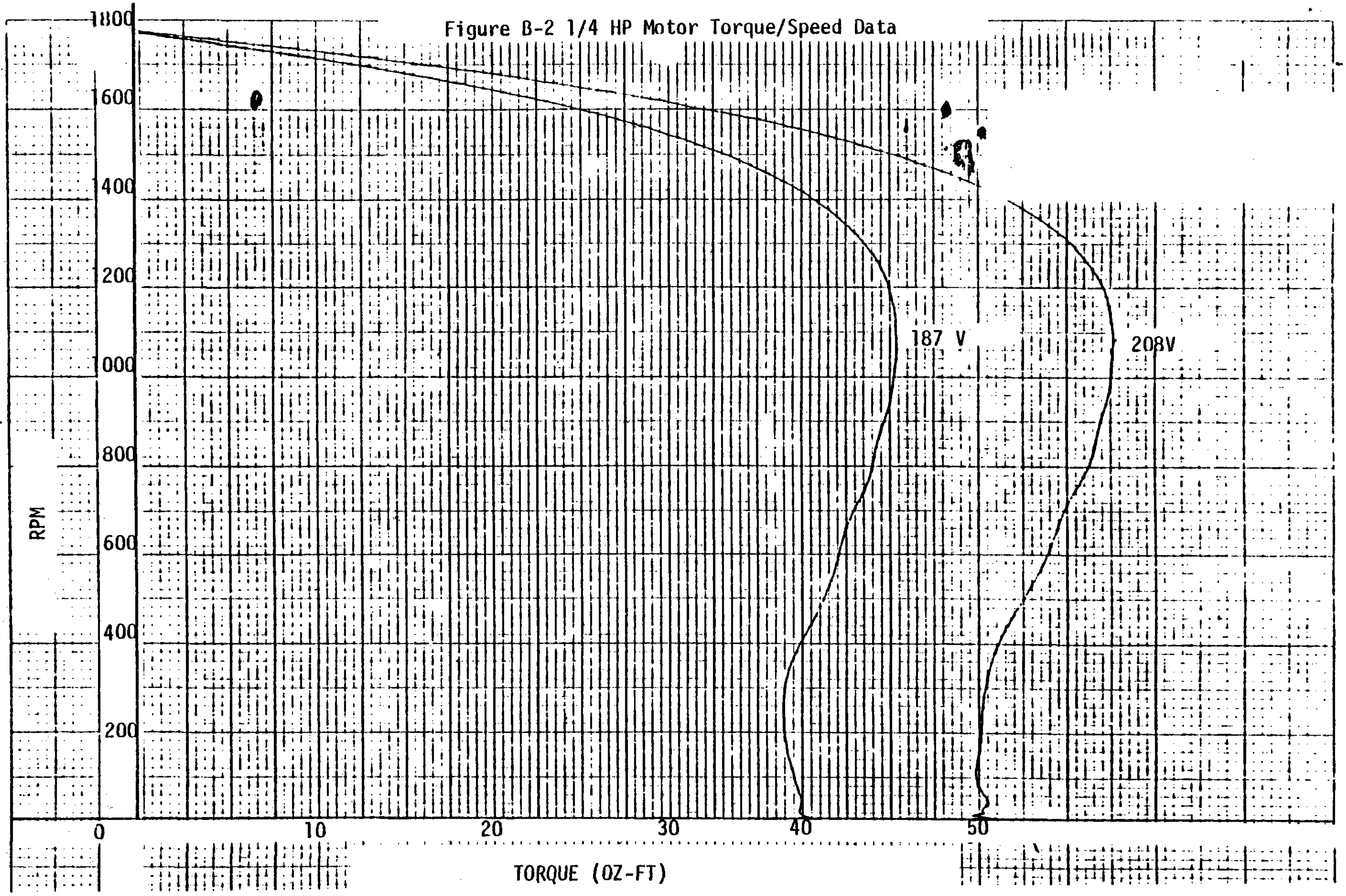

Figure B-2. 1/4 HP Motor Torque/Speed Data

Appendix C

PEDESTAL INSTALLATION PROCEDURE

This procedure may be used to install either a 1D22475, Drive Unit - Pedestal - Main Beam, or a 1D22461, pedestal onto a 1D22469, Foundation. An installation kit is used which for the prototype heliostats consists of four aluminum adapters, which bolt to the foundation and the pedestal, and some of MDAC's Structures Laboratory standard hydraulic equipment. The hydraulic equipment consists of a hydraulic pumping unit, which can be operated manually or by shop air, a 5000 psi pressure gage, two 5 square inch hydraulic actuators, interconnecting hydraulic hose equipped with quick disconnects, and a number of standard linkage elements which can be bolted to the aluminum adapters and the hydraulic jack. In addition, a plumb bob is helpful in orienting the pedestal with the foundation.

Installation Procedure

Bolt the two small adapter fittings into the nuts welded onto the foundation cone with (2) 1 inch diameter bolts for each fitting so that the hydraulic linkage attachment hole is on top. Bolt the two aluminum channel adapters into the nuts welded onto the pedestal with (2) 1 inch diameter bolts for each adapter so that the attachment hole is on the upper part of the pedestal. Bolt a clevis fitting to each channel adapter and install a hydraulic actuator with the rod end down. Lift the pedestal or drive unit - pedestal - main beam with a crane and lower over the foundation. Before contact is made, drop a plumb bob from one of the rod end holes in the hydraulic actuator. With the electrical controller box cutout on the south side, align the plumb bob with the lower adapter fitting. Lower the pedestal until it engages the pedestal, verifying that alignment is maintained. If not aligned, pull the pedestal up until it can be rotated to the correct alignment. When properly aligned and with lifting cables slack, remove the plumb bob, attach hydraulic lines lowering the actuator piston to maximum extension, and install hydraulic linkage to attach the actuator to the foundation adapter. Pressurize both jacks equally to 2000 psi to obtain 20,000 pounds of assembly force. Remove linkage and extend jack stroke as required to pull the pedestal and foundation together.

UNLIMITED RELEASE

INITIAL DISTRIBUTION

U.S. Department of Energy
600 E Street NW
Washington, D. C. 20585
Attn: W. W. Auer
G. W. Braun
K. Cherian
M. U. Gutstein
L. Melamed
J. E. Rannels

U.S. Department of Energy
San Francisco Operations Office
1333 Broadway
Oakland, CA 94612
Attn: S. D. Elliott
S. Fisk
R. W. Hughey
W. Nettleton

U.S. Department of Energy
Solar Ten Megawatt Project Office
P. O. Box 1449
Canoga Park, CA 91304
Attn: M. Slaminski

U.S. Department of Energy
Solar Ten Megawatt Project Office
5301 Bolsa Ave. MS14-1
Huntington Beach, CA 92649
Attn: R. W. Schweinberg

USAF Logistics Command
P. O. Box 33140
Wright-Patterson AFB
Ohio 45433
Attn: G. Kastanos

UCLA
900 Veteran Avenue
Los Angeles, CA 90024
Attn: F. Turner

Georgia Institute of Technology
Engineering Experiment St.
Atlanta, GA 30332
Attn: S. H. Bomar, Jr.

University of Houston
Houston
Solar Energy Laboratory
4800 Calhoun
Houston, TX 77004
Attn: A. F. Hildebrandt
L. L. Vant-Hull

U.S. Department of Interior
Water & Power Res. Service
P.O. Box 427
Boulder City, NV 89005
Attn: J. Sundberg

Acurex
485 Clyde Avenue
Mountain View, CA 94042
Attn: J. Hull

Aerospace Corporation
Solar Thermal Projects
Energy Systems Group, D-5
Room 1110
P.O. Box 92957
El Segundo, CA 90009
Attn: P. deRienzo
P. Mathur

Airesearch Manufacturing Co.
2525 West 190th Street
Torrance, CA 90509
Attn: M. G. Coombs
For: P. F. Connelly

AMFAC
700 Bishop Street
Honolulu, HI 96801
Attn: G. St. John

ARCO
911 Wilshire Blvd
Los Angeles, CA 90017
Attn: J. H. Caldwell, Jr.

Arizona Public Service
P. O. Box 21666
Phoenix, AZ 85036
Attn: D. L. Barnes
For: E. Weber

Arizona Solar Energy Commission
1700 W. Washington - 502
Phoenix, AZ 85007
Attn: R. Sears

Babcock & Wilcox
91 Stirling Avenue
Barberton, OH 44203
Attn: G. Grant
For: J. Pletcher
M. Seale

Babcock & Wilcox
P. O. Box 1260
Lynchburg, VA 24505
Attn: W. Smith

Babcock & Wilcox
20 S. VanBuren Avenue
Barberton, OH 44203
Attn: M. Wiener

Badger Energy, Inc.
One Broadway
Cambridge, MA 02142
Attn: F. D. Gardner

Battelle Pacific Northwest Labs
P. O. Box 999
Richland, WA 99352
Attn: M. A. Lind

Bechtel National, Inc.
P. O. Box 3965
San Francisco, CA 94119
Attn: E. Lam
For: J. B. Darnell
R. L. Lessley

Black & Veatch
P. O. Box 8405
Kansas City, MO 64114
Attn: C. Grosskreutz
For: J. E. Harder
S. Levy

Boeing Engineering & Construction
P. O. Box 3707
Seattle, WA 98124
Attn: R. Gillette
J. R. Gintz
R. L. Campbell

Booz, Allen & Hamilton, Inc.
8801 E. Pleasant Valley Road
Cleveland, OH 44131
Attn: W. Hahn

Brookhaven National Laboratory
Upton, NY 11973
Attn: G. Cottingham

Burns and Roe, Inc.
550 Kinderkamack Rd.
Oradell, NJ 07649
Attn: J. Willson

Busche Energy Systems
7288 Murdy Circle
Huntington Beach, CA 92647
Attn: K. Busche

California Public Utilities Commission
350 McAllister St., Room 5024
San Francisco, CA 94102
Attn: B. Barkovich
For: C. Waddell

Chevron Research
P. O. Box 1627
Richmond, CA 94804
Attn: L. Fraas

Chevron Oil Research
P. O. Box 446
La Habra, CA 90631
Attn: W. Peake
For: J. Ploeg
W. Stiles

Colt Industries
Trent Tube Division
East Troy, WI 53170
Attn: J. Thackray

Corning Glass Works
Advanced Products Dept.
M/S 25
Corning, NY 14830
Attn: W. M. Baldwin
A. Shoemaker

Custom Metals Enterprises, Inc.
3288 Main Street
Chula Vista, CA 92011
Attn: T. J. Bauer

Data Science Corp.
1189 Oddstad Drive
Redwood City, CA 94063
Attn: M. Liang

Electric Power Research Institute
P. O. Box 10412
Palo Alto, CA 93403
Attn: J. Bigger

El Paso Electric Company
P. O. Box 982
El Paso, TX 79946
Attn: J. E. Brown

Energy, Inc.
P. O. Box 736
Idaho Falls, ID 83401
Attn: G. Meredith

Exxon Enterprises-Solar Thermal Systems
P. O. Box 592
Florham Park, NJ 07932
Attn: P. Joy
For: D. Nelson
G. Yenetchi

Ford Aerospace
3939 Fabian Way, T33
Palo Alto, CA 94303
Attn: I. E. Lewis
For: H. Sund

Foster-Miller Associates
135 Second Avenue
Waltham, MA 02154
Attn: E. Poulin

Foster Wheeler Dev. Corp.
12 Peach Tree Hill Road
Livingston, NJ 07039
Attn: A. C. Gangadharan
For: R. Zoschak

GAI Consultants, Inc.
570 Beatty Rd.
Monroeville, PA 15146
Attn: H. Davidson

General Atomic Company
P. O. Box 81608
San Diego, CA 92138
Attn: H. A. Chiger

General Electric Company
Advanced Energy Programs
P. O. Box 8661
Philadelphia, PA 19101
Attn: A. A. Koenig

General Electric Company
1 River Road
Schenectady, NY 12345
tric Company
1 River Road
Schenectady, NY 12345
Attn: J. A. Elsner
For: R. N. Griffin
R. Horton

GM Transportation System Center
GM Technical Center
Warren, MI 48090
Attn: J. Britt

GM Corp. Harrison Rad. Division
A and E Building
Lockport, NY 14094
Attn: A. Stocker

Houston Lighting and Power
P. O. Box 1700
Houston, TX 77001
Attn: J. Ridgway

Institute of Gas Technology
Suite 218
1825 K Street, NW
Washington, D. C. 25006
Attn: D. R. Glenn

Jet Propulsion Laboratory
Building 520-201
4800 Oak Grove Drive
Pasadena, CA 91103
Attn: V. Truscello
For: H. Bank
W. Carley
W. Carroll
E. Cuddihy

Kaiser Engineers, Inc.
300 Lakeside Drive
Oakland, CA 94612
Attn: I. Kornyey

Lawrence Berkeley National Laboratory
University of California
Berkeley, CA 94720
Attn: A. J. Hunt

Los Alamos National Laboratory
P. O. Box 1663
Los Alamos, NM 87545
Attn: S. W. Moore

Los Angeles Water and Power
111 North Hope Street
Los Angeles, CA 90051
Attn: B. M. Tuller
R. Radmacher

Martin Marietta Corporation
P. O. Box 179
Denver, CO 80201
Attn: P. R. Brown
A. E. Hawkins
T. Heaton
L. Oldham
H. C. Wroton

McDonnell Douglas Astronautics Co.
5301 Bolsa Avenue
Huntington Beach, CA 92647
Attn: P. Drummond
R. L. Gervais
D. A. Steinmeyer
L. Weinstein

Meridian Corporation
5515 Cherokee Avenue
Alexandria, VA 22312
Attn: B. S. Macazeer

Nielsen Engineering. & Research
510 Clyde Avenue
Mt. View, CA 94043
Attn: R. Schwind

Northrup, Inc.
302 Nichols Drive
Hutchins, TX 75141
Attn: J. A. Pietsch

Northrup, Inc.
Blake Laboratory
Suite 306
7061 S. University Boulevard
Littleton, CO 80122
Attn: J. Anderson
F. Blake

Olin Corporation
275 Winchester Avenue
New Haven, CT 06511
Attn: S. L. Goldstein

OSC Department of Commerce
341 West 2d Street
San Bernardino, CA 92401
Attn: M. G. Heaviside

Pacific Gas and Electric Co.
77 Beale Street
San Francisco, CA 94105
Attn: P. D. Hindley
For: J. F. Doyle
A. Lam

Pacific Gas and Electric Co.
3400 Crow Canyon Road
San Ramon, CA 9426
Attn: H. Seielstad
For: J. Raggio

Phillips Chemical Co.
13-D2 Phillips Building
Bartlesville, OK 74004
Attn: M. Bowman

Pittsburgh Corning
800 Presque Isle Drive
Pittsburgh, PA 15239
Attn: W. F. Lynsavage

Pittsburgh Corning
723 N. Main Street
Port Allegany, PA 16743
Attn: W. J. Binder
For: R. Greene

PPG Industries, Inc.
One Gateway Center
Pittsburgh, PA 15222
Attn: C. R. Frownfelter

Public Service Co. of New Mexico
P. O. Box 2267
Albuquerque, NM 87103
Attn: A. Akhil

Research and Development
Public Service Co. of Oklahoma
P. O. Box 201
Tulsa, OK 74102
Attn: F. Meyer

Rockwell International
Energy Systems Group
8900 De Soto Avenue
Canoga Park, CA 91304
Attn: T. Springer

S. C. Plotkin & Associates
6451 West 83rd Street
Los Angeles, CA 90045
Attn: W. Raser

Safeguard Power Transmission Co.
Hub City Division
P. O. Box 1089
Aberdeen, SD 57401
Attn: R. E. Feldges

Sargent and Lundy
55 East Monroe
Chicago, IL 60603
Attn: N. Weber

Schumacher & Associates
2550 Fair Oaks Blvd., Suite 120
Sacramento, CA 95825
Attn: J. C. Schumacher

Sierra Pacific Power Co.
P. O. Box 10100
Reno, NV 89510
Attn: W. K. Branch

Solar Energy Research Institute
1617 Cole Boulevard
Golden, CO 80401
Attn: L. Duhham, TID
G. Gross
B. Gupta
D. Kearney
L. M. Murphy
R. Ortiz, SEIDB
J. Thornton

Solar Thermal Test Facility
User Association
Suite 1205
First National Bank East
Albuquerque, NM 87112
Attn: F. Smith

Solar Turbines International
P. O. Box 80966
San Diego, CA 92138
Attn: P. Roberts

Southern California Edison
2244 Walnut Grove Road
Rosemead, CA 91770
Attn: J. Reeves
For: C. Winarski

Southwestern Public Service Co.
P. O. Box 1261
Amarillo, TX 78170
Attn: A. Higgins

Standard Oil of California
555 Market Street
San Francisco, CA 94105
Attn: S. Kleespies

Stanford Research Institute
333 Ravenswood Avenue
Menlo Park, CA 94025
Attn: A. Slemmons

Stearns-Roger
P. O. Box 5888
Denver, CO 80217
Attn: W. Lang
For: J. Hopson

Stone & Webster Engineering Corp.
245 Summer Street
P. O. Box 2325
Boston, MA 02107
Attn: R. Kuhr

Townsend and Bottum
9550 Flair Drive
El Monte, CA 91731
Attn: R. Schwing

US Gypsum
101 S. Wacker Drive
Chicago, IL 60606
Attn: Ray McCleary

US Water & Power Resources Service
Bureau of Reclamation
Code 1500 E
Denver Federal Center
P. O. Box 25007
Denver, CO 80225
Attn: S. J. Hightower

Van Leer Plastics
15581 Computer Lane
Huntington Beach, CA 92649
Attn: Larry Nelson

Veda, Inc.
400 N. Mobile, Building D
Camarillo, CA 90310
Attn: L. E. Ehrhardt
For: W. Moore

Westinghouse Corporation
Box 10864
Pittsburgh, PA 15236
Attn: J. J. Buggy
For: R. W. Devlin
W. Parker

Winsmith
Division of UMC Industries
Springville, NY 14141
Attn: W. H. Heller

K. R. Miller, 3153
G. E. Brandvold, 4710; Attn: J. F. Banas, 4716
J. A. Leonard, 4717
B. W. Marshall, 4713; Attn: D. L. King
A. B. Maish, 4719
R. G. Kepler, 5810; Attn: L. A. Harrah, 5811
J. G. Curro, 5813
F. P. Gerstle, 5814
J. N. Sweet, 5824; Attn: R. B. Pettit and E. P. Roth
T. B. Cook, 8000; Attn: A. N. Blackwell, 8200
B. F. Murphey, 8300
C. S. Hoyle, 8122; Attn: V. D. Dunder
R. J. Gallagher, 8124; Attn: B. A. Meyer
D. M. Schuster, 8310; Attn: W. R. Hoover, 8312, for M. D. Skibo
A. J. West, 8314
W. R. Even, 8315
R. L. Rinne, 8320
C. T. Yokomizo, 8326; Attn: L. D. Brandt
P. L. Mattern, 8342; Attn: J. Vitko, Jr.
L. Gutierrez, 8400; Attn: R. A. Baroody, 8410
D. E. Gregson, 8440
C. M. Tapp, 8460
C. S. Selvage, 8420
V. Burolla, 8424; Attn: C. B. Frost
R. C. Wayne, 8450
T. D. Brumleve, 8451
W. R. Delameter, 8451
P. J. Eicker, 8451 (5)
R. M. Houser, 8451
C. L. Mavis, 8451
W. L. Morehouse, 8451
H. F. Norris, Jr., 8451
W. S. Rorke, Jr., 8451
D. N. Tanner, 8451
S. S. White, 8451
A. C. Skinrood, 8452
W. G. Wilson, 8453
Publications Division, 8265, for TIC (27)
Publications Division, 8265/Technical Library Processes and Systems Division, 3141
Technical Library Processes and Systems Division, 3141 (2)
M. A. Pound, 8214, for Central Technical File (3)